
Computer Modeling of Jet Mixing in INEL Waste Tanks

P. A. Meyer

January 1994

Prepared for the U.S. Department of Energy
under Contract DE-AC06-76RLO 1830

Pacific Northwest Laboratory
Operated for the U.S. Department of Energy
by Battelle Memorial Institute

RECEIVED
APR 04 1994
OSTI



PNL-9063

DISCLAIMER

This report was prepared as an account of work sponsored by an agency of the United States Government. Neither the United States Government nor any agency thereof, nor Battelle Memorial Institute, nor any of their employees, makes any **warranty, expressed or implied, or assumes any legal liability or responsibility for the accuracy, completeness, or usefulness of any information, apparatus, product, or process disclosed, or represents that its use would not infringe privately owned rights.** Reference herein to any specific commercial product, process, or service by trade name, trademark, manufacturer, or otherwise does not necessarily constitute or imply its endorsement, recommendation, or favoring by the United States Government or any agency thereof, or Battelle Memorial Institute. The views and opinions of authors expressed herein do not necessarily state or reflect those of the United States Government or any agency thereof.

PACIFIC NORTHWEST LABORATORY
operated by
BATTELLE MEMORIAL INSTITUTE
for the
UNITED STATES DEPARTMENT OF ENERGY
under Contract DE-AC06-76RLO 1830

Printed in the United States of America

Available to DOE and DOE contractors from the
Office of Scientific and Technical Information, P.O. Box 62, Oak Ridge, TN 37831;
prices available from (615) 576-8401. FTS 626-8401.

Available to the public from the National Technical Information Service,
U.S. Department of Commerce, 5285 Port Royal Rd., Springfield, VA 22161.



The contents of this report were printed on recycled paper

PNL-9063
UC-510

**Computer Modeling of Jet Mixing
in INEL Waste Tanks**

P.A. Meyer

January 1994

**Prepared for
the U.S. Department of Energy
Under Contract DE-AC06-76RLO 1830**

**Pacific Northwest Laboratory
Richland, Washington 99352**

MASTER

DISTRIBUTION OF THIS DOCUMENT IS UNLIMITED

Summary

The objective of this study is to examine the feasibility of using submerged jet mixing pumps to mobilize and suspend settled sludge materials in INEL High Level Radioactive Waste Tanks. Scenarios include removing the heel (a shallow liquid and sludge layer remaining after tank emptying processes) and mobilizing and suspending solids in full or partially full tanks. The approach used was to 1) briefly review jet mixing theory, 2) review erosion literature in order to identify and estimate important sludge characterization parameters 3) perform computer modeling of submerged liquid mixing jets in INEL tank geometries, 4) develop analytical models from which pump operating conditions and mixing times can be estimated, and 5) analyze model results to determine overall feasibility of using jet mixing pumps and make design recommendations.

Following is a summary of the important findings of this study:

- Two parameters important to mobilization and deposition modeling are the critical shear stress for erosion and deposition. The erosion literature indicates values for these parameters can vary by several orders of magnitude for materials thought to be similar to the sludge in INEL tanks.
- Computer simulations showed that the ability of a submerged jet to erode sludge material is strongly dependent on the orientation of the jet relative to cooling coil arrays located near the tank floor.
- Correlations relating floor shear stress and fluid velocities with jet operating parameters were derived from the simulations. It was determined that the jet discharge parameter (defined as the product of nozzle diameter and jet velocity), not jet horsepower, was the most important parameter contributing to mobilization as long as suspended particle concentrations were small.
- Models were developed for estimating jet operating parameters, mixing time, and pump rotation rates. These models used the correlations obtained from the simulations and other important parameters such as fluid height, sludge thickness, and sludge material characteristics. Results show that the value of critical shear stress for erosion for the sludge has a strong effect on the minimum jet discharge parameter required to mobilize the sludge.
- Based on simulation data and analytical model results, feasibility of using a single jet mixing pump located near the tank center could not be conclusively determined. The primary reason for this is uncertainty in the value of critical shear stress for erosion. The results suggest, however, if the critical shear stress for erosion is less than about 0.35 Pa, a single pump with a jet discharge parameter equal to $1.8 \text{ m}^2/\text{s}$ ($19.4 \text{ ft}^2/\text{s}$) would be sufficient to mobilize and maintain solids in sus-

pension if it were located near the center of the tank. For a circular nozzle 20 cm (8 in.) in diameter, this would correspond to a total hydraulic jet power of about 62 hp and a pump power of about 124 hp assuming a 50% pump efficiency.

- Using an estimated upper limit of critical shear stress for erosion of 1.0 Pa, model results suggest heel removal would be successful if two off-center pumps were used. These pumps should each have a jet discharge parameter of at least $1.7 \text{ m}^2/\text{s}$ ($18.3 \text{ ft}^2/\text{s}$). For a 20 cm (8 in.) diameter round jet nozzle, the models predict a total hydraulic jet power of at least 52 hp is required, corresponding to a pump power of approximately 105 hp per pump assuming a 50% pump efficiency. The mixing time for this situation would be about 5 days. For a 20 cm diameter nozzle with a pump power of about 150 hp, mixing time would be reduced to about 5 hours.

While model results indicate that a double pump configuration would be adequate for even conservative values of critical shear stress for erosion, difficulties associated with new riser additions may make this option unattractive. In light of this, it is important that INEL obtain more precise estimations of the critical shear stress for erosion in order to confirm whether a single pump located near the tank center would be sufficiently effective. Model results indicate that if the critical shear stress for erosion is determined to be less than about 0.35Pa, this option should be successful. Formulas developed in this report for mixing time and rotation rate could be used as guides for pump sizing. In using these formulas, however, it would be helpful to have more precise estimates of particle properties (such as size, density, and distribution by weight), and the sludge thickness.

The models developed in this study represent simplifications of extremely complex flow phenomenon. In light of this, it would be advisable for INEL to combine sludge characterization activities with carefully designed mobilization experiments. Experiments could identify important behaviors not captured by numerical simulations or analytical models. In particular, experimental observations of jets in shallow liquids and measurements of floor shear underneath the cooling coils would be helpful in confirming the predictions.

Acknowledgments

This work was performed for Idaho National Engineering Laboratory, operated by Westinghouse Idaho Nuclear Company for the U. S. Department of Energy (technical contact, M. Christensen, c/o EG&G, Inc.). The work was conducted by Pacific Northwest Laboratory, operated by Battelle Memorial Institute for the U. S. Department of Energy under contract DE-AC06-76RLO 1830.

Sludge critical shear property evaluations were provided by Y. Onishi, Earth and Environmental Sciences Center, Pacific Northwest Laboratory. L. L. Eyler, Applied Physics Center, Pacific Northwest Laboratory, provided invaluable assistance with the TEMPEST computer program.

Contents

Summary	iii
Acknowledgments	v
1.0 Introduction.....	1-1
1.1 Objectives	1-1
1.2 Limitations	1-1
1.3 Approach	1-3
2.0 Mixing Theory and System Definition	2-1
2.1 Jet Mixing in Tanks	2-1
2.1.1 Jet Mixing of Liquids	2-1
2.1.2 Jet Mixing of Liquid/Solid Mixtures	2-3
2.2 INEL Tank Description	2-7
2.2.1 Tank Geometry.....	2-7
2.2.2 Mixing Pump Description.....	2-10
2.3 INEL Tank Waste Physical Properties	2-12
2.3.1 Waste Properties.....	2-12
2.3.2 Erosion/Deposition Properties	2-13
2.4 Factors Affecting Jet Mixing in INEL Tanks	2-15
2.4.1 Cooling Coils	2-15
2.4.2 Sludge Characterization.....	2-15
2.4.3 Limitations on Mixing Pump Configuration and Operating Conditions.....	2-16
3.0 Computer Simulations of Mixing Jet Hydrodynamics	3-1
3.1 Modeling Objectives and Approach	3-1
3.1.1 Objectives of Computer Modeling	3-1
3.1.2 The TEMPEST Computer Code	3-1
3.1.3 Modeling Approach and Limitations.....	3-1
3.2 Code Validation and Testing	3-3
3.2.1 Free-Jet Simulations	3-4
3.2.2 Floor-Jet Simulations.....	3-4
3.2.3 Modeling Flow over Cooling Coil.....	3-6

3.2.4 Shallow Liquid Tests.....	3-8
3.3 Numerical Simulations	3-9
3.3.1 The TEMPEST Model	3-9
3.3.2 Test Cases.....	3-11
3.3.3 Centered Jets Oriented Perpendicular to Cooling Coils	3-13
3.3.4 Centered Jets Flowing Parallel to Cooling Coils	3-31
3.3.5 Simulations of Off-Center Jets.....	3-39
3.3.6 Simulations of Particle Laden Jets.....	3-49
4.0 Mixing System Requirements.....	4-1
4.1 Analytical Models	4-1
4.1.1 Necessary Conditions for Effective Mixing	4-1
4.1.2 Erosion and Deposition Models.....	4-2
4.1.3 Jet Rotation Rate and Mixing Time Models	4-5
4.1.4 Solids Suspension Models	4-7
4.2 Model Results	4-8
4.2.1 Erosion and Deposition Results	4-8
4.2.2 Mixing Time Results and Pump Rotation Results	4-12
4.2.3 Solids Suspension Results	4-18
4.3 Mixing System Design	4-18
4.3.1 Feasibility Assessment Approach.....	4-18
4.3.2 Feasibility Results.....	4-20
4.3.3 Conclusions and Recommendations	4-21
5.0 References.....	5-1

Figures

2.1	Cross-Sectional Representation of a Typical INEL Waste Tank	2-8
2.2	Plan View of INEL Waste Tank WM-182	2-8
2.3	Plan View of INEL Waste Tank WM-188	2-9
2.4	Plan View Showing Typical Placement of Cooling Coil Support Beams and Spacer Type	2-9
2.5	Detail of Cooling Coils and Support Structure	2-10
2.6	Representation of a Submergible Jet Mixing Pump with Dual-Opposed Jet Discharge	2-11
2.7	Waste Tank with Mixing Pumps Installed in Existing Risers	2-11
2.8	Envelope of Allowable Jet Velocities and Nozzle Diameters due to Maximum Pump Power Constraint	2-17
3.1	Side View of Geometry for a Three-dimensional Turbulent Floor Jet	3-4
3.2	Comparison of Maximum Velocity Decay and Floor Shear Stress for a Turbulent Floor Jet	3-5
3.3	Geometry for 2-D Cooling Coil Noding Resolution Study	3-7
3.4	Computed Floor Shear Stress for 2-D Noding Resolution Study	3-7
3.5	Rectangular Computational Grid Representation	3-9
3.6	Detail of Pump Nozzle and Inlet Model	3-10
3.7	Velocity Vectors for Tank Without Cooling Coils (T150A) (top) and Tank With Jet oriented Perpendicular to Cooling Coils (N150A) (bottom)	3-13
3.8	Recirculating Flow Near Tank Wall Due to Cooling Coils	3-14
3.9	Comparison of Jet Center-line Floor Shear Stress for Tank Without Cooling Coils (T150A) and Tank with Jet Oriented Perpendicular to Cooling Coils (N150A)	3-14
3.10	Floor Shear Stress Contours for Tank Without Cooling Coils (T150A) (top) and Tank With Jet Perpendicular to Cooling Coils (N150A) (bottom)	3-15
3.11	Effect of Jet Height Above Cooling Coils on Floor Shear Stress	3-17
3.12	Floor Shear Stress for a Jet Located Underneath Cooling Coils	3-17
3.13	Floor Shear Stress Along Jet Center-line For Jets Oriented Perpendicular to Cooling Coils with Various Operating Conditions	3-19
3.14	Correlation of Floor Shear Stress Along Jet Center-line with Nozzle Discharge Parameter	3-21

3.15	Off-Center Nondimensional Floor Shear Stress for Test Cases N150A Through N025A	3-23
3.16	Transverse Variation of Nondimensional Floor Shear Stress at for Test Cases N150A Through N025A	3-23
3.17	Effect of Liquid Depth on Center-Line Floor Shear Stress	3-25
3.18	Contours of Normalized Velocity Near the Tank Wall	3-27
3.19	Normalized Velocity Components Near Tank Wall for $h_f = 91$ cm (test case N150B)	3-27
3.20	Normalized Velocity Components Near Tank Wall for $h_f = 183$ cm (test case N150G)	3-29
3.21	Normalized Velocity Components Near Tank Wall for $h_f = 305$ cm (test case N150H)	3-29
3.22	Normalized Velocity Components Near Tank Wall for $h_f = 640$ cm (test case N150I)	3-31
3.23	Velocity Vectors for Jet Oriented Parallel to the Cooling Coils for (top) West Facing Jet (W150A) and (bottom) East Facing Jet (E150A)	3-33
3.24	Floor Shear Stress Contours for (top) West Facing Jet (W150A) and (bottom) East Facing Jet (E150A)	3-35
3.25	Normalized Center-line Floor Shear Stress for West Facing Jets	3-35
3.26	Normalized Center-line Floor Shear Stress for East Facing Jets	3-37
3.27	Normalized Velocity Components Near Tank Wall for East Facing Jet in 91 cm Depth Fluid (E150A)	3-37
3.28	Normalized Velocity Components Near Tank Wall for East Facing Jet in 183 cm Depth Fluid (E150B)	3-39
3.29	Velocity Vectors for Off-center Jet Oriented Perpendicular to Cooling Coils (test case N150M)	3-41
3.30	Floor Shear Stress Contours for Off-center Jet Oriented Perpendicular to Cooling Coils (test case N150M)	3-41
3.31	Normalized Jet Center-line Floor Shear Stress for Off-center Jets Oriented Perpendicular to Cooling Coils	3-43
3.32	Normalized Velocity Components Near Tank Wall for Off-center Jet in 91 cm Depth Fluid Oriented Perpendicular to Cooling Coils (N150M)	3-43
3.33	Normalized Velocity Components Near Tank Wall for Off-center Jet in 305 cm Depth Fluid Oriented Perpendicular to Cooling Coils (N150N)	3-45
3.34	Normalized Center-line Floor Shear Stress for East Facing Off-center Jets	3-45

3.35	Normalized Velocity Components Near Tank Wall for Off-center Jet in 91 cm Depth Fluid Oriented Parallel to Cooling Coils (E150D)	3-47
3.36	Normalized Velocity Components Near Tank Wall for Off-center Jet in 305 cm Depth Fluid Oriented Parallel to Cooling Coils (E150E)	3-47
3.37	Density Contours in Particle Laden Jets Oriented Perpendicular to Cooling Coils for 91cm Fluid Height (P150A) (top) and 305 cm Fluid Height (P150B) (bottom)	3-51
3.38	Normalized Floor Shear Stress for Tank-centered Particle-laden Jets	3-51
3.39	Normalized Floor Shear Stress for Off-center Particle-laden Jets	3-53
3.40	Normalized Velocity Components Near Tank Wall for Dense Jet in 91 cm Height Fluid (P150A)	3-55
3.41	Normalized Velocity Components Near Tank Wall for Dense Jet in 305 cm Height Fluid (P050B)	3-55
3.42	Normalized Velocity Components Near Tank Wall for Off-center Dense Jet in 305 cm Height Fluid (P050C)	3-57
3.43	Normalized Particle Concentrations of Smallest Particles Along Tank Wall for Various Test Cases	3-57
3.44	Normalized Particle Concentrations of Medium Particles Along Tank Wall for Various Test Cases	3-59
3.45	Normalized Particle Concentrations of Largest Particles Along Tank Wall for Various Test Cases	3-59
4.1	Erosion and Deposition Areas Within the Effective Cleaning Radius	4-3
4.2	Jet Discharge Parameter Required to Erode Sludge Near Tank Wall	4-8
4.3	Effect of Particle Size on $u_0 d_0$ for Tank-centered Jet	4-10
4.4	Effect of Erodibility Constant on $u_0 d_0$ for Tank-centered Jet	4-10
4.5	Effect of Jet Location on $u_0 d_0$	4-11
4.6	Effect of Background Shear Constant \bar{c}_d on $u_0 d_0$ for Tank-centered Jet	4-11
4.7	Effect of Particle Size on Mixing Time for Tank-centered Jet	4-13
4.8	Effect of Erodibility Constant on Mixing Time for Tank-centered Jet	4-13
4.9	Effect of Fluid Height on Mixing Time for Tank-centered Jet	4-14
4.10	Effect of Sludge Thickness on Mixing Time for Tank-centered Jet	4-14
4.11	Effect of Critical Shear Stress for Erosion on Mixing Time for Tank-centered Jet	4-15

4.12	Effect of Critical Shear Stress for Erosion on Mixing Time for Off-center Jet	4-15
4.13	Effect of Particle Size on Jet Rotation Rate for Tank-centered Jet	4-16
4.14	Effect of Degree of Uniformity on Pump Rotation Rate for Tank-centered Jet	4-16
4.15	Effect of Fluid Height on Jet Rotation Rate for Tank-centered Jet	4-17
4.16	Effect of Critical Shear Stress for Erosion on Jet Rotation Rate for Tank-centered Jet	4-17
4.17	Graphical Illustration of Feasibility Assessment Approach	4-19
4.18	Recommended Mixing Pump Locations in INEL Waste Tank WM-182	4-22
4.19	Recommended Mixing Pump Locations in INEL Waste Tank WM-188	4-22

Tables

2.1	Sludge Solids Composition Used for Analysis.....	2-12
2.2	Fluid and Bulk Sludge Properties Used for Analysis	2-13
2.3	Erosion and Deposition Properties Used for Analysis.....	2-15
3.1	Test Case Parameters	3-11

1.0 Introduction

There are eleven 300,000 gallon high-level radioactive liquid waste storage tanks at the Idaho Chemical Processing Plant (ICPP) located on the tank farm at the Idaho National Engineering Laboratory (INEL). Following normal tank farm emptying operations, there remains a heel of approximately 500 to 15,000 gal of liquid/solid solution in the bottom of each storage tank. One of the tasks of the High Level Waste Tank Farm Replacement Project (HLWTFRP) includes removing these heels. A recently completed Heel Removal Special Study (HRSS) recommended the use of jet mixing pumps to re-suspend solids that settled out of solution during interim storage. This mixed solution of liquid and solids would then be transferred out of the tanks and undergo a calcination process in the New Waste Calcinator Facility (NWCF). Further evaluations have identified the need to minimize solids concentrations in the feed to the NWCF. In light of this, the concept of using mixing pumps to suspend solids in a full or partially full tank and maintaining solids suspension during feed-out to NWCF was generated.

1.1 Objectives

The main objective of this work is to examine the feasibility of using submerged jet mixing pumps to remove the remaining heel in emptied waste storage tanks and to suspend solids in full and partially full tanks. This will be accomplished by the following:

- Perform computer simulations of submerged liquid jets in the heel.
- Perform computer simulations of submerged liquid jets in partially full and full tanks.
- Perform modeling of solids erosion and settling in heels and full/partially full tanks.
- Evaluate modeling results in order to determine the feasibility of using jet mixing pumps and make recommendations on pump characteristics and configurations in order to accomplish heel removal and solids suspension.

Computer simulations in this study are performed with the TEMPEST computer program which is described in Section 3.

1.2 Limitations

Limitations are inherent to any analysis because of uncertainties in defining the system and applicability of analytic tools. The limitations on this study are listed below:

- The computational model of the free liquid surface at the liquid/air interface is

non-deformable. At low liquid levels, the model does not represent surface effects such as waves, rolling, or splashing.

- Incomplete knowledge of the physical properties of the solids in the INEL waste tanks provides an uncertainty in the ability of mixing pumps to resuspend settled solids and maintain solids in suspension.
- Accurate modeling of turbulence phenomena in complex flows, in general, remains beyond the ability of modern engineering science. While there are models which are applicable to certain flows, there is no model which can solve every problem. The effects of solid particulates on turbulent phenomena remains the subject of present research.
- The speed of modern high-performance computers is insufficient to perform highly resolved simulations of large physical systems. Therefore, errors associated with coarse “nodeing” of geometric detail are inherent.
- The computational model being used for this analysis has not yet been developed for rotating jets. Therefore, only fixed jets are modeled.

The first limitation can only be addressed in a general way. Several models will be developed to estimate the minimum liquid level which can be accurately modeled. While surface deformation is expected, especially at low liquid levels, its occurrence should be primarily related to surface effects (e. g., aerosol generation, waves) and not to mixing in the liquid volume.

The second limitation is related to uncertainties associated with deposition and resuspension of material on the tank floor. A critical shear stress model is used in the analysis. This model requires constants for the critical shear stress for deposition, erodibility of a material, and critical shear stress for erosion. Lack of knowledge of the physical characteristics of the INEL tank contents limits applicability of erosion constants obtained from the literature. The effects of uncertainty in values for erosion constants will be quantified by determining the dependence of jet performance on these constants. Mixing results will be presented for a range of erosion constant values.

The third limitation can be addressed by comparing simulated turbulent flow results with available experimental data. While there is limited experimental data available for turbulent particulate flows, for small concentrations, the effects of particulates are minimized. Since the settled sludge layer in INEL tanks is thin (approximately 1 to 3 in.) the effects of suspended particles on turbulent motions should be minimal.

The fourth limitation can be addressed by performing resolution studies on test problems similar to INEL flow geometries. The effects of coarse nodeing can be quantified by increasing the resolution incrementally and observing the change in the flow solution.

The final limitation is not critical to this analysis. Results for rotating jets can be obtained from analytical models which incorporate simulation results for fixed jets.

1.3 Approach

The approach used to accomplish the objectives of this study is as follows:

- Briefly review jet mixing theory in order to establish the pertinent physical processes affecting jet mixing in tanks.
- Review erosion literature in order to identify and estimate important sludge characterization parameters.
- Perform computer code validation tests which address shallow liquid surface effects, node resolution requirements, and turbulent jet predictive capability.
- Perform computer modeling of submerged liquid jets in INEL tank geometries. Derive correlations relating floor shear stress and fluid velocities with jet operating parameters.
- Develop analytical models for estimating jet operating parameters, mixing time, and pump rotation rates. These models will use the correlations obtained from the simulations and be dependent on parameters such as fluid height, sludge thickness, and sludge material characteristics.
- Analyze model results to determine overall feasibility of using jet mixing pumps in INEL tanks and provide design recommendations.

2.0 Mixing Theory and System Definition

This section presents a brief review of jet mixing theory and a description of the INEL Waste Tank system to be modeled. Section 2.1 reviews important aspects of jet mixing in tanks. In Section 2.2, a description of typical INEL tank geometries is presented. Characterization of INEL tank waste is addressed in Section 2.3. Finally, Section 2.4 addresses important factors anticipated to affect mixing in INEL tanks.

2.1 Jet Mixing in Tanks

Mixing in tanks involves the reduction in concentration gradients of different constituents by means of fluid motions. The constituents may be separate fluids, chemical species, or solid materials which are dissolved or suspended. The fluid motions may occur naturally (such as buoyant actions due to density differences) or may be forced by some means of agitation. Historically, much of the literature on mixing in tanks has addressed systems with mechanical agitators. More recently, there has been increased attention on understanding principles of jet mixing in tanks. Much of the mixing literature addresses mixing in fluid-only systems. The presence of solids has been found to add an additional degree of complexity. An extensive review of mixing literature was recently performed by Bamberger, Liljegren, and Lowery (1993). Their findings were consistent with Tatterson (1991), who performed a brief review of jet mixing in tanks.

2.1.1 Jet Mixing of Liquids

Fundamental to mixing theory is the mixing time concept. The mixing time, T_m , is defined as the amount of time required to produce uniform concentrations of constituents within a tank. In general, the mixing time will be a function of the fluid properties, tank geometry, jet location and orientation, and jet characteristics such as nozzle diameter and jet velocity. In studying any complex physical system, it is often useful to formulate nondimensional quantities which remove the effects of physical scale from the system. For example, a nondimensional mixing time can be constructed by dividing the mixing time by the ratio of jet diameter to jet velocity. Bamberger, Liljegren, and Lowery (1993) suggest that a nondimensional mixing time is found to be affected by four dimensionless parameters; the jet Reynolds number (Re), the Froude number (Fr), the relative density ratio (N_ρ), and the aspect ratio of the liquid in the tank (AR). These parameters are defined as

$$Re = (\rho_j u_0 d_0) / \mu_f \quad (2.1)$$

$$Fr = u_0^2 / (N_\rho g d_0) \quad (2.2)$$

$$N_\rho = (\rho_j - \rho_f) / \rho_j \quad (2.3)$$

$$AR = h_f/R_T, \quad (2.4)$$

where u_0 and d_0 are the jet velocity and diameter^(a), respectively, ρ_j is the density of the fluid exiting the jet, and μ_f and ρ_f are the mean tank fluid viscosity and density, respectively. Also, g is the acceleration caused by gravity, h_f is the fluid height, and R_T is the tank radius.

If the jet Reynolds number is large enough, the jet will be turbulent-- greatly enhancing mixing. Once the jet is turbulent, however, the nondimensional mixing time is relatively unaffected by changes in the jet Reynolds number. The Froude number takes into account buoyancy effects due to density differences between the jet and the surrounding fluid. If the Froude number is small, the jet may have insufficient kinetic energy to convect fluid upward against the force of gravity. If the Froude number is large, the jet can easily move fluid to the liquid surface and density effects are unimportant. The aspect ratio of the tank seems to effect mixing primarily by setting large-scale recirculating flow patterns.

In addition to the above-mentioned parameters, some additional factors are thought to be important in jet mixing processes in tanks. For example, the vertical location of the jet is particularly important when buoyant effects are present. For jets that are more dense than the surrounding fluid, locating the jet near the top of the tank should decrease mixing time. Conversely, locating lighter jets near the bottom of tanks would enhance mixing. Another factor involves rotating jets. For a fixed jet, mixing is dependent on large-scale currents which set up throughout the tank. When the jet is rotated, these large-scale motions are continuously changing with time. It is not immediately obvious which rotation rate would have the most favorable effect on mixing time. For a centrally located jet that rotates at a very high rate, the effect would be that of a jet which flows radially outward without angular dependence. A dimensionless jet rotation rate (Ω_j) can be defined as

$$\Omega_j = \dot{\omega}_j d_0 / u_0, \quad (2.5)$$

where $\dot{\omega}$ is the rotation rate of the jet mixing pump.

Finally, when multiple jets are used, jet interaction effects could constructively or destructively interfere. Evidently, for a given tank geometry, the jet locations (both vertically and horizontally) could be very important. For the case of multiple rotating jets, the complexity of the system is certainly increased.

(a) In general, d_0 is the square root of the nozzle cross-sectional area. Throughout this report, d_0 will be referred to as the nozzle diameter even though the analysis is not limited to jets with circular nozzles.

2.1.2 Jet Mixing of Liquid/Solid Mixtures

All parameters involved in mixing liquids are expected to be important when solids are present. There are, however, two additional important aspects of jet mixing in tanks with solids. These are 1) mobilizing the settled solids (sludge) at the bottom of a tank and 2) maintaining the solids in a suspension of uniform concentration. The processes involved in each of these have been addressed by Bamberger, Eyster, and Dodge (1993). Their findings will be summarized here, and some additional information will be provided.

Mobilizing Settled Solids

There are two basic mechanisms thought to be involved in sludge mobilization. First, jets may mobilize settled solids by erosion due to shearing when fluid flows parallel to the sludge layer. When the flow is turbulent, the erosion is enhanced due to small-scale nonsteady turbulent motions. The degree of erosion is thought to be dependent on shear stress which the fluid applies to the solid layer. Second, jets can mobilize solids in bulk by impinging normal to the sludge layer. This boring action is thought to be dominated by normal momentum exchange (as opposed to shear) between the fluid and the solids. Which mechanism dominates in a given physical situation will depend on a number of factors including fluid velocity (or momentum) near the sludge, sludge bank shape, and solids characteristics, such as particle size and cohesiveness.

The effective cleaning radius (*ECR*) of a jet is defined as the distance from the jet nozzle beyond which no mobilization occurs. For a rotating jet, the *ECR* is the radius of the circle where the sludge has been mobilized (or where mobilization is occurring). Liljegren (1993) proposed that the nondimensional *ECR* is a function of the Reynolds number (*Re*) and a yield parameter (N_τ) according to

$$ECR/d_0 = f(Re, N_\tau) \quad (2.6)$$

$$N_\tau = (\rho_j u_0^2) / \tau_{ss} \quad (2.7)$$

where τ_{ss} is the shear strength of the sludge. The use of shear strength was proposed by Powell^(a) who suggests it is an indicator of the sludge's ability to resist mobilization. Some researchers, however, suggest that the sludge tensile strength may be a more useful parameter to characterize sludge resistance. In general, the function dependence between the nondimensional effective cleaning radius and the Reynolds number and the yield parameter is unknown.

(a)M. R. Powell, C. L. Fow, G. A. Whyatt, P. A. Scott, and C. M. Ruecker. November 1990. *Proposed Test Strategy for the Evaluation of Double-Shell Tank Sludge Mobilization*. A letter report for Westinghouse Hanford Company by Pacific Northwest Laboratory, Richland, Washington.

Historically, much of the research pertaining to the erosion of settled solids has been in the field of hydrology where transport of silt and sediment in rivers has been of interest. Expressions to determine erodibility of solids are usually formulated differently for cohesive and non-cohesive sediments. There are no data available to indicate which INEL tank solids are cohesive. In general for soils, clay (0.24 to 4 μm diameter particles), and silt (4 to 64 μm diameter particles), are often treated as cohesive, while sand (64 to 200 μm diameter particles) is treated as non-cohesive. Onishi (1993) summarized the comparisons of 23 different formulas used to predict erosion and deposition of solids. He recommended a widely used expression originally suggested by Partheniades (1962) which gives a relationship between erosion rate and fluid shear stress in the form;

$$\dot{m}_e = E(\tau_f/\tau_e - 1) \quad \tau_f \geq \tau_e. \quad (2.8)$$

In Equation (2.8), τ_f is the shear stress exerted on the sludge by the fluid and \dot{m}_e is the mass flux of solids away from the sludge layer. The terms E and τ_e are the erodibility and critical shear stress for erosion, respectively. These are empirical constants that must be determined for a given sludge. To determine the net mass transport of solids into the fluid, Equation (2.8) must be integrated over the area where erosion is occurring.

A similar expression for the solids deposition flux to the floor (or, for example, a river bed) due to particle settling was suggested by Krone (1962). This relation, which has the same form as Equation (2.8), is given by

$$\dot{m}_d = u_s \phi_s (1 - \tau_f/\tau_d) \quad \tau_f \leq \tau_d. \quad (2.9)$$

Here u_s is the particle settling velocity, ϕ_s is the species mass fraction, and τ_d is the critical shear stress for deposition that must be determined from measurements for a given sludge material.

The settling velocity is the speed at which a particle falls due to a balance of gravitational force and particle drag. For low concentrations of small particles, the settling velocity can be computed according to the Stokes settling relation,

$$u_s = \frac{1}{18} g d_s^2 (\rho_s - \rho_f) / \mu_f \quad (2.10)$$

where d_s is the particle diameter and ρ_s is the particle density. Equation (2.10) is valid for particle Reynolds number (Re_s):

$$Re_s = (\rho_f d_s u_s) / \mu_f < 1. \quad (2.11)$$

For particles $Re_s > 1$, Equation (2.10) can be modified.

The shear stress (τ_f) in Equation (2.8) will generally be related to the jet momentum. For a turbulent jet located on a tank floor in a pure liquid, Rajaratnam (1976) showed that the parameter $\tau_f / (\rho_f u_m^2)$ is approximately constant far from the jet nozzle. The velocity u_m is the maximum velocity in the fluid jet above the floor. As in the case of a free jet (far from walls), the maximum velocity divided by the jet velocity is inversely proportional to the dimensionless distance from the jet, x/d_0 . From these relationships, the following dependence between floor shear stress on jet momentum can be derived:

$$\tau_f / (\rho_f u_0^2) \sim (d_0/x)^2 \quad (2.12)$$

Although Equation (2.12) is derived from experimentally determined relationships that are strictly valid only for floor jets in pure liquids, it may be valid for jets that are located above the tank floor as well. This would be true if 1) density effects were relatively unimportant, 2) the floor shear stress was proportional to the local jet momentum, and 3) the local maximum velocity decayed inversely with distance from the nozzle.

In order to make Equation (2.12) an equality, the constant of proportionality would need to be determined. If this could be achieved, then Equation (2.12) could be combined with Equation (2.8) to relate the erosion mass flux to the jet momentum. Therefore, if the erodibility (E) and the critical shear stress for erosion (τ_c) were known for a given sludge, the effective cleaning radius could be determined.

Maintaining Solids in Suspension

Once solids have been mobilized from the floor of a tank, large-scale circulating motions induced by the jet are expected to mix the particles throughout the tank. Small-scale diffusive motions are expected to complete the mixing process by locally smoothing out particle concentration gradients. Gravity will act to cause heavy particles to settle to the bottom of the tank. Suspension maintenance should occur if 1) the jet is particle laden, 2) the particle-laden jet has sufficient momentum to travel to the upper regions of the tank, and 3) either the large-scale motions far from the jet are sufficient to counter the effects of gravity or the jet is rotated so that all fluid parcels near the bottom of the tank are eventually carried upward.

Density differences in the tank can greatly affect the large-scale circulation patterns created by the jet. The average density of the jet is dependent on the concentration of particles. If the jet intake is located near the bottom of the tank, the jet density may be greater than the average fluid density surrounding the jet. As the jet travels upward along the tank wall, the excess density relative to the surrounding fluid may increase. Excess density combined with low momentum can

prevent the jet from rising towards the surface. The height to which the jet will rise (h_j) is a function of the Froude number, the Reynolds number, the relative density parameter (N_ρ), and the jet angle relative to the floor (θ_j):

$$h_j/d_0 = f(Fr, Re, N_\rho, \theta_j). \quad (2.13)$$

Geisler, Buurman, and Mersmann (1992) considered scaling laws for stirred vessels with suspensions. They concluded that no single scaling law existed (i.e., no universal relationship exists between, say, jet momentum and suspendability). However, they did find an interesting criterion for suspension maintenance in large tanks. This criterion can be explained as follows: Gravity does work on particles by attracting them toward the tank bottom. The rate of work (i.e., power) per particle is the vertical component of particle drag multiplied by the particles relative velocity with the surrounding fluid. In order to satisfy the conservation of energy principle, the mixing jet must have sufficient power to overcome gravitational work. Jet power will also be converted to thermal energy through viscous dissipation; however, if the jet power is less than the gravitation work rate, suspension maintenance will be impossible. Liljegren (1993) introduced a gravitational settling parameter (N_s) which scales the rate of gravitational work on the particulates with the jet power. This parameter is given by

$$N_s = (\phi_s f_s u_s V_T) / (\rho_j u_0^3 d_0^2), \quad (2.14)$$

where f_s is the average drag force on a settling particle and V_T is the tank volume.

In general, it is expected that dimensionless mixing time in tanks with solids concentrations will be a function of Reynolds number, Froude number, yield parameter, relative density, gravitational settling parameter, aspect ratio, jet angle, jet rotation rate, and number of pumps (n). This is expressed as

$$\frac{T_m}{(d_0/u_0)} = f(Re, Fr, N_\tau, N_\rho, N_s, AR, \theta, \Omega, n). \quad (2.15)$$

Experiments are being planned as part of double-shell tank retrieval investigations at Pacific Northwest Laboratory (PNL) to investigate the effects of Reynolds number, Froude number, and gravitational settling parameter. These experiments will be used to augment validation of computer model results.

2.2 INEL Tank Description

There are eleven 300,000 gal high-level radioactive liquid waste tanks in the tank farm at the Idaho Chemical Processing Plant (ICPP) at the Idaho National Engineering Laboratory (INEL). The locations of risers and man-ways that could be used for mixing pump installment vary from tank to tank. Most of the tanks are equipped with internal cooling coils which are located near the tank floors and walls. Because no two tanks are identical, two representative tanks will be considered for purposes of modeling. In Section 2.2.1 these representative geometries will be described. Section 2.2.2 describes typical jet mixing pump operations.

2.2.1 Tank Geometry

A cross-section of a typical INEL tank is shown in Figure 2.1. The tank is 15.25 m (50 ft) in diameter with a 6.4 m (21 ft) maximum liquid height capacity. There are several risers located at the top of the tank along with a man-way opening. Steam jets extend to the bottom of the tank. Also shown is a representation of cooling coil banks near the bottom and side of the tank. Figure 2.2 and Figure 2.3 show plan views of two different tanks. These two tanks (designated Tank WM-182 and Tank WM-188, respectively) are considered to be representative of the other tanks at INEL. Because steam jet usage may continue during various operational scenarios, only the man-ways and existing risers are being considered for possible mixing pump installation. The man-ways in both tanks are 28 in. in diameter while the risers are 12 in. in diameter.

Also shown in Figure 2.2 and Figure 2.3 are a representation of the cooling coils at the tank bottom. Each solid grey lines represent two adjacent pipes which are supported off the tank floor. These cooling coils are connected to another network of coils on the tank walls (not shown). Figure 2.4 shows a plan view detail of the support beam structure underneath the cooling coils. Also shown are the location and types of spacers that fasten the main support beams to the tank floor. Figure 2.5 shows details of the cooling coil and support structures.

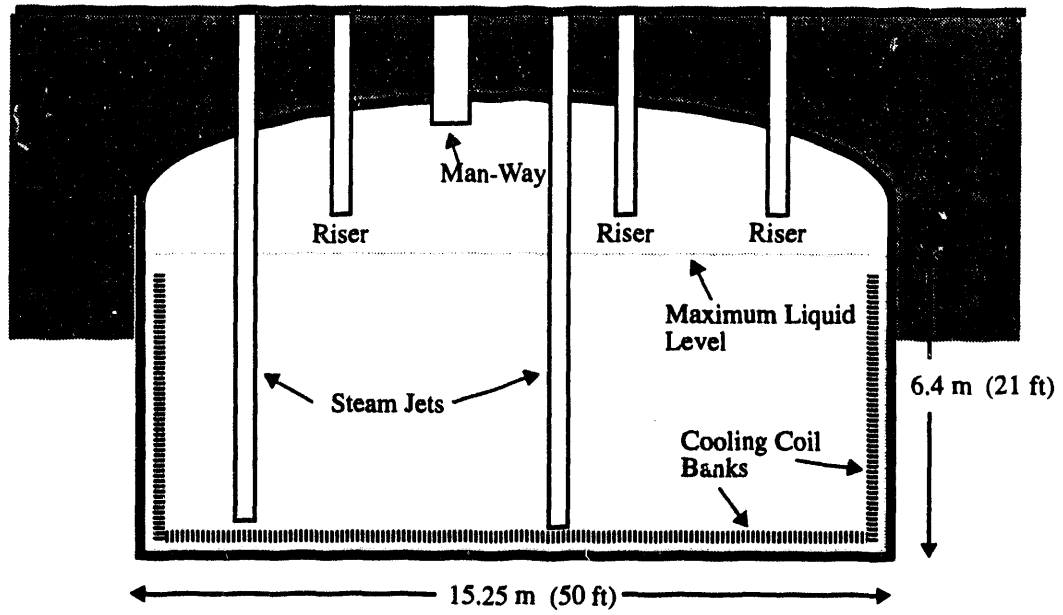


Figure 2.1 Cross-Sectional Representation of a Typical INEL Waste Tank

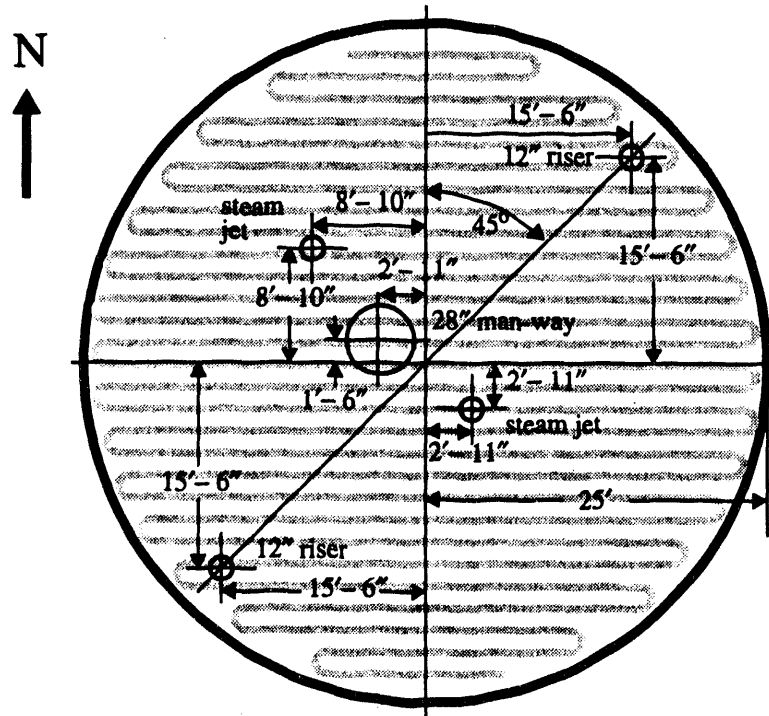


Figure 2.2 Plan View of INEL Waste Tank WM-182. Shaded lines represent cooling coils near tank floor

Figure 2.4 Plan View Showing Typical Placement of Cooling Coil Support Beams and Spacer Type

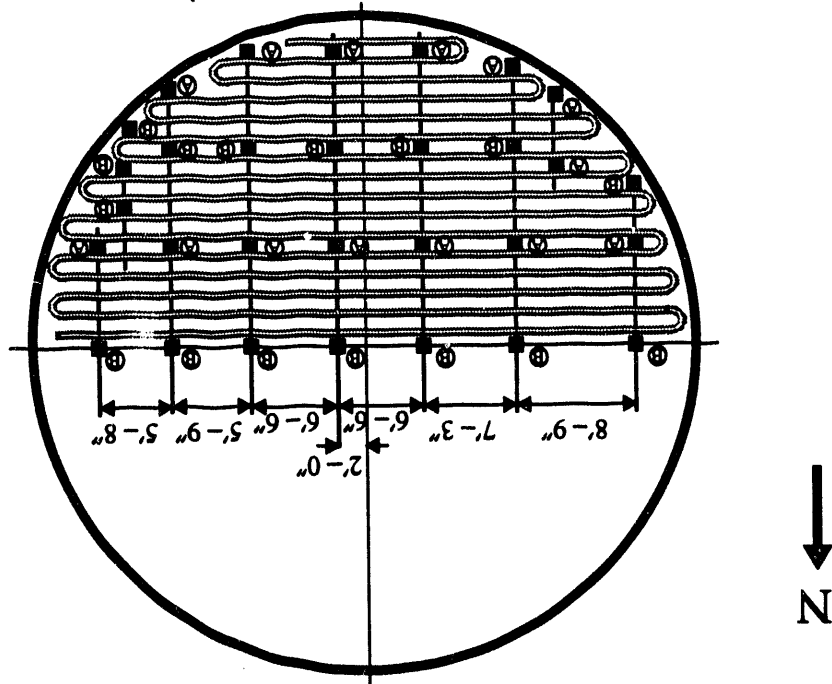
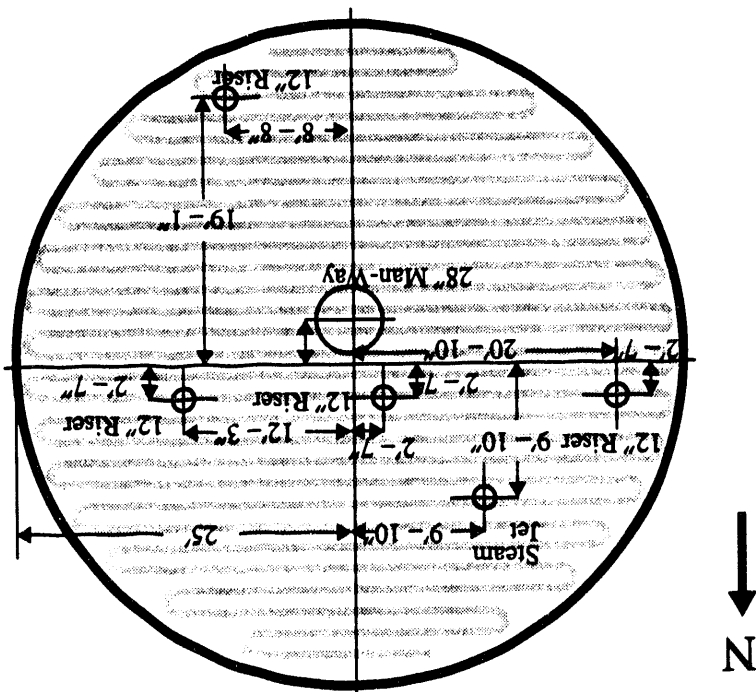


Figure 2.3 Plan View of INEL Waste Tank WM-188. Shaded lines represent cooling coils near tank floor.



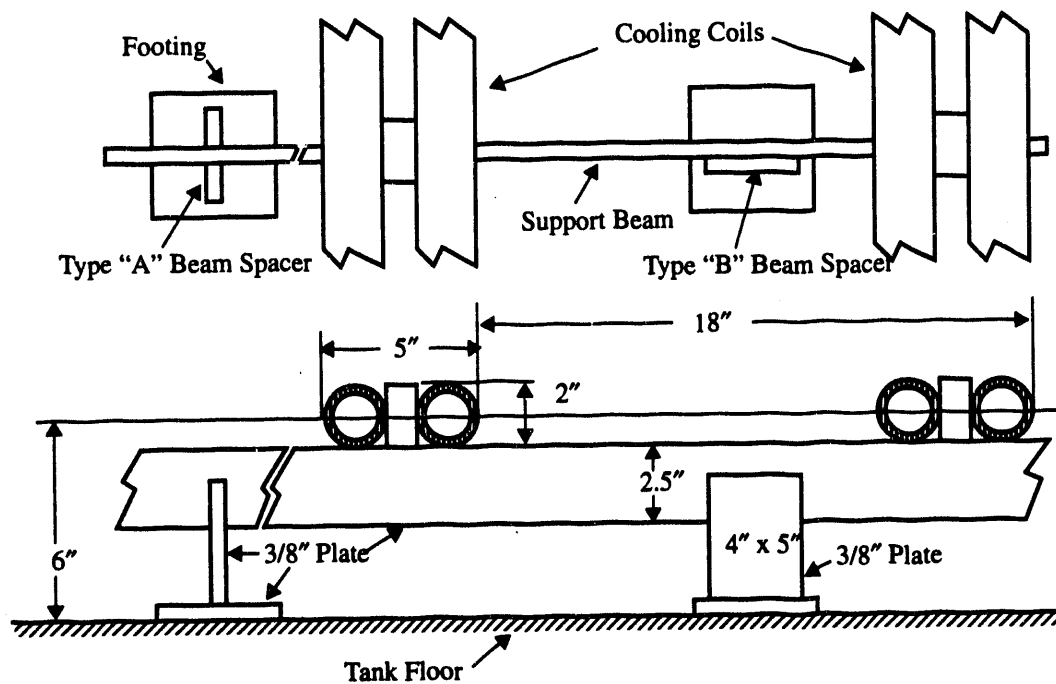


Figure 2.5 Detail of Cooling Coils and Support Structure

2.2.2 Mixing Pump Description

A representation of a typical jet mixing pump expected to be similar to those planned for the INEL tanks is shown in Figure 2.7. The pump has two identical dual-opposed jet discharge nozzles designed to eliminate torque on the support column. The inlet is on the bottom of the pump unit. The pump may continuously rotate 360° or oscillate in a 180° period. Figure 2.6 shows a representative cross-section of a waste tank with jet mixing pumps installed in existing risers.

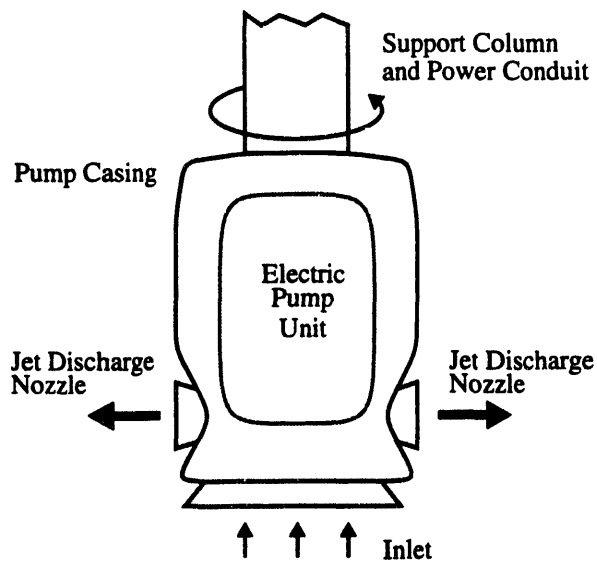


Figure 2.6 Representation of a Submersible Jet Mixing Pump with Dual-Opposed Jet Discharge

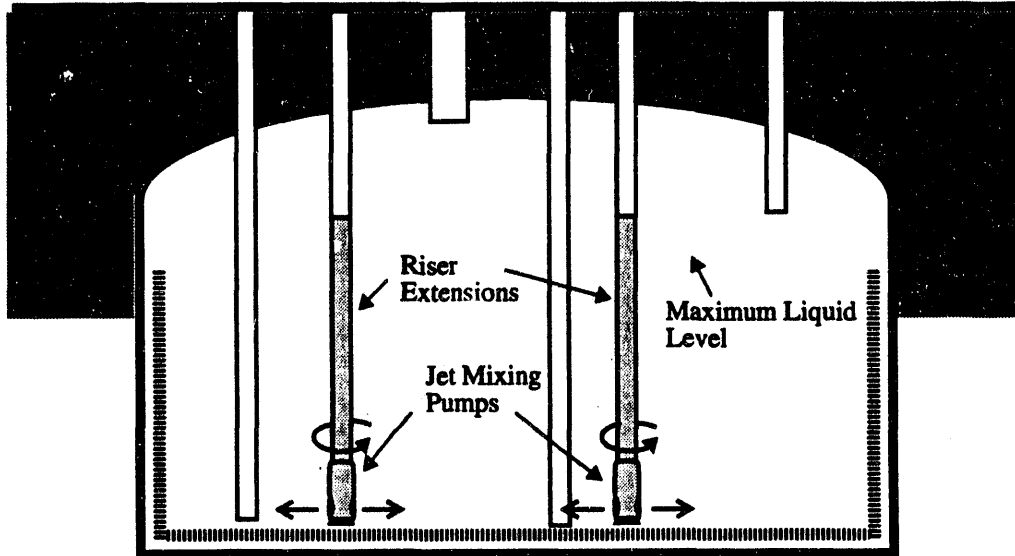


Figure 2.7 Waste Tank with Mixing Pumps Installed in Existing Risers

2.3 INEL Tank Waste Physical Properties

This section presents a description of the liquid and solid waste in the INEL waste tanks. Characterization of radioactive waste remains one of the highest priorities and greatest challenges facing hazardous waste remediation efforts. Computational, experimental, and analytical models of waste mobilization and retrieval systems require knowledge of the waste's physical characteristics. Useful data on waste properties can be difficult to obtain and may greatly vary for different waste samples. In light of this difficulty, it is necessary to estimate certain physical properties based on the best available known data for similar materials. In Section 2.3.1, properties of the solids and liquid waste are presented. Section 2.3.2 gives estimations of the parameter values required for solids erosion and deposition modeling.

2.3.1 Waste Properties

The INEL waste tanks contain a clear acidic liquid solution with a settled sludge layer at the tank floor. The sludge layer is known to be less than 3 in. deep, but may be considerably less. Some characterization of the liquid and solid materials have been completed by INEL. Based on these analyses, primary parameter values for the present study are presented here. Table 2.1 gives the sludge solids composition used for this study^(a). The solid particles are grouped into three representative categories; largest, smallest, and most populous. The largest and smallest particles are thought to represent a conservative outer range of particle sizes. The large particles are resin beads which could be silicon gel or glass. The composition of the other particles is uncertain

Table 2.2 gives fluid and bulk sludge properties used in this study^(a). The sludge dry bulk density (the density of sludge which has had all liquid removed) is computed from the solids composition data shown in Table 2.1. The wet bulk density was computed assuming a solids void fraction of 50%. This value was chosen somewhat arbitrarily but is thought to be similar to typical dense sludges. The density and viscosity of liquid aluminum nitrate is also shown in Table 2.2. This fluid may be added to the waste prior to convenience to the calcination facility.

Table 2.1 Sludge Solids Composition Used for Analysis

Property	Largest Particles	Most Populous	Smallest Particles
Particle diameter, d_s	200 μm	70 μm	13 μm
Particle density, ρ_s	3000 kg/m^3	3000 kg/m^3	5540 kg/m^3
Distribution by weight	4%	70%	26%

(a) From private communications with Max Christensen, EG&G Idaho Inc., 9/93.

Table 2.2 Fluid and Bulk Sludge Properties Used for Analysis

Property	Value	Observation
Fluid density, ρ_f	1400 kg/m ³	mostly water-like liquid, acidic
Fluid viscosity, μ_f	1.6 cP	measured quantity
Sludge dry bulk density	3406 kg/m ³	from solids property data (see Table 2.1)
Sludge wet bulk density	2402 kg/m ³	based on assumed void fraction of 50%
Aluminum Nitrate density	1300 kg/m ³	may be added to liquid waste
Aluminum Nitrate viscosity	0.8 cP	measured quantity

2.3.2 Erosion/Deposition Properties

To model the erosion and deposition of solids at the sludge layer, the critical shear parameters in Equations (2.8) and (2.9) need to be estimated, because no data are available for the INEL sludge. To accomplish this, the literature was surveyed to obtain representative sedimentation parameters for sludge materials thought to be similar to those in INEL tanks. Additionally, video tape images of an in-tank washing process and instrument placement in an INEL tank were viewed in order to obtain a qualitative understanding of sludge erodibility.

Bamberger, Eyler, and Dodge (1993) conducted a brief review of sedimentation literature to determine values of the critical shear stress for erosion (τ_e), deposition (τ_d), and the erodibility constant (E). They found a very wide range of values for small (less than 100 μ m) particles. Most data are for sand and silt transport in moving surface water such as rivers and bays. Teeter (1988) measured critical shear stress for erosion of .0599 N/m² and an erodibility constant of 4.00x10⁻⁶ kg/m²-s for very fine silt (1 to 2 μ m in diameter). O'Brien et al. (1988) measured a much larger value of critical shear stress for erosion (3.58 N/m²) for a lightly packed layer of larger particulate material (approximately 70 μ m) and a significantly larger value of erodibility constant than Teeter's. Powell^(a) reports erodibility constants ranging from 0.15 to 147 kg/m²-s and critical shear stress for erosion ranging from 0.0072 to 1.47 N/m² for various simulated sludges. Powell's data were obtained by curve-fitting data from for effective cleaning radius during mobilization in scaled experiments.

Other studies provide a wide range of values for the critical shear stress for erosion for very small particles such as Dunn (1959), 0.058 - 0.24 N/m²; Smerdon and Beasley (1961),

(a) M. R. Powell. 1991. "Current Status of DST Sludge Mobilization Research". An Interim Draft Report to Westinghouse Hanford Company. Pacific Northwest Laboratory, Richland Washington.

0.0038 - 0.024 N/m²; Flaxman (1963), 0.11 - 0.72 N/m²; and Abdel and Rahmann (1964), 0.0072 - 0.043 N/m². Recently obtained unpublished data^(a) on erosion in rivers gives erosion and deposition parameters for various compositions of clay (less than 4 μm), silt (4 to 62 μm), and sand (62 - 200μm). These data give values of critical shear stress for erosion from 0.1 to 6.8 N/m², critical shear stress for deposition from 0.33 to 3.0 N/m², and erodibility constants from 0.00027 to 0.023 kg/m²-s. Critical shear stresses for some of the samples tested were unavailable because the samples yielded and eroded in bulk. Some of these samples had a similar particle size distribution as the INEL sludge.

An analytical method for estimating critical shear stress for erosion was developed by Shield (1936) and discussed by Vanoni (1975). A Shield diagram, which relates a dimensionless shear stress for initiation of particle motion with a boundary Reynolds number, can be used to estimate critical shear stress for erosion based on particle size, diameter and fluid properties. Based on this theory (not presented here), the critical shear stresses for erosion for the INEL sludge were estimated to be 0.24, 0.10, and 0.42N/m² for the largest (200 μm), most populous (70 μm), and smallest (13 μm) particles, respectively. Shield's theory does not take into account any cohesive effects which are characteristically present for very small particles. Therefore, the value of critical shear stress for erosion for the smallest particles is probably unrealistic.

Video images of the in-tank washing process and instrument placement in the INEL tanks seem to indicate that much of the sludge particulate is very light and easily suspendable. Slight motions seem to disturb the sludge, causing the fluid above the sludge to cloud. This cloud seems to persist (on the order of 10 to 20 minutes), indicating very light particulates. Given the very wide range of values in the literature for the sedimentation parameters, and the uncertainty in characterizing the INEL sludge, conservative estimations of parameter value ranges were made and are shown in Table 2.3. Also shown are the settling velocities and particle Reynolds numbers for the different particles calculated from Equation (2.10) and (2.11). Because the largest particles have a Reynolds number greater than 1, the Stokes settling relation does not hold. A correction to this relation was made according to the data of Rouse (1937).

Table 3.3 lists estimations of the erosion and deposition properties for the INEL waste sludge. Critical shear stresses for erosion are estimated to be in the range 0.01 to 1.0Pa (1Pa = 1N/m²) and erodibility constants are estimated to be 0.001 to 0.1kg/m²s. In the absence of better data, it is assumed that the critical shear stress for erosion and deposition are of equal value.

(a) Printed data obtained from Ray Krone, University of California at Berkeley, 9/93.

Table 2.3 Erosion and Deposition Properties Used for Analysis

Property	Largest Particles	Most Populous	Smallest Particles
Critical shear stress for erosion τ_e	0.01 - 1.0Pa	0.01 - 1.0Pa	0.01 - 1.0Pa
Critical shear stress for deposition τ_d	0.01 - 1.0Pa	0.01 - 1.0Pa	0.01 - 1.0Pa
erodibility constant E	.001 - 0.1kg/m ² s	.001 - 0.1kg/m ² s	.001 - 0.1kg/m ² s
Stokes settling velocity u_s	2.18 cm/s	.267 cm/s	.024 cm/s
Particle Reynolds number Re_s	3.82	.164	.0027
Corrected settling velocity	1.7 cm/s		

2.4 Factors Affecting Jet Mixing in INEL Tanks

In general, analyzing jet mixing pumps for mobilization and suspension of solids in tanks can be a complex undertaking. For the INEL tanks, there are a number a factors that increase the level of complexity and require focused attention. This section presents some issues that are thought to be most important in determining the feasibility of using jet mixing pumps for heel removal and solids suspension in INEL waste tanks.

2.4.1 Cooling Coils

The cooling coils and support structure located on the tank floors may create an impediment to sludge mobilization. Horizontal jets that are elevated above a tank floor will generally attach themselves to the floor at some distance away from the jet nozzle. This attachment creates high shear stress which acts to erode the sludge layer. It is uncertain what effect the cooling coils will have on this attachment process. The jet will lose momentum due to both viscous and form drag on the cooling coils. However, turbulent intensity should be increased due to vortex shedding in the wakes of the cooling coils-- thereby enhancing erosion. Additionally, the effect of the cooling coils would seem to be strongly dependent on the horizontal orientation of the jets because the cooling coils run predominantly East and West (see Figure 2.4). Cooling coils oriented North or South may have a smaller effect on the jets ability to erode the sludge.

2.4.2 Sludge Characterization

The success of using jet mixing pumps in the INEL tanks for sludge mobilization and suspension may be strongly dependent on the physical characteristics of the sludge material. If some

of the solids in the sludge are strongly cohesive, excessive pump horsepower requirements may prohibit a practical implementation of a mobilization system. Additionally, some solids may adhere to the tank floor. The physical properties of the solid particulates are important for several reasons. The density of the solids can greatly effect buoyant actions on the jet and large-scale circulation patterns. The rate at which particles settle out of suspension and accumulate on the tank floor will be dependent on their settling velocity, which is a function of both particle density and size.

2.4.3 Limitations on Mixing Pump Configuration and Operating Conditions

One of the current priorities of the High Level Waste Tank Replacement Project is to utilize existing riser penetrations to install mixing pump equipment. This priority is important for two reasons. First, the diameter of the risers puts a constraint on the size of pump that can be installed. In general, the physical size of a pump will be dependent on horsepower. For positive displacement pumps, the diameter of the pump will be dependent on horsepower. In order to overcome the pump diameter limitation, some manufactures are attempting to develop staged turbine pumps. These pumps utilize "stacked" compression stages to increase horsepower without increasing pump diameter. Consultations with pump manufactures indicated the largest pump that can realistically be installed in a 12 in. riser would require 150 horsepower. Because each pump drives two dual-opposed mixing jets, the maximum allowable jet hydraulic horsepower would be $75\eta_p$ where η_p is the pump efficiency. This upper limit on horsepower puts a constraint on the jet velocity and diameter since total pump power is given by

$$\dot{P}_0 = \frac{1}{\eta_p} \rho_j (u_0 d_0)^3 / d_0. \quad (2.16)$$

Equation (2.16) is true for all nozzle geometries so long as d_0 is taken as the square root of the nozzle cross-sectional area. Figure 2.8 shows an envelope of allowable jet velocities and nozzle diameters which will produce a total pump power less than or equal to 150 horsepower for an assumed pump efficiency of 50%. This efficiency is that of jet mixing pumps being considered for use in Hanford waste tanks.

The second reason the use of existing risers is important is due to their locations within the tanks. In an optimal mixing pump configuration, risers would be strategically located to minimize the number of risers (pumps) and maximize their mobilization capability. The existing risers in the INEL tanks do not appear to be in optimum locations. Therefore, pump operating conditions such as power, jet velocity, nozzle diameter, and rotation rate may need to be different for pumps located in different risers.

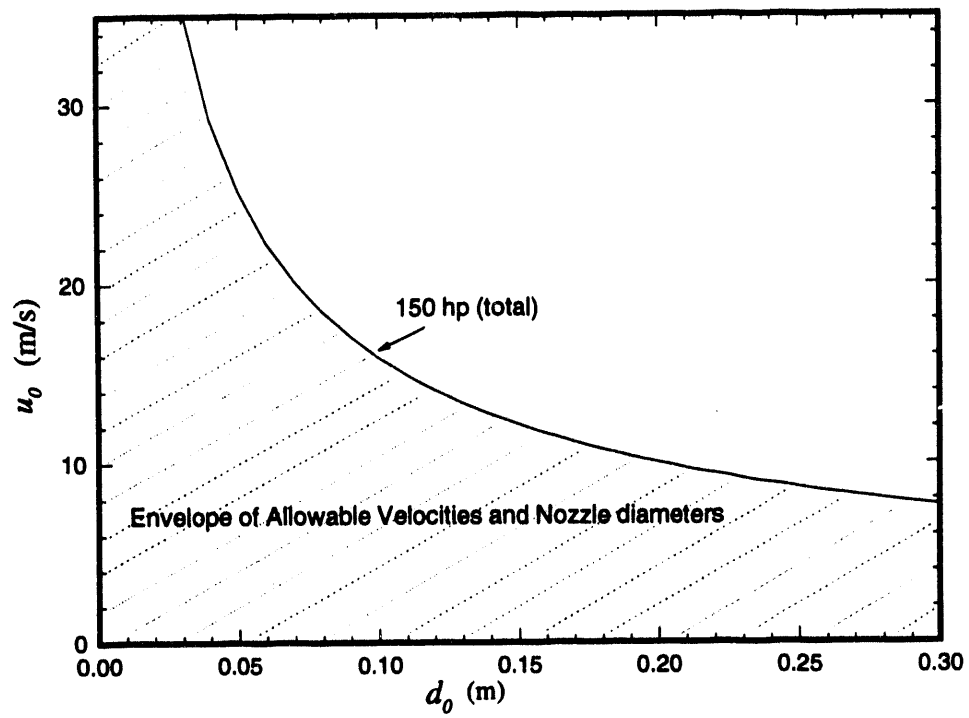


Figure 2.8 Envelope of Allowable Jet Velocities and Nozzle Diameters due to Maximum Pump Power Constraint

3.0 Computer Simulations of Mixing Jet Hydrodynamics

This section presents results of computer simulations of submerged liquid jets in INEL Tanks. Floor shear stress distributions and jet flow patterns were examined for a number of jet parameter conditions and tank configurations. These results will be combined with analytical erosion, deposition, and suspension models in Section 4 in order to make recommendations on suitable pump configurations and operating conditions. Section 3.1 states the objectives of computer modeling and describes the TEMPEST computer code, modeling approach, and limitations to the modeling task. Section 3.2 presents some code testing and validation results for basic jets and flow over cooling coils. These results are presented in order to establish the credibility of the more complex simulations and to identify modeling limitations. Section 3.3 presents the results of the hydrodynamic simulations.

3.1 Modeling Objectives and Approach

3.1.1 Objectives of Computer Modeling

The objective of computer modeling is to analyze the hydrodynamics of the mixing of turbulent jets in INEL Tanks in order to determine their propensity for mobilizing the sludge layer.

3.1.2 The TEMPEST Computer Code

Computer modeling of jet mixing in waste storage tanks is an on-going effort within several programs at the Pacific Northwest Laboratory (PNL). These efforts support a wide range of remediation and retrieval efforts at the Hanford site as well as other DOE sites. These include the Hanford Double Shell Tank Retrieval Project, the Waste Tank Safety Program, and the Oak Ridge National Laboratory (ORNL) Storage Tank Sludge Mobilization and Mixing Project. While each of these programs has special analysis needs, computer modeling of the fluid dynamics of mixing and solid/liquid transport are inherent to each. The modeling in progress at PNL uses the TEMPEST^(a) computer code (Trent and Eyster 1992).

TEMPEST is a three-dimensional, time-dependent, computational fluid dynamics analysis computer program that solves discrete equations for the conservation of mass, momentum, thermal energy, turbulence, and species transport. The code is well suited to model the turbulent, jet-induced mixing in waste storage tanks.

3.1.3 Modeling Approach and Limitations

Performing a parametric jet mixing study in tanks can be a complex task when the number of variables involved is large. Given the complexity of the INEL tank geometries, the uncertainty

(a) Transient, Energy, Momentum, and Pressure Equation Solution in Three-dimensions.

in sludge characteristics, and the absence of specified design configurations for pump locations, horsepower, etc., it is necessary to identify the most important aspects of problem and focus on understanding them so that usable results can be obtained. Limitations inherent with the modeling tool and computational speed put additional constraints on the modeling approach. Limitations associated with the TEMPEST computer program and computational speed relevant to this study are as follows:

- A Cartesian computational grid is required in order to accurately model the cooling coils and support structure. This grid prevents simulation of rotating jets and requires the jets to be oriented in one of the two principle coordinate directions. Rotating jets can be directly simulated by using a cylindrical coordinate system; however, the cooling coils cannot be accurately represented in this way.
- The TEMPEST computer program uses a solid, free-slip boundary condition to represent the free liquid surface. This boundary condition is thought to be correct so long as the free surface is very far from the jet. When the surface is close to the jet (as in the case of the heel) the solid boundary can effect the jet flow patterns.
- The solution time increment used by the TEMPEST program is severely limited when high-speed jets flow through small computational cells. Also, the computer time for one solution time increment is proportional to the total number of computational cells. Therefore, accurately modeling high speed jets in large tanks is a computationally intensive task. For typical jet mixing simulations in large tanks, about one hour of computer time is required for one second of simulation on an IBM 560 superworkstation (this machine is approximately 0.5 of Cray XMP speed). These computational speed limitations put constraints on resolution and simulation time.
- In order to accurately represent the geometric detail of individual cooling coils and support structures, a high level of resolution is required. Given the size of the INEL tanks and the number of structures present, the total number of computational cells (finite volumes of liquid or solid) would be prohibitive. Therefore, it is necessary to minimize the number of computational cells while preserving enough resolution to capture essential phenomena.

In light of the complexity of the physical system to be modeled and the limitations associated with the modeling tool and computational speed, the approach taken was to identify the key aspects of the hydrodynamic mixing processes and then perform parametric studies in order to understand their behavior. The following are the important elements of the modeling approach:

- Model a simple, pure-liquid jet located on the tank floor and compare results for velocity and floor shear stress with experimental data in order to validate the predictive capability of the TEMPEST code.
- Perform a numerical study to determine the minimum amount of resolution required to accurately model perpendicular flow over the cooling coils.
- Model a single, dual-opposed, jet above the cooling coils. This jet will be located at the tank center and have a fixed orientation perpendicular to the cooling coils (North on Figure 2.4). Perform a study to determine the minimum liquid depth which can be modeled with reasonable accuracy.
- Consider a non-rotating jet located at the tank center and oriented in the North, East and West directions. Perform a parametric study varying jet velocity and diameter and analyze floor shear stress distributions and flow patterns. These studies should reveal the fundamental effects that the cooling coils will have on jet attachment and erosion.
- Examine the effects of jet height above the tank floor.
- Examine the effects of varying liquid depth on floor shear stress and flow patterns.
- Model off-center jets by reducing the diameter of the tank.
- Examine the effects of particle laden jets which likely will result from sludge particulates being entrained in the pump inlet.

This approach to analyzing jet mixing in the INEL Tanks should provide fundamental insight into the feasibility of heel mobilization and suspension. It will also produce the required inputs for the analytic models used to examine mixing system requirements in Section 4.

3.2 Code Validation and Testing

In performing a numerical simulation of a complex fluid dynamic system, it is important to demonstrate that the computer program can accurately predict basic features of the flow. The TEMPEST computer program is regularly tested by comparing code predictions with analytical flow solutions or experimental data. Code assessment and validation results have been reported by Trent and Eyler (1991) and Meyer and Fort (1993). The most essential and basic fluid dynamic feature of the mixing process in the INEL tanks is the turbulent jet located near the floor. While no data is available for the unique geometry in the INEL tanks, basic jet data is available.

3.2.1 Free-Jet Simulations

A free-jet is a jet that is located far from any walls or other obstructions. A jet located above the floor, such as those considered for the INEL tanks, initially behaves like a free-jet. As the jet spreads, however, restricted entrainment due to the solid floor causes the jet to turn towards the floor and eventually attach. The TEMPEST program's ability to accurately model high-speed turbulent free-jets in large tanks has been extensively tested and reported by Trent and Michener (1993). They found that computed jet velocity decay agreed well with experimental data. They also determined that excellent results could be obtained with fairly coarse nodding resolution. The fact that TEMPEST accurately predicts turbulent free-jet behavior is not surprising in light of the $k - \epsilon$ turbulence model in TEMPEST. This model, which approximates true turbulence by using turbulent energy production and decay equations, utilizes empirical constants that have been "tuned" in order to match free-jet behavior. The model also accurately predicts other turbulent flows such as pipe and channel flows, and is the industry standard for simulation of turbulent flows.

3.2.2 Floor-Jet Simulations

A floor-jet refers to a jet that is located directly on a floor and flows horizontally as shown in Figure 3.1. Jets located above the floor behave like true floor-jets once they have attached to the floor. Therefore, the floor-jet serves as an excellent test problem to examine TEMPEST's ability to predict off-floor jet behavior. Velocity and floor shear stress data for turbulent floor jets have been reported by Rajaratman (1976). Figure 3.2 shows a comparison between TEMPEST predictions and experimental data for a turbulent floor-jet. The velocities shown are the maximum, or peak velocity, normalized by the initial jet velocity and plotted as a function of distance (normalized by jet diameter) from the nozzle. Shear stresses are normalized by initial jet momentum. The TEMPEST program derives turbulent shear stress from computed turbulent kinetic energy. The results shown for the experimental data are mean curve fits.



Figure 3.1 Side View of Geometry for a Three-dimensional Turbulent Floor Jet

Figure 3.2 shows that the TEMPEST program over-predicts both maximum velocity and floor shear stress. At a distance of 60 nozzle diameters down stream, the maximum velocity is over-predicted by 75% and the floor shear stress is over-predicted by 50%. Extensive testing and consultations were undertaken in order to improve these results. It was finally determined that the results are consistent with assumptions implicit to the $k - \epsilon$ turbulence model. One of the fundamental assumptions in the $k - \epsilon$ turbulence model is that there is no preferential direction locally for small turbulent scales. This is to say the turbulence is locally isotropic. Experimental observations of turbulent floor-jets have shown that the jets spread faster in the horizontal plane (the plane of the floor) than in the vertical plane. This is contrary to free-jets which spread uniformly in all planes. Evidently, the characteristics of small turbulent structures in the horizontal plane of a floor-jet are different than those in the vertical plane. Developing turbulence models which account for nonisotropic effects such as these is the subject of current research in the computational fluid dynamics community and at PNL. Presently, there is no robust model available that has been successfully tested.

The jet growth rates (spreading angle) predicted by TEMPEST are also found to differ from the experimental data (not shown here). Horizontal growth is under predicted by a factor of 2 to 3 and vertical growth is over predicted by about a factor of 2. These results explain the over-prediction in maximum velocity. Because the horizontal jet growth is limited due to the turbulence model, the maximum velocity must increase in order to conserve momentum. Therefore, the total momentum for the two jets would be similar. Floor shear stress along the axis of the jet is over-predicted by TEMPEST due to the over-prediction of jet velocity.

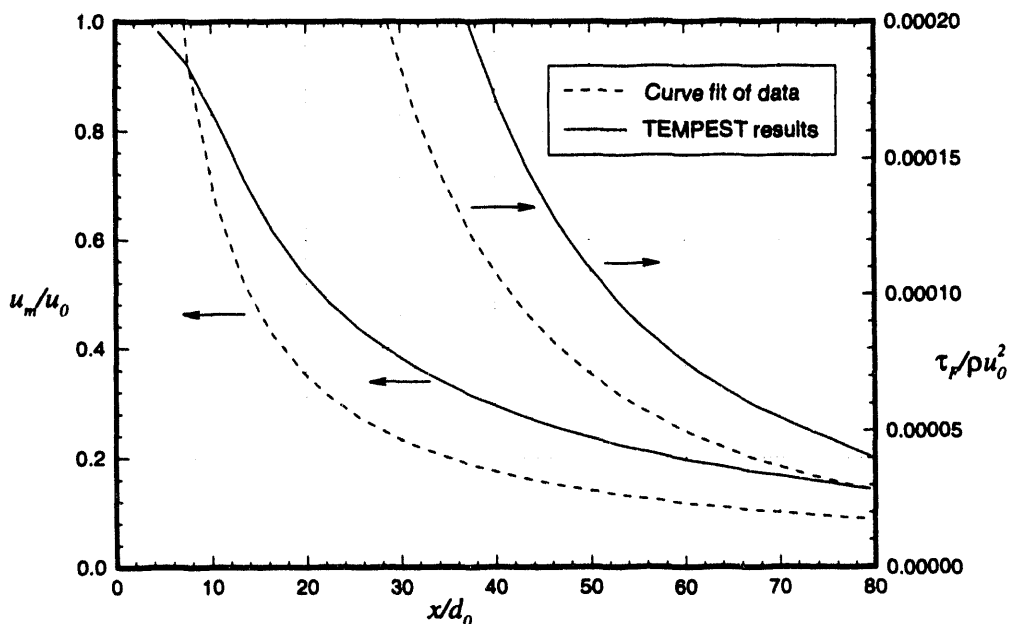


Figure 3.2 Comparison of Maximum Velocity Decay and Floor Shear Stress for a Turbulent Floor Jet

Because the TEMPEST program accurately predicts free-jet behavior, but over estimates floor-jet velocity and shear stress, it is reasonable to assume that TEMPEST's ability to predict near-floor jets would fall somewhere between these two limiting cases. Furthermore, the presence of cooling coils adds an additional complexity to the flow. If the limitations of the isotropic turbulence model affect off-floor jets over cooling coils in the same way they affect the floor-jet simulations, then the under-predicted horizontal spread angle is conservative because the width of the effective cleaning area would be reduced. The over-prediction of floor shear stress, however, is not conservative because erosion rates will be artificially high. Therefore, over-predicted floor shear stresses will be accounted for when considering erosion models. In this way, potential error due to turbulence model limitations will be minimized.

3.2.3 Modeling Flow over Cooling Coils

A study was performed to examine the noding resolution required in order to accurately model the cooling coil blockages. Accurate modeling of these features is required in order to get reasonable predictions of shear stress distributions on the floor below the cooling coils. Noding resolution requirements are dependent on the magnitude of velocity gradients. The largest velocity gradients are thought to occur near the cooling coils when the jet is flowing perpendicular to them. Each cooling coil section, formed by two cooling coils separated by a spacer as shown in Figure 2.5, will shed vortices in their wake. These turbulent actions will interact and create local flow patterns which produce shear on the tank floor. The cross section of a cooling coil pair is only about 2 in. high by 5 in. wide. If these structures were highly resolved, the total number of computational nodes in the tank simulation domain would be prohibitively large.

In order to examine noding resolution, a two-dimensional, uniform flow above representative cooling coil sections was modeled. The node geometry is shown in Figure 3.3 (the jet flows towards the North). Each cooling coil section is modeled as a 2 in. by 5 in. rectangle, located 5 in. above the floor, and separated by 13 in. The boldest lines represent a coarse noding base test case. For this base case, each cooling coil section is represented by a single node. There are 2 nodes separating each cooling coil section and 3 nodes between the section and the floor. The finer lines represent higher degrees of vertical and horizontal resolution. Computed floor shear stress for the different test cases is shown in Figure 3.4. The oscillations in the floor shear stress curves are due to turbulent eddies behind each cooling coil section. Shear stress peaks occur approximately at the leading edge of a cooling coil section, and the minima occur between sections. The base test case produced the lowest floor shear stress of all the cases. As resolution was increased, shear stress increased with horizontal resolution having the greatest effect. Above 2X horizontal resolution, the shear stress curves begin to converge. The case with 2X horizontal and vertical resolution lies below the converging curves, but captures both the oscillations and the mean spatial increase. This case was chosen as an acceptable noding because it produces conservative floor shear stresses while keeping the total number of computational cells within reasonable limits.

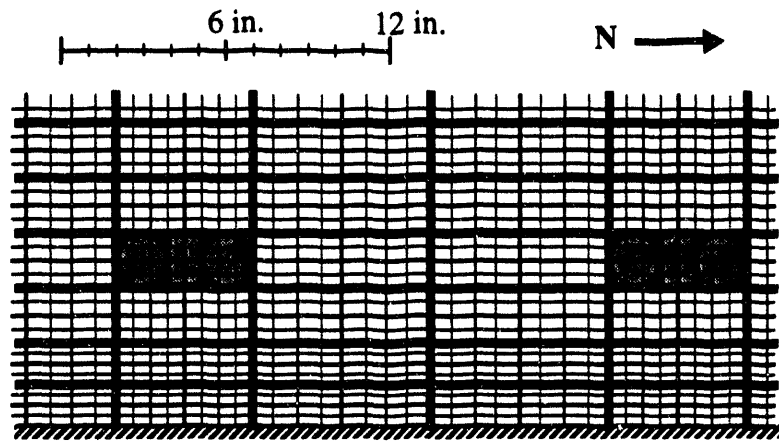


Figure 3.3 Geometry for 2-D Cooling Coil Noding Resolution Study

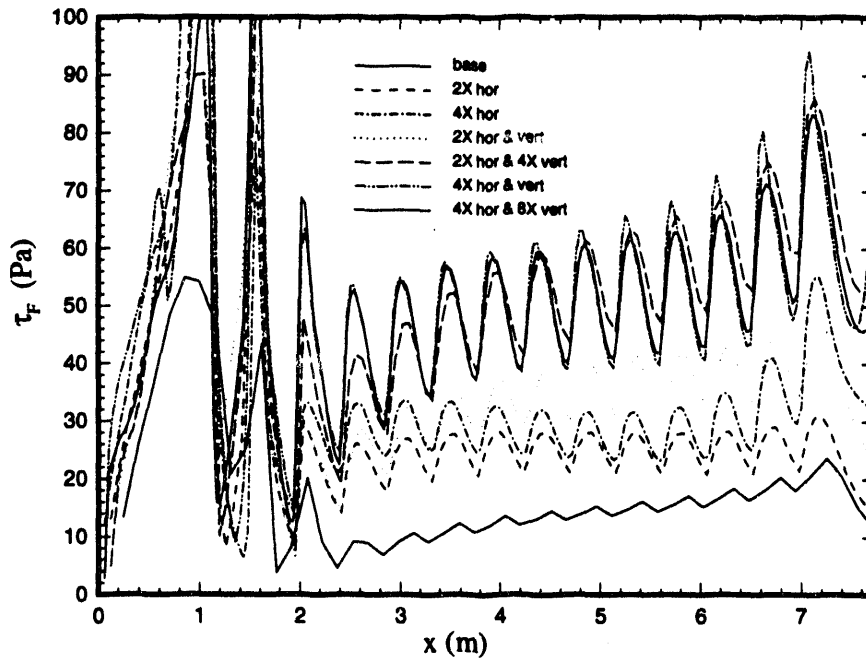


Figure 3.4 Computed Floor Shear Stress for 2-D Noding Resolution Study

3.2.4 Shallow Liquid Tests

A series of tests were performed to determine the minimum acceptable liquid level that could be accurately modeled using the free slip solid boundary at the liquid surface. The free slip boundary, while producing no drag on the simulated fluid, forces fluid elements impinging normal to the surface to turn and flow in the horizontal plane. Bubbling and churning effects, which would be present in an actual flow, are not reproduced by the model. Additionally, the free slip boundary will modify pressure forces which, in turn, may affect the flow throughout the tank. Generally, if fluid velocities near the surface are small, the effect of the free slip boundary will be negligible. The question of determining the minimum liquid level that can accurately be modeled is difficult because the effects of the free slip boundary are implicit in simulated results. It is possible, however, to determine the liquid level above which surface effects are unimportant.

Three tests were devised to estimate an acceptable minimum liquid level. The first test examined the vertical flow component near the tank wall. This flow pattern is due to jet impingement on the wall. By considering the dynamic pressure of upward flowing fluid elements, the height to which a fluid element would ascend (if the free slip boundary were not present) can be estimated with a simple conservation of energy argument. If this height is less than the height of the liquid, then surface effects may not be important. The second, more qualitative test, examines the horizontal component of flow at the free slip boundary. Generally, when a jet attaches to the floor of a tank, horizontal velocities near the surface will be small. If the fluid surface is located just above the jet nozzle, however, the jet can break the surface. The final test examined the effect of fluid height on shear stress distributions at the floor.

A 4 in. jet was modeled at the tank center located 11 in. above the floor. Jet velocities ranged from 5 m/s (16.4 ft/s) to 20 m/s (65.6 ft/s) and liquid depths ranged from 0.46 m (18 in.) to approximately 3 m (10 ft). Test cases with liquid levels above 1 m showed floor shear stress to be virtually unaffected by liquid level changes. Dynamic pressures near the wall and horizontal velocities near the surface were found to be quite small. For fluid depths less than 60 cm (2 ft), velocities near the surface approached maximum jet velocities. Also, floor shear stress increased considerably. Based on these results, a minimum liquid level of 91 cm (3 ft) was chosen.

3.3 Numerical Simulations

This Section presents results from the numerical simulations of submerged jets in INEL tanks. The TEMPEST model is described first, followed by a description of the various test cases. Detailed results are then presented.

3.3.1 The TEMPEST Model

The INEL tank geometry was modeled using a Cartesian (rectangular) computational grid. This allowed accurate modeling of the cooling coil structures and permitted jets to be oriented in both the North and East (or, equivalently, South and West) directions. A representation of the computational domain (for a jet oriented to the North) is shown in Figure 3.5. The symmetric geometry of centrally located, dual-opposed jets allowed the use of 1/4 segment of symmetry computational domains with free-slip boundaries along the East (jet axis) and South. Due to the Cartesian computational grid, curvature of the tank walls could not be modeled. Tests were performed to examine the effects of approximating 1/4 of a circular tank with the rectangular segment. These tests indicated that jet flow detail and floor shear stress distributions were virtually unaffected for two reasons: First, the curvature of the tank wall at the location of jet impingement is insufficient to affect the flow patterns in the vicinity of the jet. Secondly, the jet structure was found to be insensitive to the location or curvature of the tank boundary to the West, because flow velocities in this region were very small.

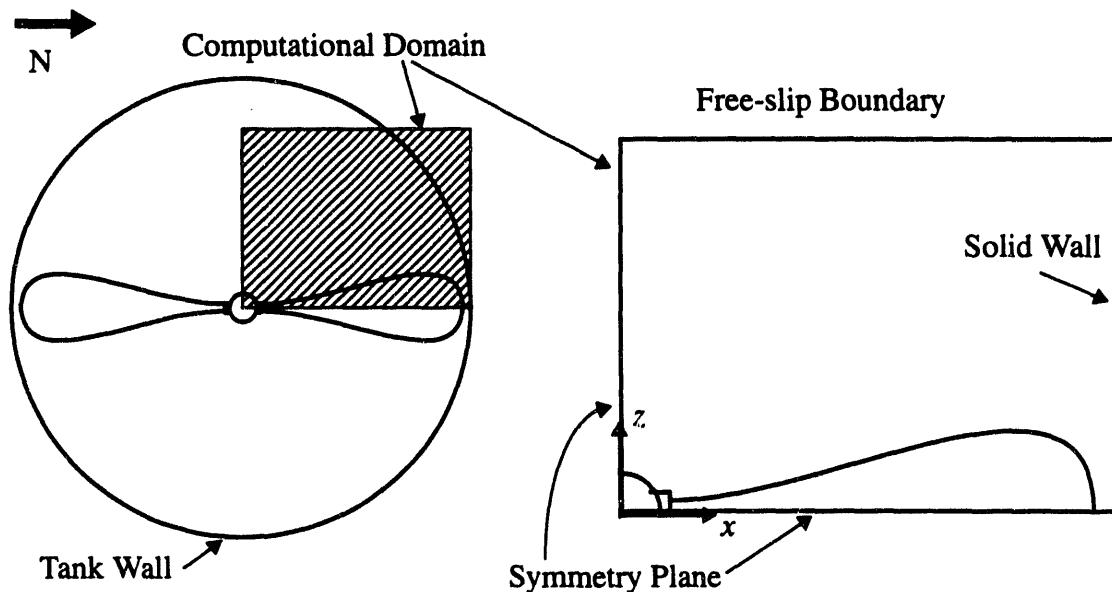


Figure 3.5 Rectangular Computational Grid Representation

A 1/4 segment of symmetry model of the jet mixing pump is shown in Figure 3.6. The riser column, jet nozzle, and jet inlet were all modeled as rectangular geometries. For the majority of the simulations, the jet nozzle was located 28 cm (11 in.) above the floor with the pump inlet 20 cm (8 in.) above the floor, allowing 2.5 cm (1 in.) between the top of the cooling coils and the inlet. Representing a round jet nozzle as a square was not considered to be a problem because jet behavior downstream of the nozzle is known to be independent of nozzle geometry.

The cooling coils were modeled as described in Section 3.2.3. Variable computational cell spacing was used to minimize the total number of cells required, while maintaining good resolution in the vicinity of the jet and floor. Most simulations required approximately 100 computational cells in the flow-wise direction, 20 to 30 cells in the vertical (depending on fluid height simulated), and 20 computational cells normal to the jet. Simulations were carried out until jet flow patterns reached steady state. Flow velocities continued to change far from the jet; however, these changes did not effect the basic jet flow features. Steady jet flows were obtained within approximately 25 s to 60 s depending on jet velocity. Approximately 2 to 4 days of computer time was required for each simulation.

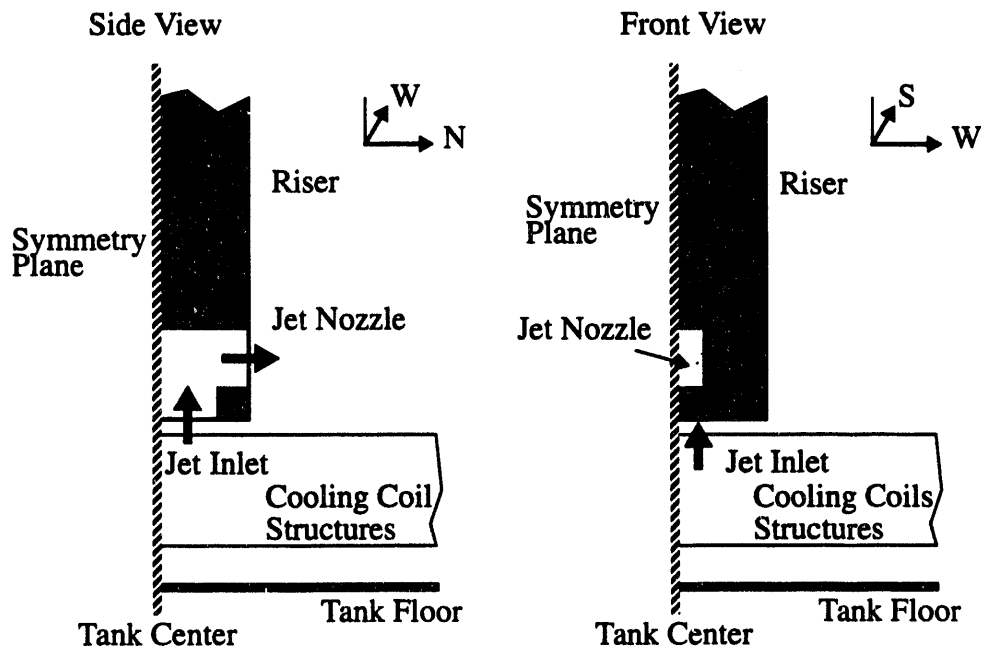


Figure 3.6 Detail of Pump Nozzle and Inlet Model

3.3.2 Test Cases

Table 3.1 describes the parameter values and configurations of the hydrodynamic simulations performed. The majority of the simulations were performed for jets oriented perpendicular to the cooling coils (North) because this orientation seemed to pose the greatest challenge to successful mixing. Nozzle diameters from 5 cm (2 in.) to 20 cm (8 in.) and jet velocities from 6.9 m/s to 31.4 m/s (22 ft/s to 103 ft/s) were considered. These corresponded to total hydraulic jet horsepower ratings of 12.5 hp to 150 hp. The majority of the cases had jet horse powers of 25 hp to 75 hp; however, the lower and higher values were added in order to demonstrate some particular power scaling trends.

Table 3.1 Test Case Parameters

Test Case	Nozzle Diameter d_0 (cm)	Jet Velocity u_0 (m/s)	Discharge Parameter $u_0 d_0$ (m ² /s)	Hydraulic Horsepower $\rho_j u_0^3 d_0^2 / 746$	Fluid Depth h_f (cm)	Comments
N150A	10.2	15.7	1.59	75	91.4	Perpendicular to cooling coils
N150B	5.1	24.9	1.27	75	91.4	Perpendicular to cooling coils
N150C	15.2	12.0	1.83	75	91.4	Perpendicular to cooling coils
N150D	20.3	9.89	2.01	75	91.4	Perpendicular to cooling coils
N300A	5.1	31.4	1.59	150	91.4	Perpendicular to cooling coils
N100A	15.2	10.5	1.59	50	91.4	Perpendicular to cooling coils
N075A	20.3	7.85	1.59	37.5	91.4	Perpendicular to cooling coils
N100A	5.1	21.8	1.11	50	91.4	Perpendicular to cooling coils
N100B	10.2	13.72	1.39	50	91.4	Perpendicular to cooling coils
N100C	20.3	8.64	1.76	50	91.4	Perpendicular to cooling coils
N050A	5.1	17.3	.878	25	91.4	Perpendicular to cooling coils
N050B	10.2	10.9	1.11	25	91.4	Perpendicular to cooling coils
N050C	20.3	6.86	1.39	25	91.4	Perpendicular to cooling coils
N300B	20.3	12.46	2.53	150	91.4	Perpendicular to cooling coils
N025A	5.1	13.7	.697	12.5	91.4	Perpendicular to cooling coils
T150A	10.2	15.7	1.59	75	91.4	No cooling coils
N150E	10.2	15.7	1.59	75	91.4	Perpendicular to cooling coils
N150F	10.2	15.7	1.59	75	61.0	Perpendicular to cooling coils
N150G	10.2	15.7	1.59	75	183.	Perpendicular to cooling coils
N150H	10.2	15.7	1.59	75	305.	Perpendicular to cooling coils
N150I	10.2	15.7	1.59	75	640.	Perpendicular to cooling coils
N050D	10.2	10.9	1.11	25	61.0	Perpendicular to cooling coils
N050F	10.2	10.9	1.11	25	183.	Perpendicular to cooling coils
N050G	10.2	10.9	1.11	25	305.	Perpendicular to cooling coils

Table 3.1 Test Case Parameters (cont.)

Test Case	Nozzle Diameter d_0 (cm)	Jet Velocity u_0 (m/s)	Discharge Parameter $u_0 d_0$ (m ² /s)	Hydraulic Horsepower $\rho_j u_0^3 d_0^2 / 746$	Fluid Depth h_f (cm)	Comments
N050H	10.2	10.9	1.11	25	640.	Perpendicular to cooling coils
E150A	10.2	15.7	1.59	75	91.4	Parallel to cooling coils (East)
E150B	10.2	15.7	1.59	75	305	Parallel to cooling coils (East)
E150C	10.2	15.7	1.59	75	640.	Parallel to cooling coils (East)
W150A	10.2	15.7	1.59	75	91.4	Parallel to cooling coils (West)
W150B	10.2	15.7	1.59	75	305	Parallel to cooling coils (West)
W150C	10.2	15.7	1.59	75	640	Parallel to cooling coils (West)
E050A	10.2	10.9	1.11	25	91.4	Parallel to cooling coils (East)
E050B	10.2	10.9	1.11	25	305	Parallel to cooling coils (East)
E050C	10.2	10.9	1.11	25	640	Parallel to cooling coils (East)
W050A	10.2	10.9	1.11	25	91.4	Parallel to cooling coils (West)
W050B	10.2	10.9	1.11	25	305	Parallel to cooling coils (West)
W050C	10.2	10.9	1.11	25	640	Parallel to cooling coils (West)
N150J	10.2	15.7	1.59	75	91.4	Perpendicular, nozzle 36cm above floor
N150K	10.2	15.7	1.59	75	91.4	Perpendicular, nozzle 24cm above floor
N150L	10.2	15.7	1.59	75	91.4	Perpendicular, nozzle under cooling coils
N150M	10.2	15.7	1.59	75	91.4	Perpendicular, off-center jet
N150N	10.2	15.7	1.59	75	305	Perpendicular, off-center jet
N050I	10.2	10.9	1.11	25	91.4	Perpendicular, off-center jet
N050J	10.2	10.9	1.11	25	305	Perpendicular, off-center jet
E150D	10.2	15.7	1.59	75	91.4	Parallel, off-center jet
E150E	10.2	15.7	1.59	75	305	Parallel, off-center jet
P050A	10.2	10.9	1.11	25	91.4	Parallel, particle-laden
P050B	10.2	10.9	1.11	25	305	Parallel, particle-laden
P150A	10.2	15.7	1.59	75	91.4	Parallel, particle-laden
P150B	10.2	15.7	1.59	75	305	Parallel, particle-laden
P050C	10.2	10.9	1.11	25	305	Parallel, particle-laden, off-center jet
P150C	10.2	15.7	1.59	75	305	Parallel, particle-laden, off-center jet

3.3.3 Centered Jets Oriented Perpendicular to Cooling Coils

In order to understand the effects of the cooling coils on jets flowing perpendicular to cooling coils (North), comparisons were made with jet flows in tanks without cooling coils. Figure 3.7 shows a comparison of velocity vectors in the vertical plane of the jet center-line for test cases N150A and T150A. These cases are for 75 hp jets with 10 cm nozzles located 28 cm above the floor. Cooling coils are absent in the latter case. The locations of the cooling coils (not shown in the plot) correspond to the regions of zero velocity seen near the floor. Several general effects of the cooling coils are demonstrated by these comparisons. First, the cooling coils appear to prevent the jet from attaching to the floor. Velocities near the floor are reduced considerably. Recirculating eddies are found between the cooling coils and the floor. These are barely visible in the plots due to reduced resolution. The peak jet velocity far from the nozzle is also reduced, implying a loss of jet momentum due to the cooling coils. Another significant difference is the flow pattern near the tank wall. In the absence of cooling coils, the jet impinges on the wall and turns upward. For the case with cooling coils, the jet impinges on the wall and then turns downward, forming a recirculation near the wall. This recirculating region is shown in Figure 3.8.

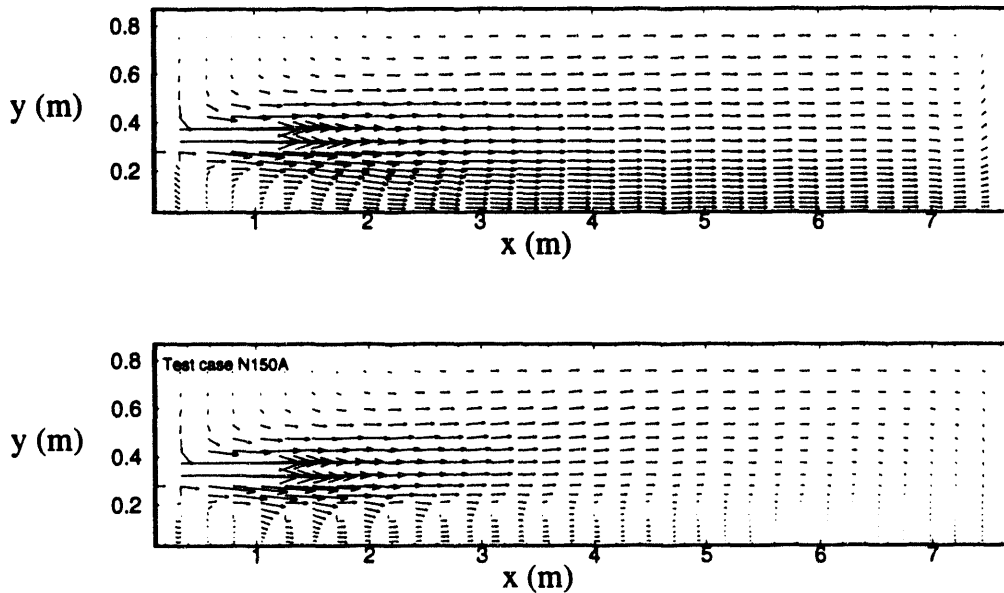


Figure 3.7 Velocity Vectors for Tank Without Cooling Coils (T150A) (top) and Tank With Jet oriented Perpendicular to Cooling Coils (N150A) (bottom)

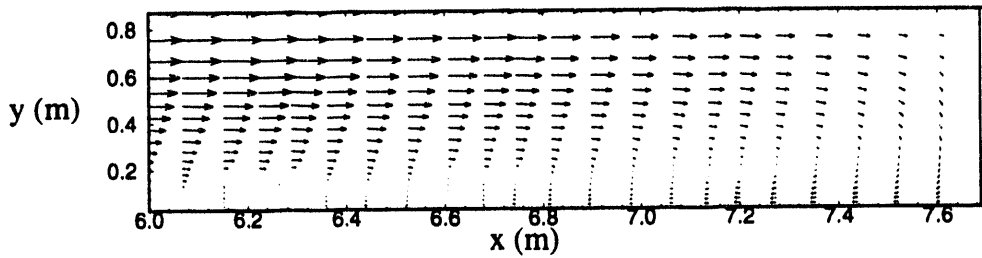


Figure 3.8 Recirculating Flow Near Tank Wall Due to Cooling Coils

Figure 3.9 shows a comparison of floor shear stress along the jet center-line for test cases T150A and N150A. A significant shear stress reduction occurs for the case with cooling coils. Near the tank wall, floor shear stress is reduced by about a factor of 30. The region of higher shear stress directly under the pump inlet (not shown) is due to entrained fluid. The shear stress is low just in front of the jet, due to a stagnation point dividing flow into the inlet and the jet flow. The cooling coils have a periodic effect on the floor shear stress distribution. This is caused by the eddy-like flow patterns behind each cooling coil. Figure 3.10 shows contour plots of the floor shear stress distributions for the two cases. For the case without cooling coils, the shear stress decreases near the tank wall. This is due to the jet slowing as it impinges on the wall. Shear stresses at the wall for the case with cooling coils increase, however. This is attributed to the fact that once the jet begins to turn and flow parallel with the cooling coils, it is no longer hindered from attaching itself to the floor. The velocity in the West and East directions (z -direction in Figure 3.10) is larger than the axial velocity (x -direction).

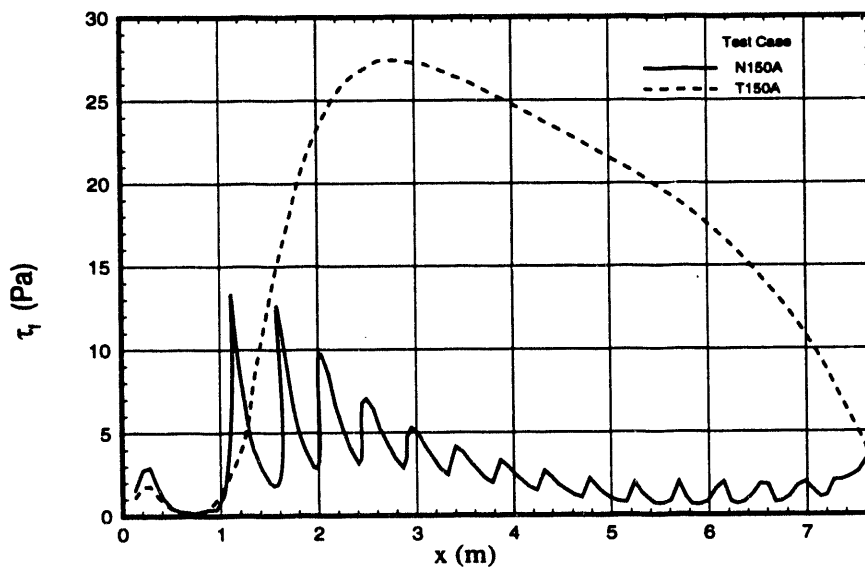


Figure 3.9 Comparison of Jet Center-line Floor Shear Stress for Tank Without Cooling Coils (T150A) and Tank with Jet Oriented Perpendicular to Cooling Coils (N150A)

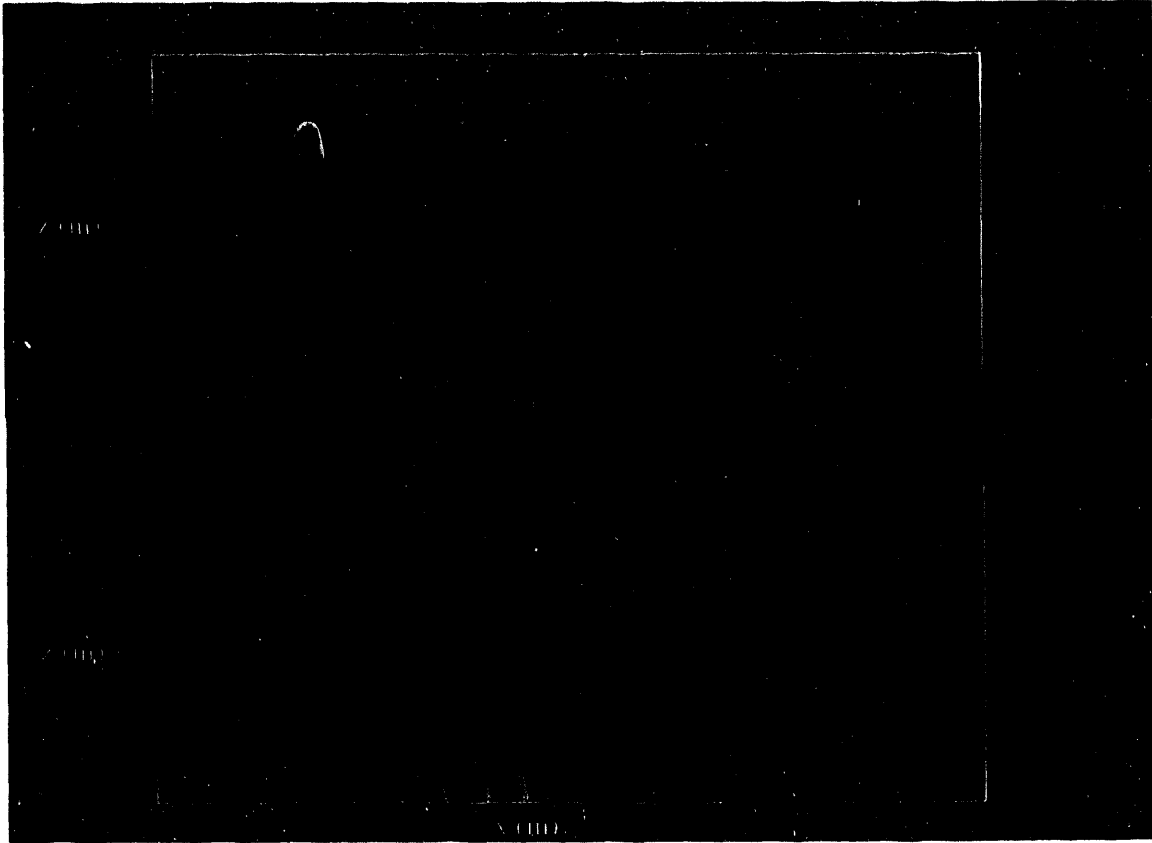


Figure 3.10 Floor Shear Stress Contours for (a) Tank Without Cooling Coils (T150A) and (b) Tank With Jet Perpendicular to Cooling Coils (N150A)

The effects of jet height above the floor was examined by simulating jets at three different locations above the cooling coils and one by simulating the jet nozzle underneath the cooling coils. Figure 3.11 shows floor shear stress along the jet center-line for test cases N150J, N150A, and N150K which have nozzles located 36 cm, 28 cm, and 24 cm above the floor respectively. Shear stress decreases with increasing jet height near the tank center. This seems to be due to the fact that the jet has to travel farther before it reaches the floor. The opposite trend occurs near the tank wall where shear stress increases with increasing jet height. Because the jet is further above the cooling coils, there is initially less momentum loss due to interactions with the cooling coils. The jet persists with higher velocity downstream and thereby causes greater shear on the floor. Figure 3.12 shows contours of floor shear stress for a jet located underneath the cooling coils (test case N150L). For this geometry, the inlet is located on the riser above the cooling coils. Floor shear stress is increased drastically in the region from the tank center to about half-way to the wall. Closer to the wall, however, the jet is dissipated and shear stresses are reduced. This configuration is not considered practical for INEL tanks due to uncertainty in precise riser locations relative to the cooling coils. Jets located 28 cm above the floor will be used for the remainder of the simulation, keeping in mind that shear stress may be increased by increasing the jet height.

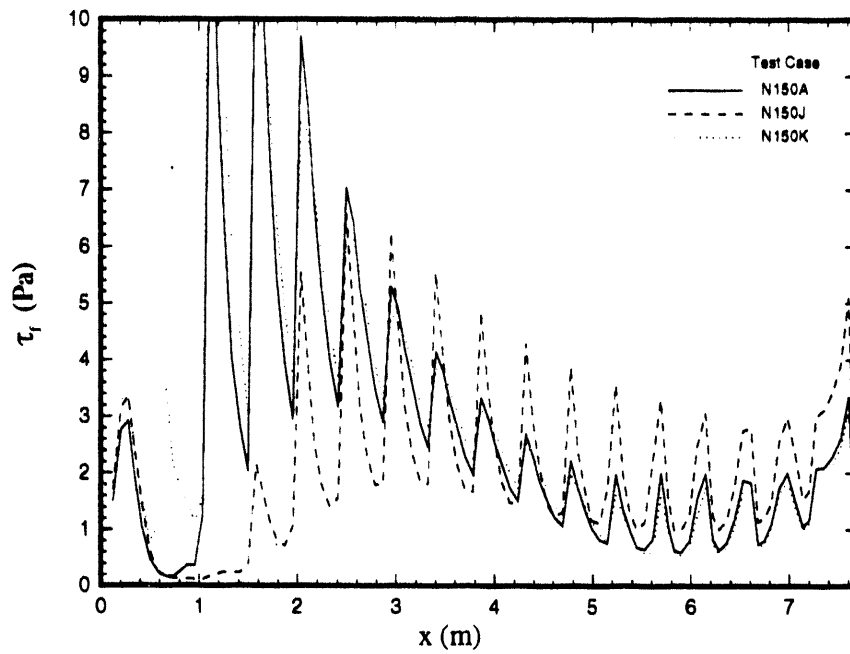


Figure 3.11 Effect of Jet Height Above Cooling Coils on Floor Shear Stress

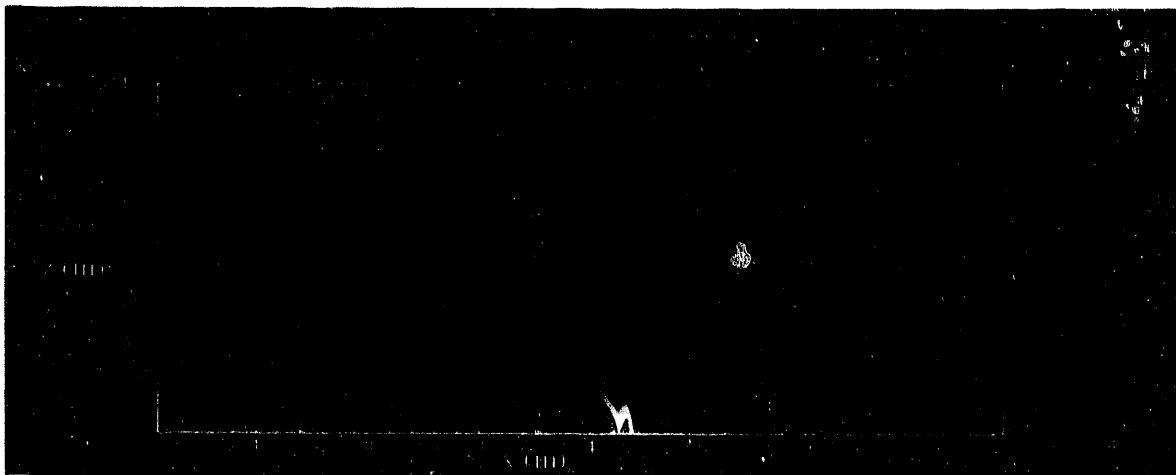


Figure 3.12 Floor Shear Stress for a Jet Located Underneath Cooling Coils

Figure 3.13 shows floor shear stress along jet center-line for test cases N150A through N025A. These test cases all have jets oriented perpendicular to the cooling coils and have a fluid depth of 91 cm (3 ft). Jet velocities are varied from 6.9 m/s to 31.4 m/s and nozzle diameters range from 5.1 cm to 20.3 cm corresponding to total hydraulic horsepowers from 12.5 hp to 150 hp. Variations in the jet velocity and nozzle diameter are seen to have considerable effect on the floor shear stress. On careful examination of Figure 3.13, it is evident that the value of shear stress at some axial location is not proportional to horsepower. In an attempt to relate floor shear stress to jet nozzle parameters, the scaling relationship given by Equation (2.12) was applied to the floor stress data. Figure 3.14 shows the quantity $\tau_f / \rho_j (u_0 d_0)^2$ plotted along the jet center-line. Near the tank wall, all the curves are seen to collapse onto one. This result demonstrates that jet horsepower is not the critical parameter affecting floor shear stress. Rather, the shear stress is proportional to the jet momentum, $\rho_j (u_0 d_0)^2$. Minimum shear stress near the tank wall is given by $\tau_f = 0.00019 \rho_j (u_0 d_0)^2 \pm 10\%$. This relationship will be useful in the analytic model for erosion and deposition of solids discussed in Section 4.

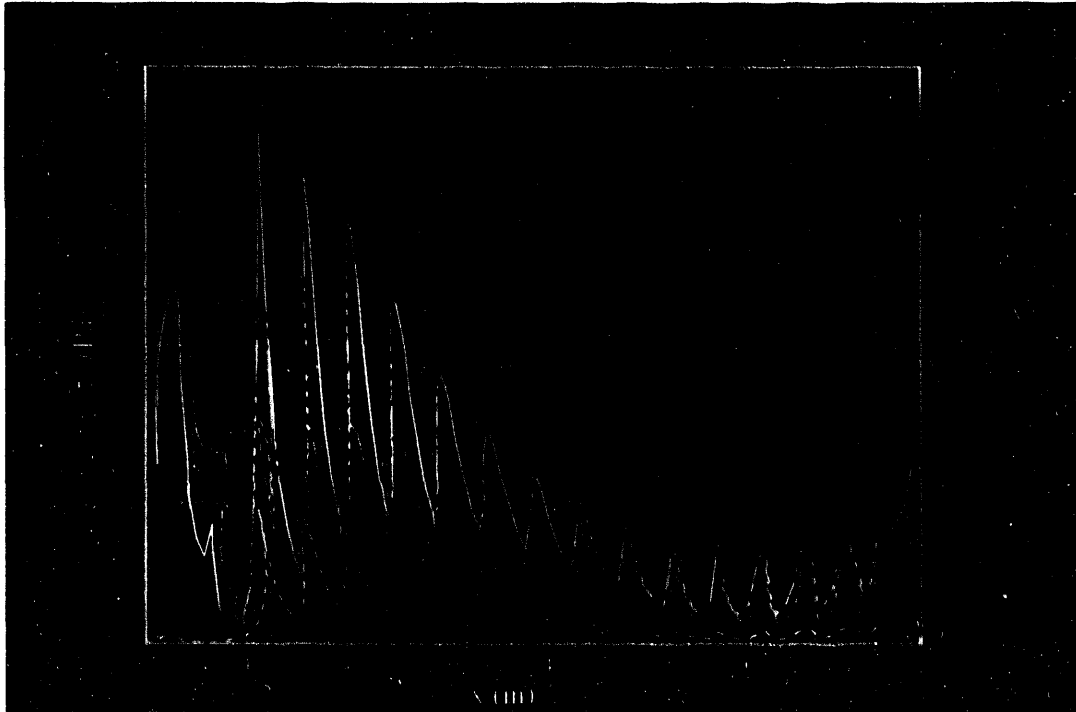


Figure 3.13 Floor Shear Stress Along Jet Center-line For Jets Oriented Perpendicular to Cooling Coils with Various Operating Conditions

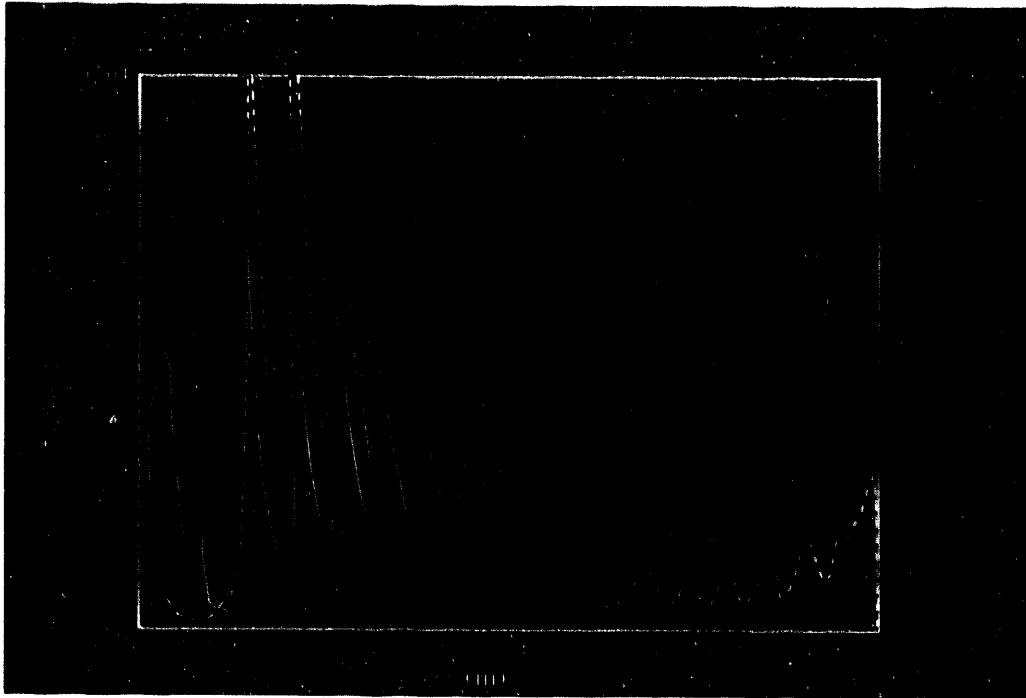


Figure 3.14 Correlation of Floor Shear Stress Along Jet Center-line with Nozzle Discharge Parameter $u_0 d_0$

Because the center-line floor shear stress scales nicely with jet momentum, it is reasonable to see if the same scaling holds for off-axis floor shear stress. Figure 3.15 shows a line of constant $\tau_f / \rho_j (u_0 d_0)^2$ plotted for test cases N150A through N025A. Near the pump, there is much scatter in the contours; however, far from the pump the lines nearly converge. The slight variation in the contours seems to be primarily due to nozzle diameter. Lines of constant nondimensional floor shear stress for small nozzles are further from the jet center-line than ones for large nozzles. This is consistent with the fact that smaller diameter jets begin spreading sooner than large diameter ones.

Figure 3.16 shows the radial (off-center) distribution of nondimensional floor shear stress for test cases N150A - N025A. The curves are for a plane normal to the jet at an axial location $x = 4.3$ m from the tank center. The shear stress for each of the test cases approaches zero at a transverse distance $z = 1$ m. For each curve, the transverse location where the shear stress has a value equal to 1/2 its center-line (maximum) value is approximately $z \approx 0.5$ m. The jet spread angle based on the half-maximum floor shear is approximately 13° . The spread angle based on near zero floor shear is 26° .

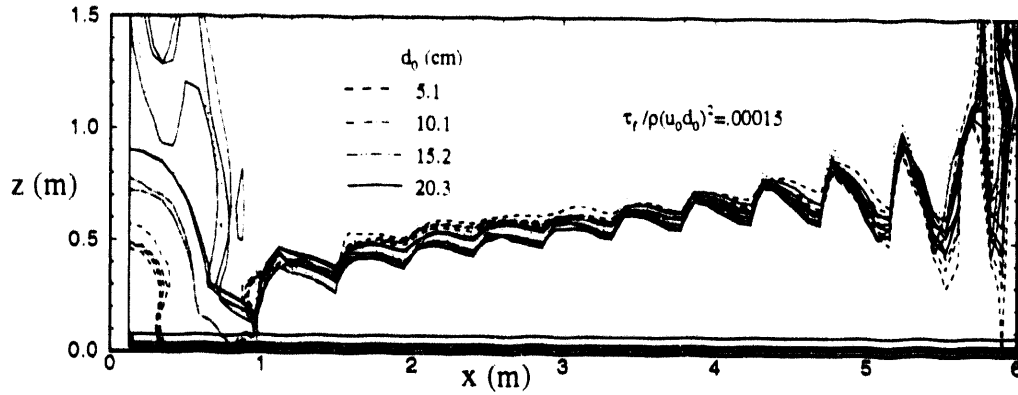


Figure 3.15 Off-Center Nondimensional Floor Shear Stress for Test Cases N150A Through N025A

The effects of fluid depth on nondimensional floor shear are shown in Figure 3.17. Fluid depths from 91 cm (3 ft) to 640 cm (21 ft) were considered for 25 hp and 75 hp jets. No effects of fluid height are observed near the center of the tank. However, close to the wall shear stress is reduced due to increasing fluid height. Floor shear appears to be independent of liquid levels for fluid heights greater than 183 cm (6 ft). The minimum value of nondimensional floor shear stress for fluid heights of 183 cm and above is $\tau_f = 0.00013\rho_j(u_0 d_0)^2$, corresponding to a 30% reduction below the 91 cm fluid depth cases discussed previously.

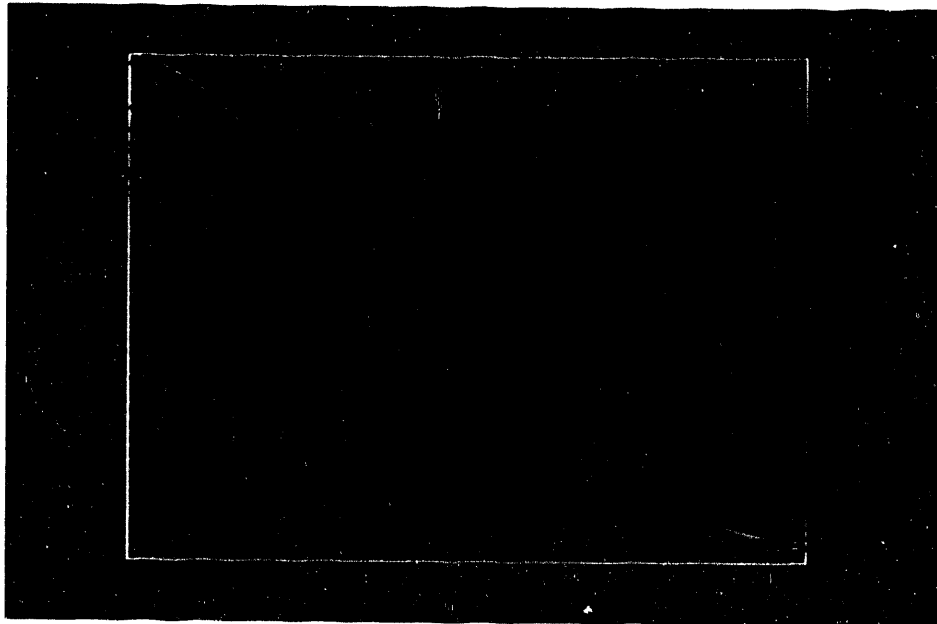


Figure 3.16 Transverse Variation of Nondimensional Floor Shear Stress at $x = 4.3\text{m}$ for Test Cases N150A Through N025A

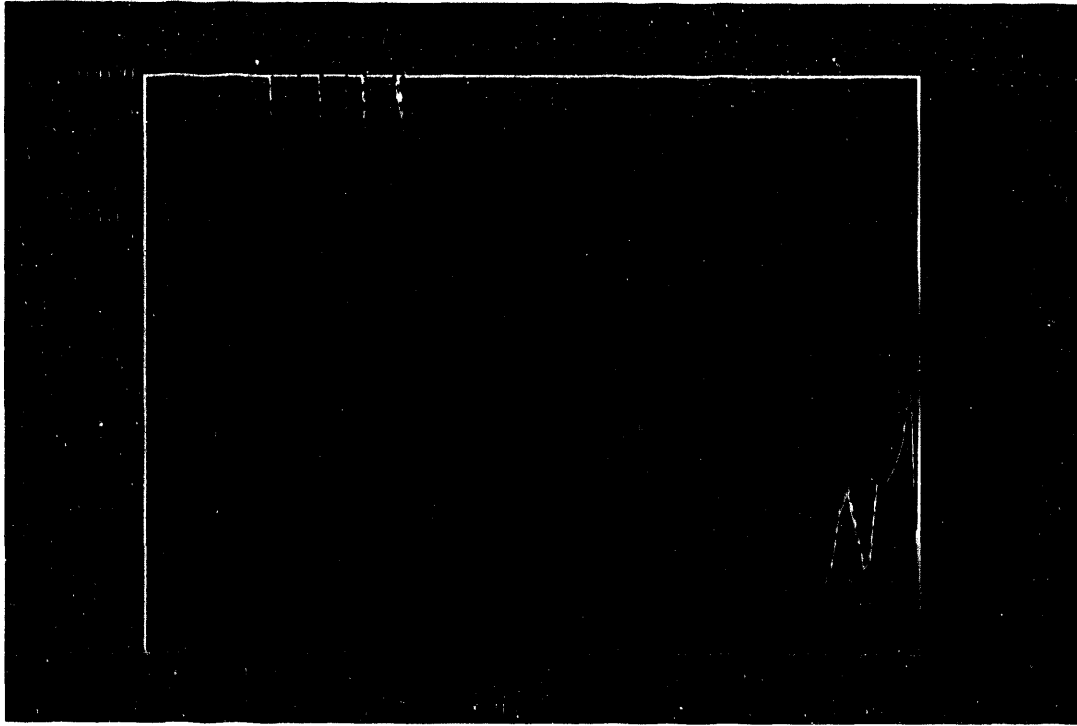


Figure 3.17 Effect of Liquid Depth on Center-Line Floor Shear Stress

The flow patterns and velocity magnitudes near the tank wall are important in understanding the jets ability to transport eroded solids off the tank floor. In order to understand how jet operating parameters effect velocities near the wall, a correlation similar to the one for floor shear stress was attempted. Figure 3.18 shows contours of vertical and horizontal velocity near the tank wall for test cases N150A through N025A. By normalizing the velocity components with the jet discharge parameter $u_0 d_0$, the contours collapse on each other.

Figure 3.19 through Figure 3.22 show contours of normalized velocity components for test cases N150B, N150G, N150H, and N150I. These cases have fluid depth ranging from 91 cm (3 ft) to 640 cm (21 ft). For the 91 cm case, the recirculating flow region (rotating clockwise) near the wall is clearly seen. Vertical velocities near the wall are all negative (downward). At about $x = 6$ m there is a small upward velocity component implying some fluid elements turn upward on encountering the eddy. As the fluid height is increased to 183 cm fluid streamlines divide at the wall. Above $y = 60$ cm, fluid moves upward along the wall. This effect persists as the fluid height is increased further, with a large counterclockwise recirculation above the lower eddy. Figure 3.22 shows horizontal velocities at the liquid surface flowing back towards the center of the tank. These velocities may be somewhat artificial due to the solid free-slip boundary at the surface.

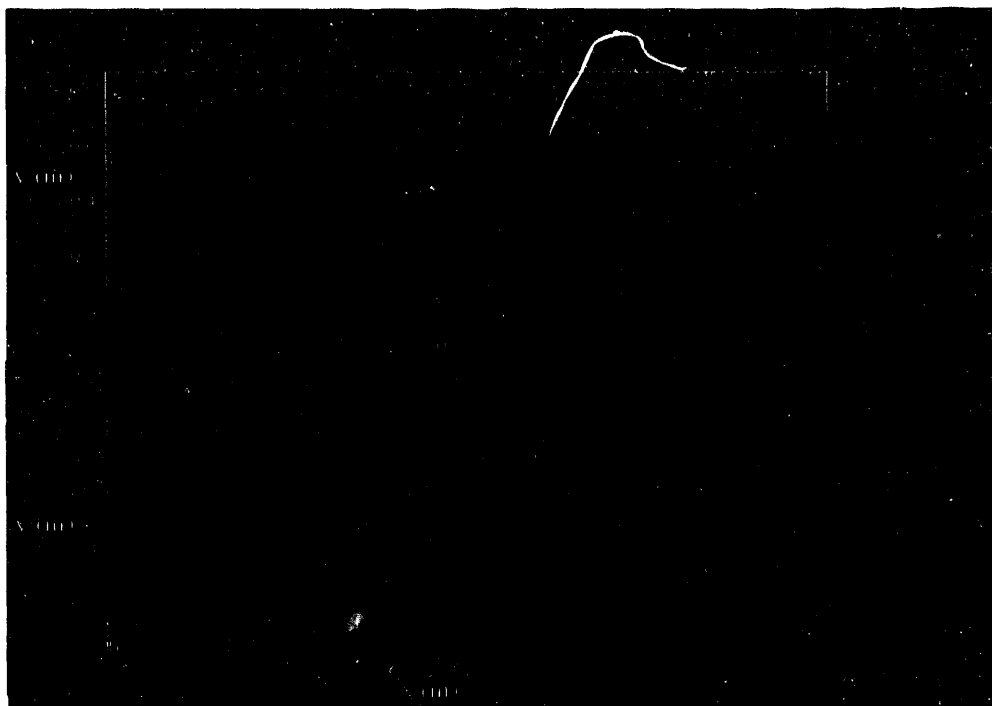


Figure 3.18 Contours of Normalized Velocity Near the Tank Wall



Figure 3.19 Normalized Velocity Components Near Tank Wall for $h_f = 91$ cm (test case N150B). Horizontal velocity (top) and Vertical velocity (bottom).

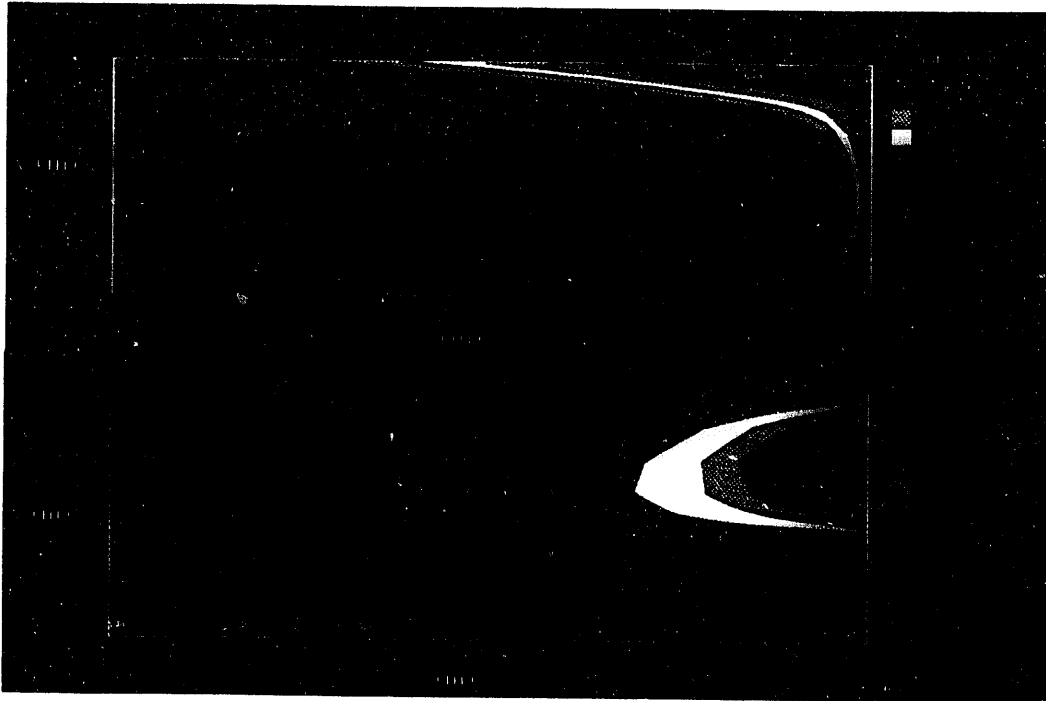


Figure 3.20 Normalized Velocity Components Near Tank Wall for $h_f = 183$ cm (test case N150G). Horizontal velocity (top) and Vertical velocity (bottom).

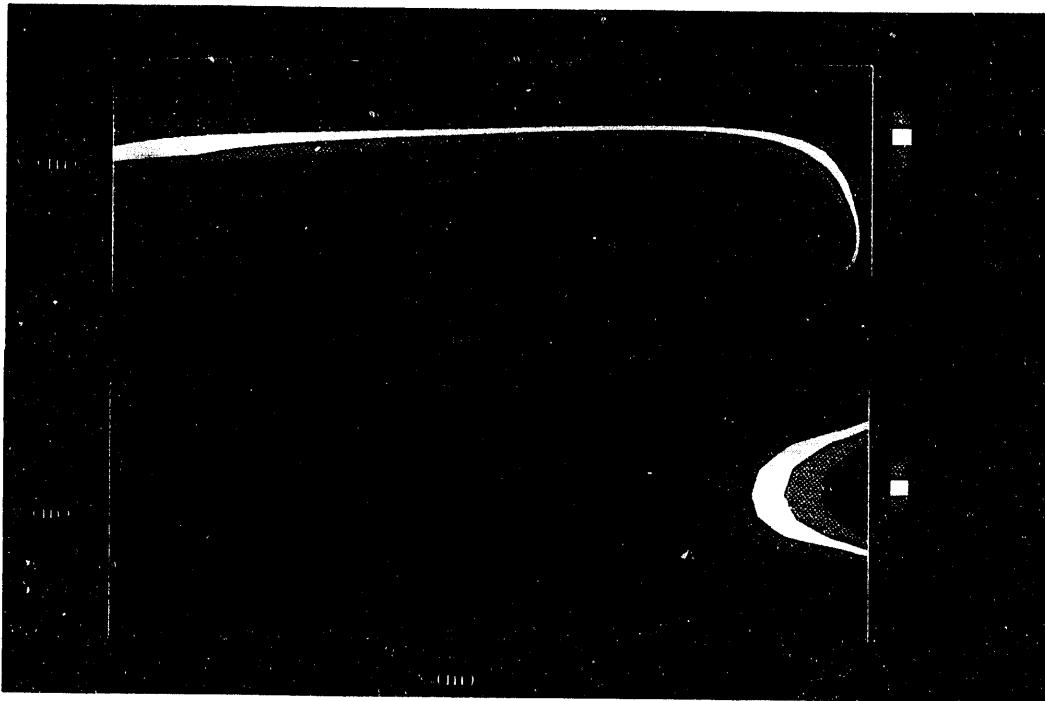


Figure 3.21 Normalized Velocity Components Near Tank Wall for $h_f = 305$ cm (test case N150H). Horizontal velocity (top) and Vertical velocity (bottom).

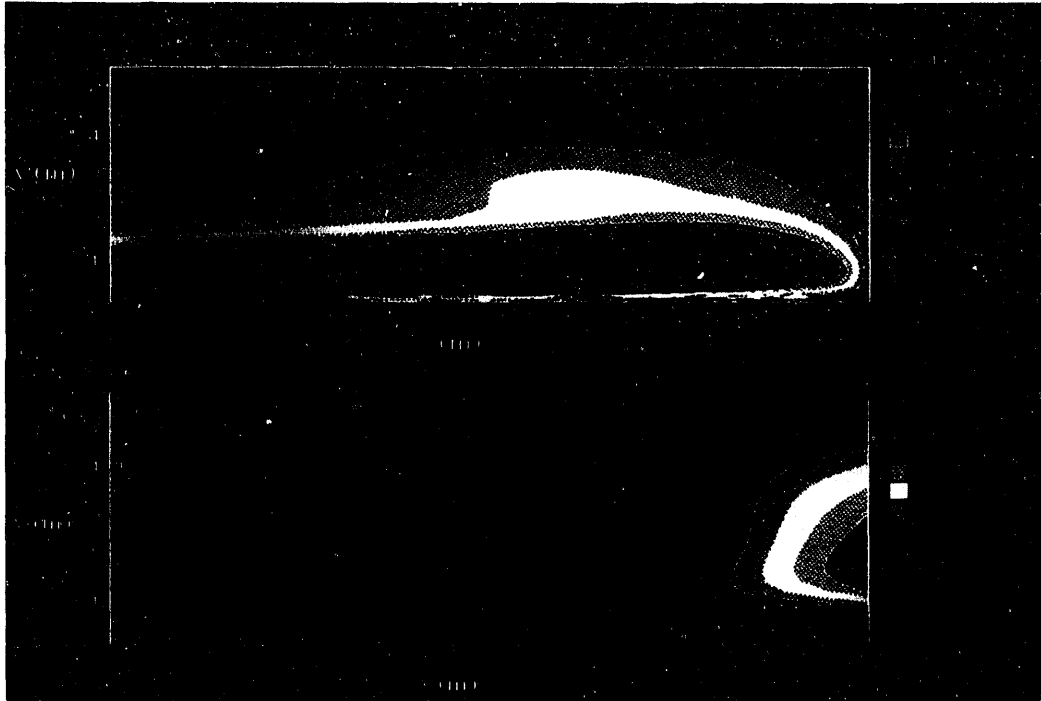


Figure 3.22 Normalized Velocity Components Near Tank Wall for $h_f = 640$ cm (test case N150I). Horizontal velocity (top) and Vertical velocity (bottom).

3.3.4 Centered Jets Flowing Parallel to Cooling Coils

This section presents results of jet simulations for jets oriented parallel to the cooling coils (East and West in Figure 2.4). Tank-centered jets with these orientations will impinge on the cooling coil support beams. There are three of these structures in the West orientation and four in the East. Figure 3.23 shows velocity vectors in the plane of the jet center-line for the two different orientations (test cases W150A and E150A). The jet is seen to attach to the floor for both cases, with a region of velocity reduction behind each support beam. The recirculating region near the tank wall is much smaller than for the case of jets oriented perpendicular to the cooling coils. Also, fluid stream lines near the wall and above the cooling coils turn upward, unlike the perpendicular flow case.

Figure 3.24 shows floor shear stress contours for the two cases. The jet spreads in front of each of the support beams, causing floor shear to decrease near the stagnation point of the impinging jet and increase laterally. The shear stress then slightly increases in the wake behind the beams. Figure 3.25 and Figure 3.26 show normalized floor shear stress along the jet center-line

for several different jet operating conditions and fluid depths ranging from 91 cm to 640 cm. From these plots, it is apparent that fluid height has little effect on the shear stresses. Also, the dependence of floor shear on the jet discharge parameter is clearly seen. Normalized shear stresses near the wall ($x = 7$ m) are approximately $\tau_f = 0.0012\rho_j(u_0d_0)^2$ for the West orientation and $\tau_f = 0.0008\rho_j(u_0d_0)^2$ for the East compared with $\tau_f = 0.00019\rho_j(u_0d_0)^2$ for jets oriented perpendicular to the cooling coils. From these results, it is evident that perpendicular orientations of cooling coils relative to fluid motions pose the greatest challenge to eroding the sludge.

Figure 3.27 shows normalized velocity contours in the plane of the jet center-line near the tank wall for an East facing jet with a 91 cm (3 ft) fluid height. The support beam causes a deficit in the horizontal component of velocity but creates an upward vertical component. A small recirculating region is seen at the wall near the floor. This recirculation is much smaller than for the case of flow perpendicular to the cooling coils. Stream-lines above the cooling coils turn upward at the wall. Figure 3.28 shows normalized velocity contours when the fluid height is 183 cm (10 ft). With the exception of the perturbation due to the support beam, flow near the wall behaves much like that for the case of flow perpendicular the cooling coils. However, vertical and horizontal velocity magnitudes are increased for this case.

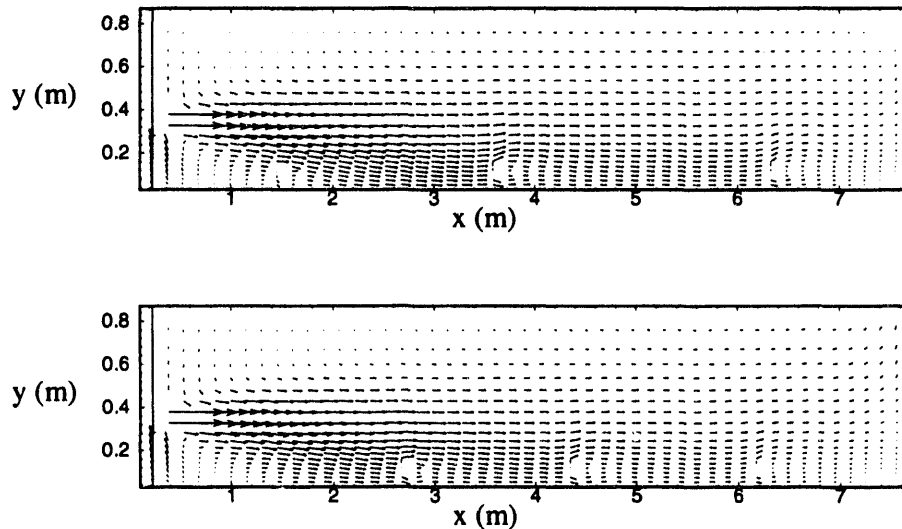


Figure 3.23 Velocity Vectors for Jet Oriented Parallel to the Cooling Coils for (top) West Facing Jet (W150A) and (bottom) East Facing Jet (E150A)

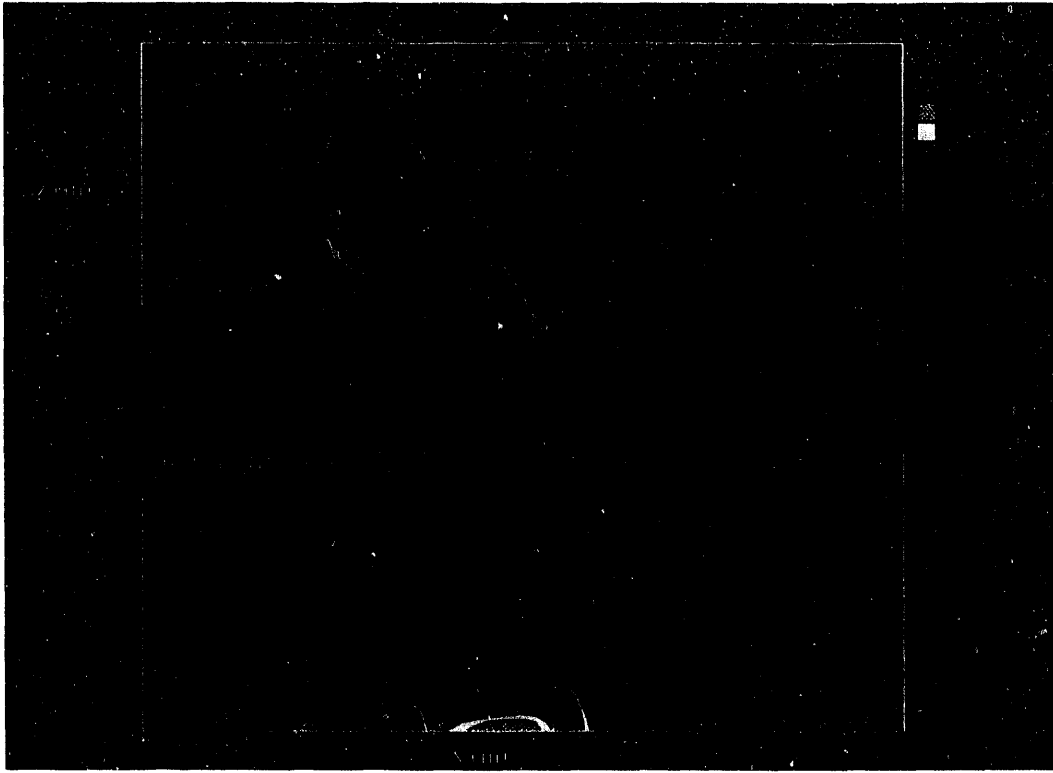


Figure 3.24 Floor Shear Stress Contours for (top) West Facing Jet (W150A) and (bottom) East Facing Jet (E150A)

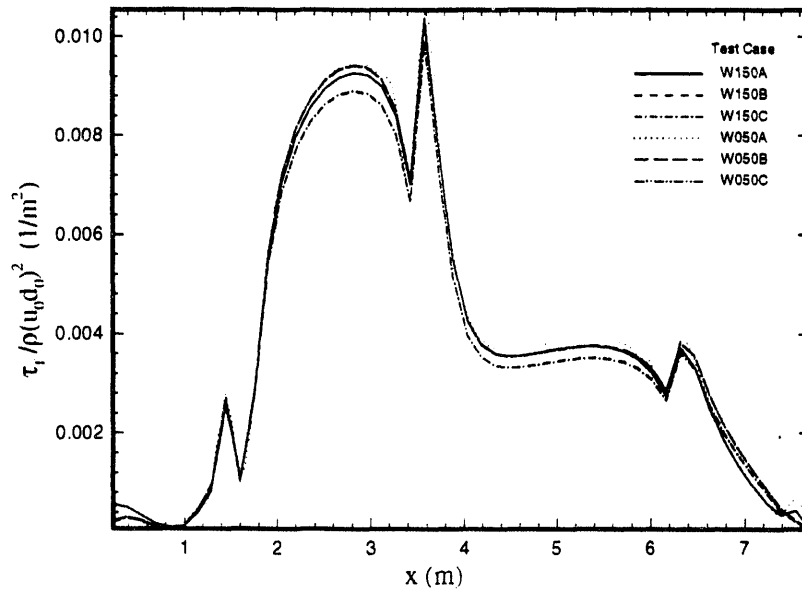


Figure 3.25 Normalized Center-line Floor Shear Stress for West Facing Jets

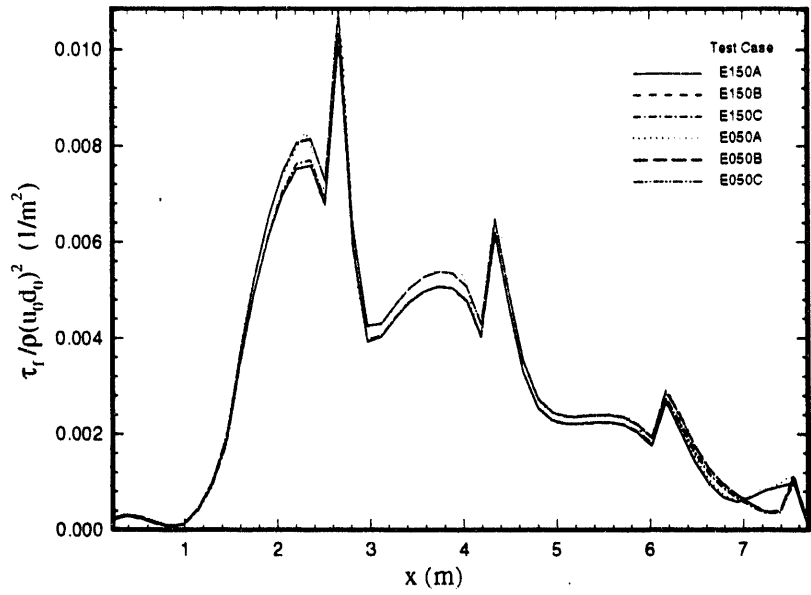


Figure 3.26 Normalized Center-line Floor Shear Stress for East Facing Jets

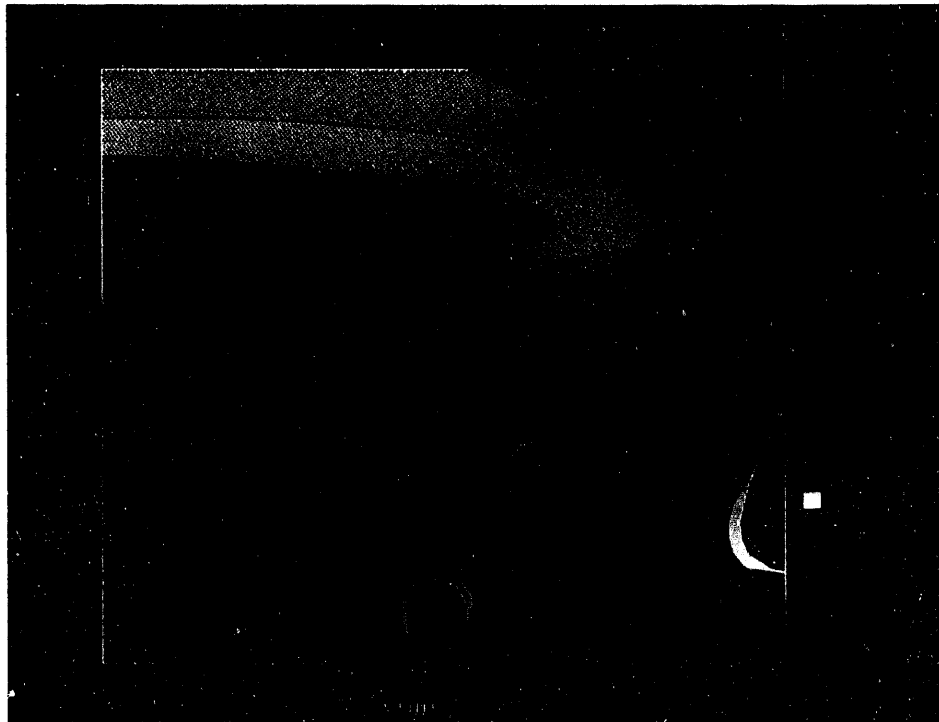


Figure 3.27 Normalized Velocity Components Near Tank Wall for East Facing Jet in 91 cm Depth Fluid (E150A). Horizontal velocity (top) and Vertical velocity (bottom).

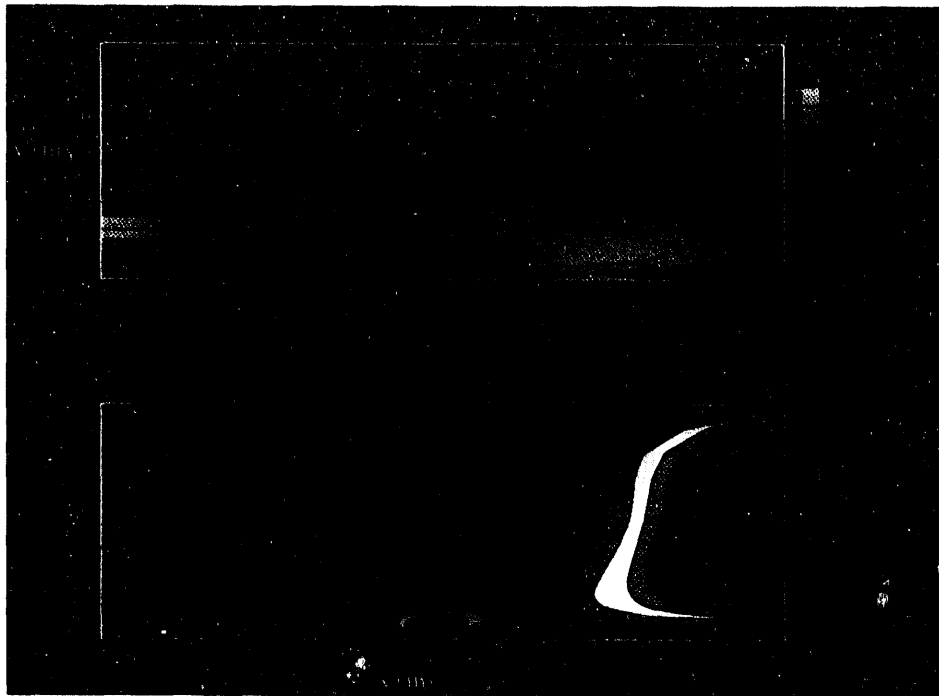


Figure 3.28 Normalized Velocity Components Near Tank Wall for East Facing Jet in 183 cm Depth Fluid (E150B). Horizontal velocity (top) and Vertical velocity (bottom).

3.3.5 Simulations of Off-Center Jets

Simulations of off-center jets were performed by reducing the distance from the jet (still located at the tank center) to the tank wall by a factor of two. While this approach does not capture all of the effects of off-center jets, it is believed that the essential behavior in the vicinity of the jet, particularly along the jet axis, is preserved.

Figure 3.29 shows velocity vectors in the plane of the jet center-line for an off-center jet oriented perpendicular to the cooling coils. The axial coordinate is the distance from the location of the jet ($x = 0$) to the wall ($x = 3.8$ m (12.5 ft)). The jet is seen to impinge on the tank wall and turn upward, unlike the behavior of the tank-centered jet. Figure 3.30 shows floor shear stress contours for the same case. The behavior is similar to the tank-centered case, except the shear stress near the wall is considerably higher, due to the closer proximity to the jet nozzle.

Figure 3.31 Shows normalized floor shear stress along the jet center-line for jets with different operating conditions and fluid heights. The shear stress scaling with nozzle discharge parameter established for the tank-centered jets still holds for this case. The variation of normalized floor shear near the wall is due primarily to fluid height. The minimum floor shear stress near the wall is approximately $\tau_f = 0.0005\rho_j(u_0d_0)^2$ for 91 cm (3 ft) depth and $\tau_f = 0.0004\rho_j(u_0d_0)^2$ for 305 cm (10 ft) depth. These values are slightly more than twice the values for tank-centered jets flowing perpendicular to the cooling coils.

Figure 3.32 and Figure 3.33 show normalized velocity components near the tank wall for off-center jets with liquid depths of 91 cm (3 ft) and 305 cm (10 ft) respectively. For the 91 cm case, the recirculating region near the wall is reduced in size compared with tank-centered jets. Also, a region of reverse horizontal flow occurs near the liquid surface. Magnitudes of both vertical and horizontal velocity are increased by about a factor of three over those for tank-centered jets. This is consistent with the jet being closer to the wall. Flow patterns for the 305 cm fluid height case are somewhat different from those of the equivalent tank-centered case (Figure 3.21). The region of upward moving fluid near the wall extends further from the wall than it does in the tank-centered case. Reverse horizontal velocities near the surface are also reduced.

Figure 3.34 shows normalized floor shear stress along the jet center-line for East facing off-center jets with different fluid heights. The behavior is similar to tank-centered East facing jets, with an increase in the shear at the wall. Figure 3.35 and Figure 3.36 show velocity contours at the wall for the same cases. Again, the behavior is similar to the tank-centered cases.

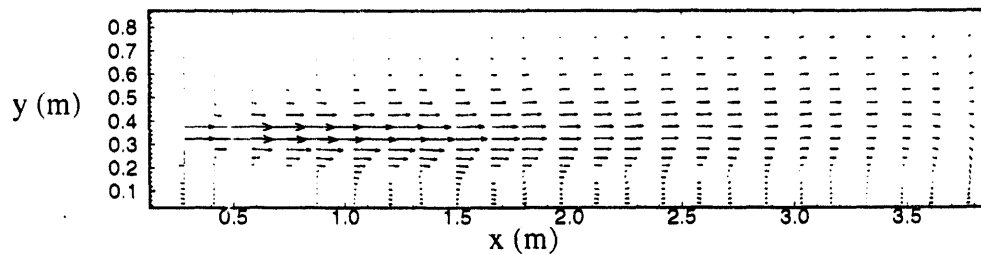


Figure 3.29 Velocity Vectors for Off-center Jet Oriented Perpendicular to Cooling Coils (test case N150M)

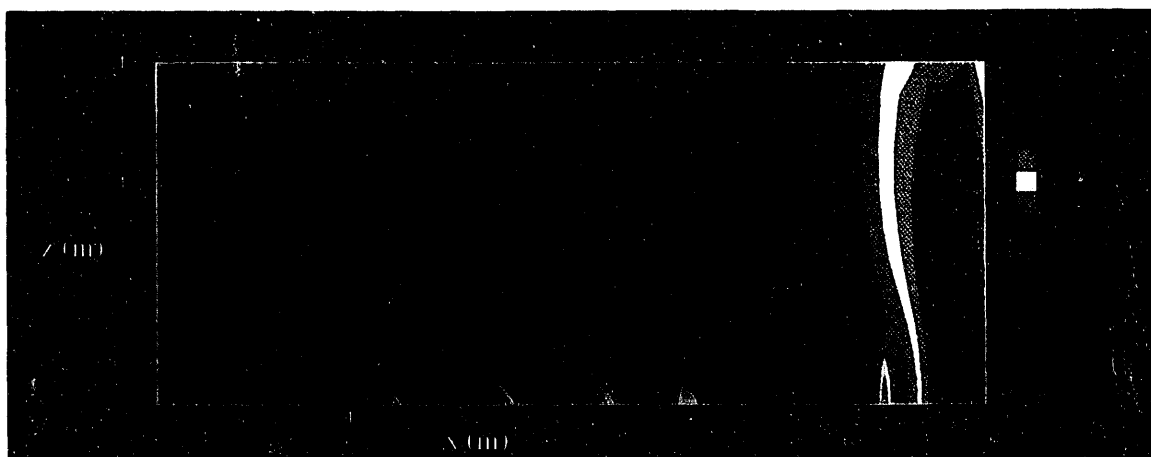


Figure 3.30 Floor Shear Stress Contours for Off-center Jet Oriented Perpendicular to Cooling Coils (test case N150M)

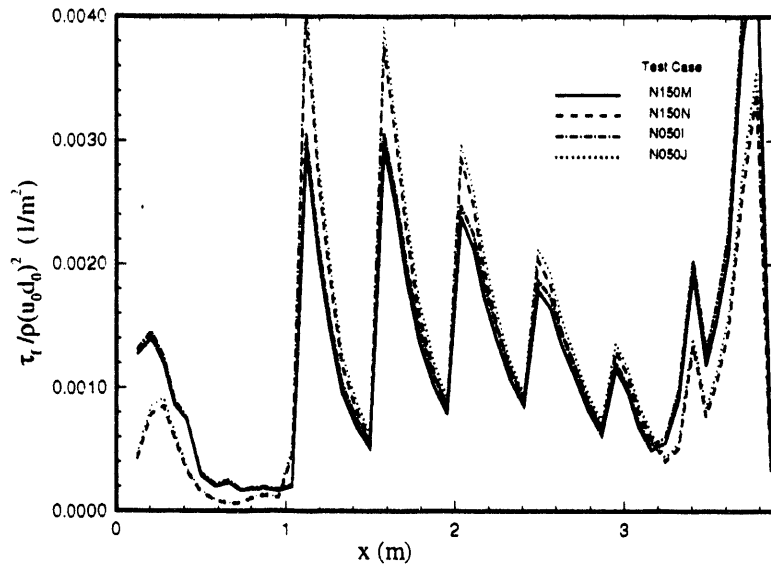


Figure 3.31 Normalized Jet Center-line Floor Shear Stress for Off-center Jets Oriented Perpendicular to Cooling Coils

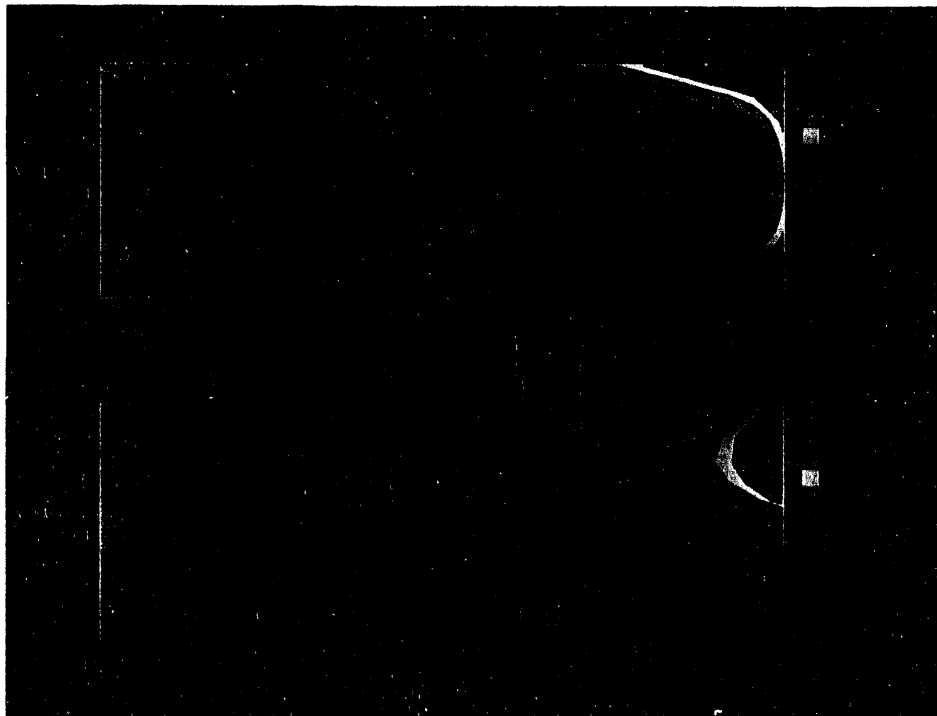


Figure 3.32 Normalized Velocity Components Near Tank Wall for Off-center Jet in 91 cm Depth Fluid Oriented Perpendicular to Cooling Coils (N150M). Horizontal velocity (top) and Vertical velocity (bottom).

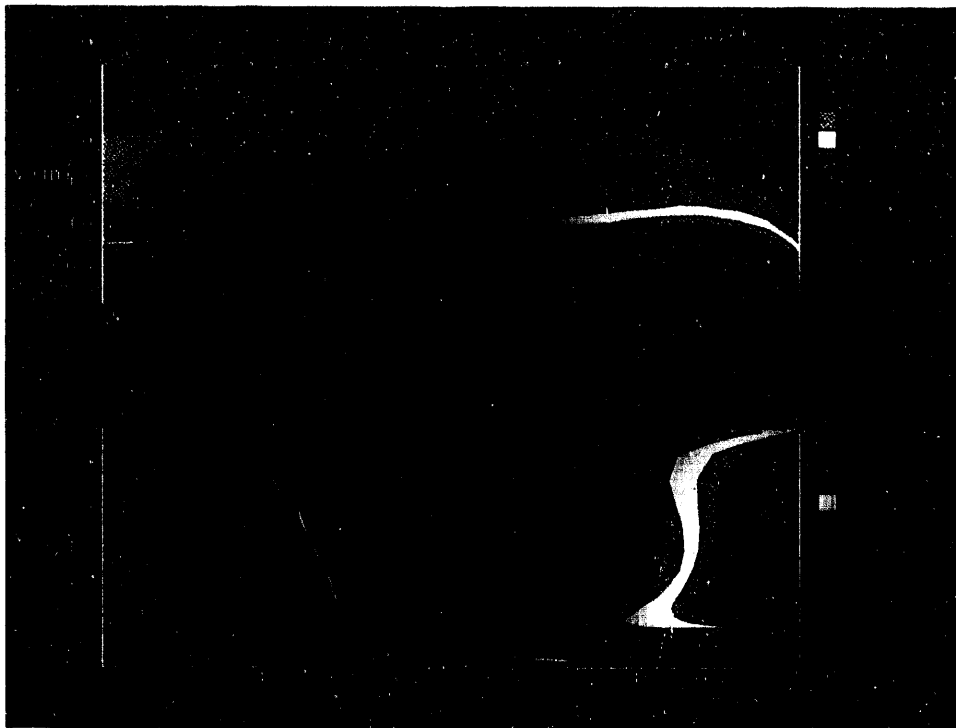


Figure 3.33 Normalized Velocity Components Near Tank Wall for Off-center Jet in 305 cm Depth Fluid Oriented Perpendicular to Cooling Coils (N150N). Horizontal velocity (top) and Vertical velocity (bottom).

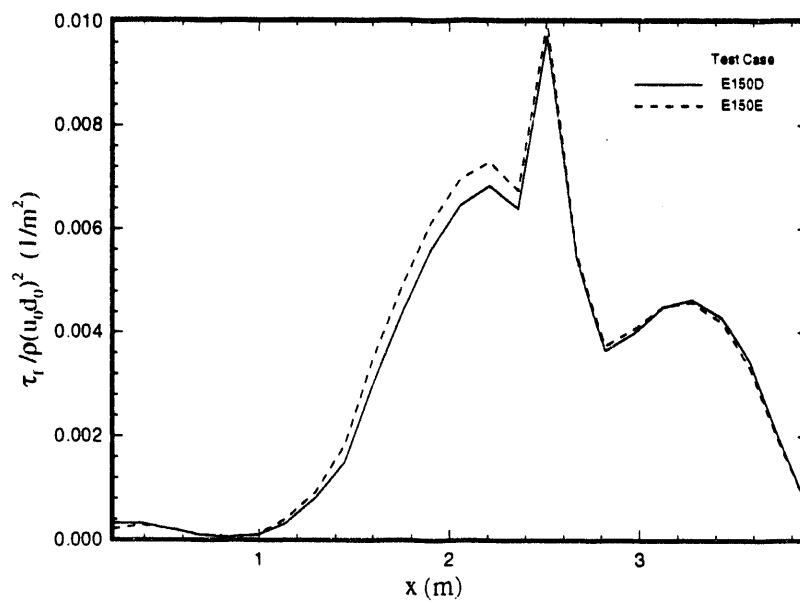


Figure 3.34 Normalized Center-line Floor Shear Stress for East Facing Off-center Jets

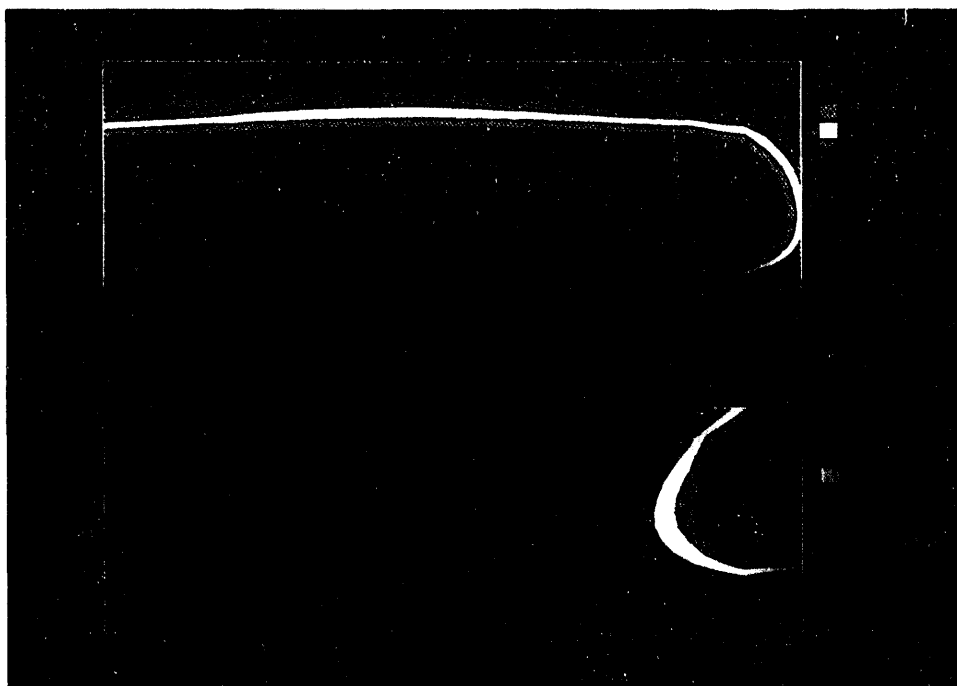


Figure 3.35 Normalized Velocity Components Near Tank Wall for Off-center Jet in 91 cm Depth Fluid Oriented Parallel to Cooling Coils (E150D). Horizontal velocity (top) and Vertical velocity (bottom).



Figure 3.36 Normalized Velocity Components Near Tank Wall for Off-center Jet in 305 cm Depth Fluid Oriented Parallel to Cooling Coils (E150E). Horizontal velocity (top) and Vertical velocity (bottom).

3.3.6 Simulations of Particle Laden Jets

This section presents results for particle laden, dense jet simulations. An extremely conservative approach was taken in order to reveal potential areas of difficulty during periods of jet start-up. In a fully mixed scenario, particle effects should be minimal, with the only significant effect being a slight increase in effective fluid density due to suspended particles. However, during pump start-up, jets may be heavier than surrounding fluid because particles will be entrained into the pump inlet from the floor. For these simulations, a 5.7 cm (2.25 in.) sludge layer was modeled at the tank floor. The sludge was made up of three particle species corresponding to the largest (200 μ), most populous (70 μ), and smallest (13 μ) particles described in Section 2. The simulation began by initializing particle concentrations at the tank floor to correspond to the assumed sludge mass distributions of 4%, 70%, and 26% for the largest, most populous, and smallest particles, respectively, and to take into account the assumed void fraction of 50%. This approach essentially represents a fully fluidized model. When the jet is turned on, the solid particles freely convect with the fluid motion. In light of this, the fluid entrained into the pump inlet is significantly more dense than it would be in a true eroding situation. The model also included particle settling, with settling velocities specified for each of the particle species.

Tests were performed for jets oriented perpendicular to the cooling coils with 91 cm fluid heights (P150A and P050A), 305 cm fluid heights (P150B and P050B), and off-center jets with 305 cm fluid heights (P150C and P050C).

Figure 3.37 shows contours of solid/liquid mixture density for test cases P150A and P150B. The density is highest underneath the pump inlet and in the core of the jet. A small vertical density gradient occurs near the tank wall. This gradient is larger for the 305 cm fluid height case. The density of fluid above the jets is nearly equal to the waste solution density, implying negligible solids concentrations are present.

Figure 3.38 shows the effect of particulates on normalized floor shear stress for the 91 cm (3 ft) fluid height cases. Comparisons are made with floor shear for the fluid-only cases. Shear stress near the wall are seen to be considerably reduced due to the particles. This means that the scaling of floor shear with jet momentum does not strictly hold for the case of dense jets. This is reasonable, because the jet can exchange momentum with the particles in accelerating them. There is also a power dissipation associated with particle drag on the fluid jet. From the trends shown in Figure 3.38, the floor shear stress near the wall is a function of jet horse power as well as jet momentum. This additional dependence is expected to diminish as particles in the tank become mixed. Figure 3.39 shows, for off-center jets, the reduction in floor shear due to particles is significantly smaller. This occurs because fluid velocities near the wall are significantly higher and jet momentum still dominates.



Figure 3.37 Density Contours in Particle Laden Jets Oriented Perpendicular to Cooling Coils for 91cm Fluid Height (P150A) (top) and 305 cm Fluid Height (P150B) (bottom)

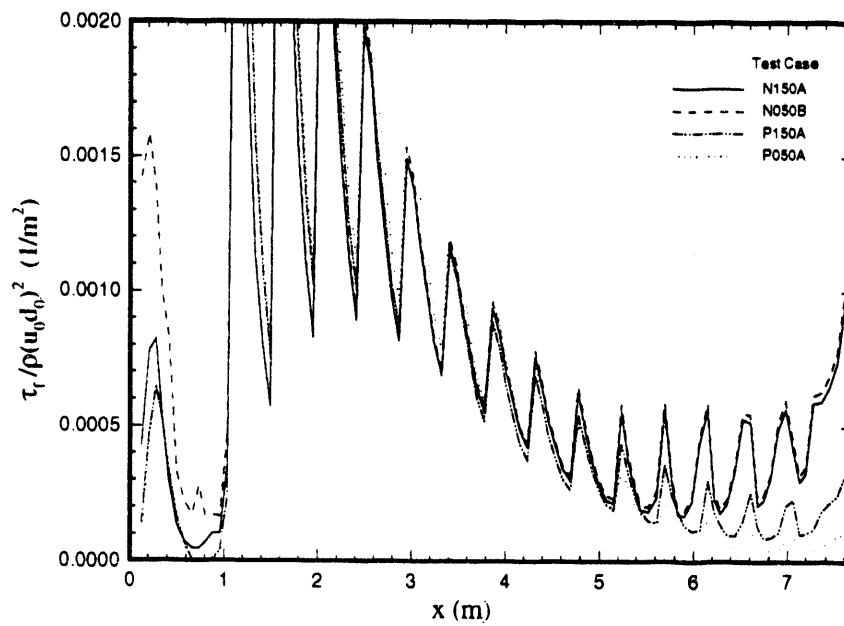


Figure 3.38 Normalized Floor Shear Stress for Tank-centered Particle-laden Jets

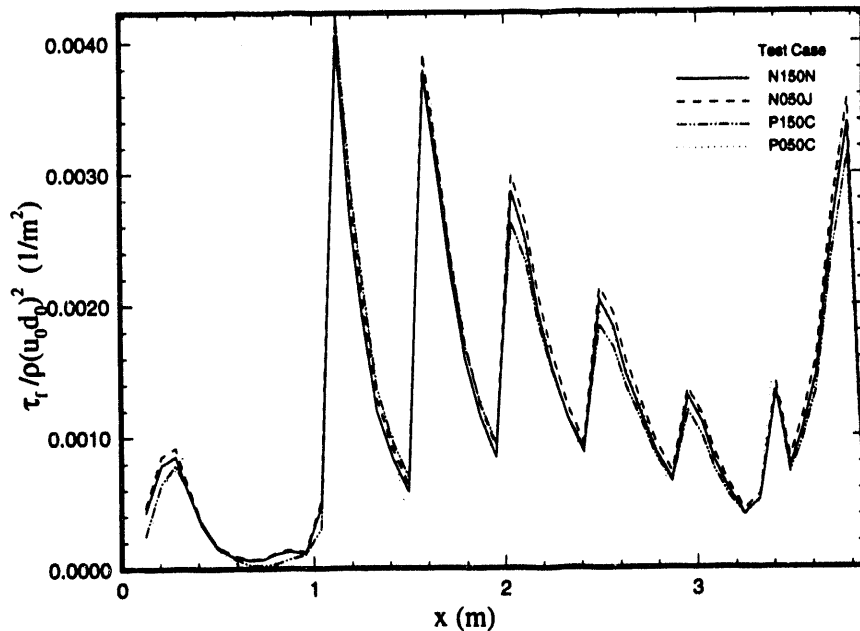


Figure 3.39 Normalized Floor Shear Stress for Off-center Particle-laden Jets

Figure 3.40 shows normalized velocity components near the tank wall for a tank-centered dense jet in a fluid of height 91 cm (3 ft). Both vertical and horizontal velocities are similar to those for the corresponding pure liquid case (see Figure 3.19), except that the velocities in the recirculation zone are slightly reduced. Since velocities are similar for the two cases, the observed reduction in shear stress due to particles must be attributed to modified turbulence intensity and not velocities. Figure 3.41 shows normalized velocity components near the tank wall for a tank-centered dense jet in a fluid of height 305 cm (3 ft). Upward vertical velocities at the wall are considerably smaller than for the corresponding pure liquid case (Figure 3.22). When the jet is located in the off-center position closer to the wall, the effects on velocity are diminished. This case is shown in Figure 3.22.

Figure 3.43 through Figure 3.45 show the vertical variation in particle concentrations along the jet center-line at the tank wall for the three different particle sizes. The concentrations are normalized by their initial value on the tank floor. For tank-centered jets with fluid heights of 91 cm (test cases W050A and W150A) the concentrations show little variation in the vertical direction, implying the jet is able to transport all particles to the surface. For tank centered jets with fluid heights of 305 cm, the variation of concentration with height depends on horsepower. For test case W150, concentrations decrease with vertical distance by about 30% for the small particles and about 50% for the medium and large particles. For test case W050 (which has a lower hydraulic horsepower) concentrations for all particle sizes fall to near zero values. For off-center jets (test cases W150C and W050C), relatively uniform concentrations are seen for higher power jets with concentration falling off for lower power jets.

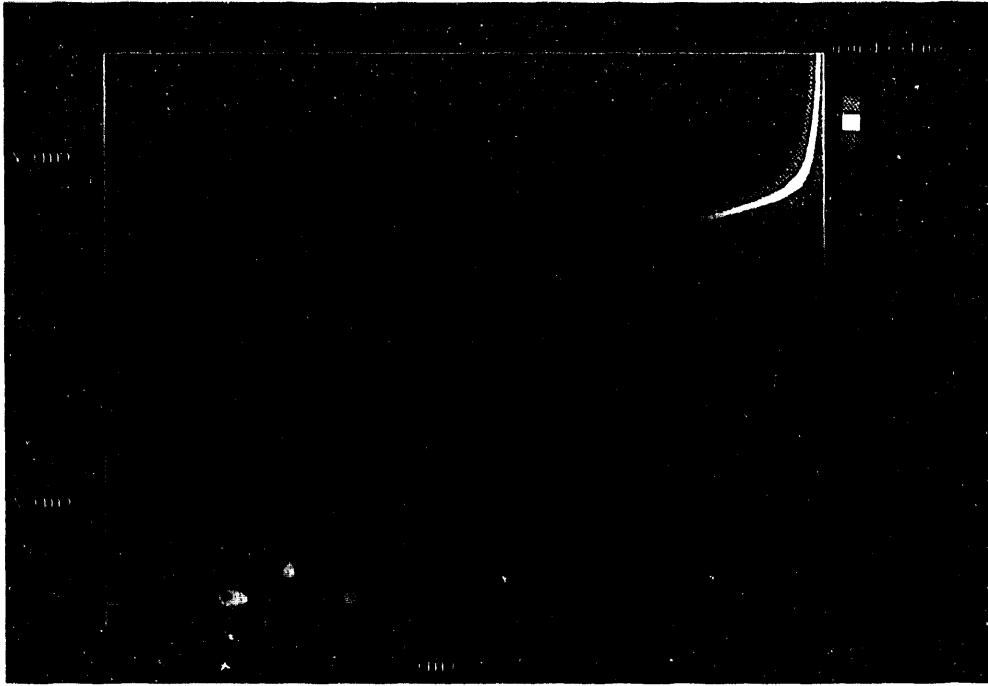


Figure 3.40 Normalized Velocity Components Near Tank Wall for Dense Jet in 91 cm Height Fluid (P150A). Horizontal velocity (top) and Vertical velocity (bottom).

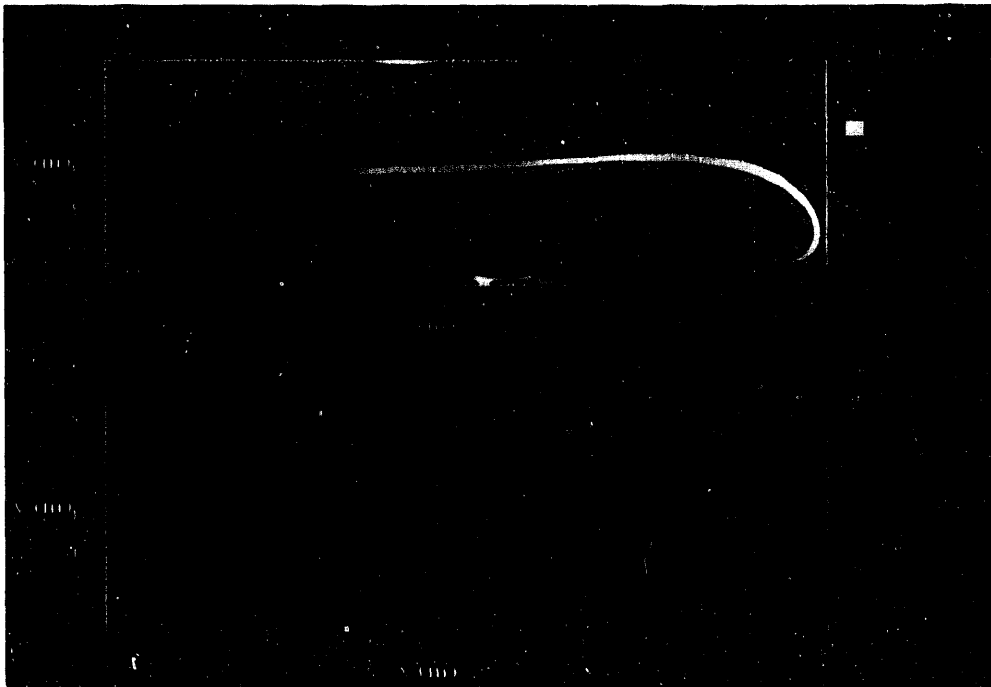


Figure 3.41 Normalized Velocity Components Near Tank Wall for Dense Jet in 305 cm Height Fluid (P050B). Horizontal velocity (top) and Vertical velocity (bottom).

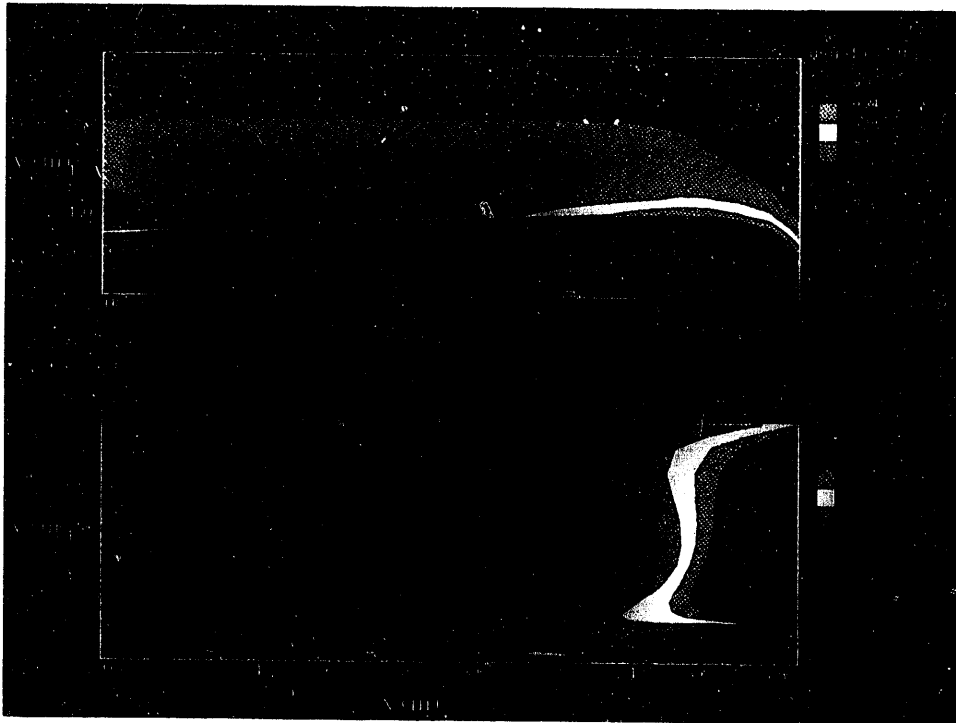


Figure 3.42 Normalized Velocity Components Near Tank Wall for Off-center Dense Jet in 305 cm Height Fluid (P050C). Horizontal velocity (top) and Vertical velocity (bottom).

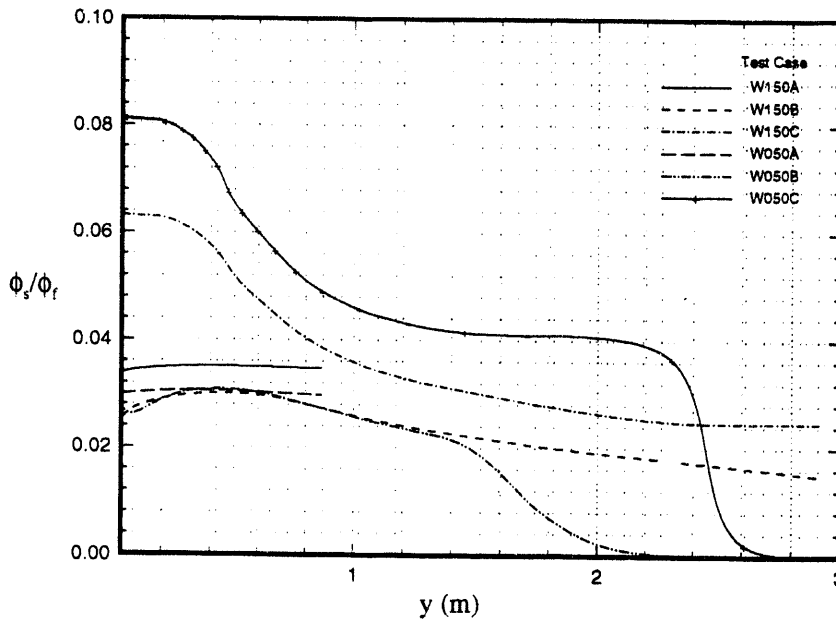


Figure 3.43 Normalized Particle Concentrations of Smallest Particles Along Tank Wall for Various Test Cases

Figure 3.45 Normalized Particle Concentrations of Largest Particles Along Tank Wall for Various Test Cases

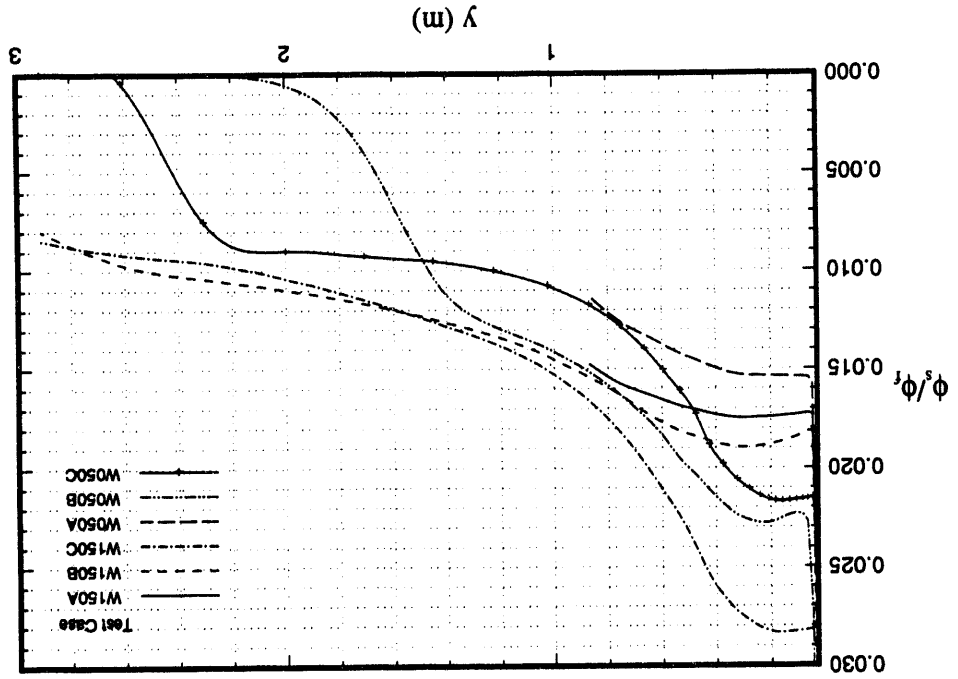
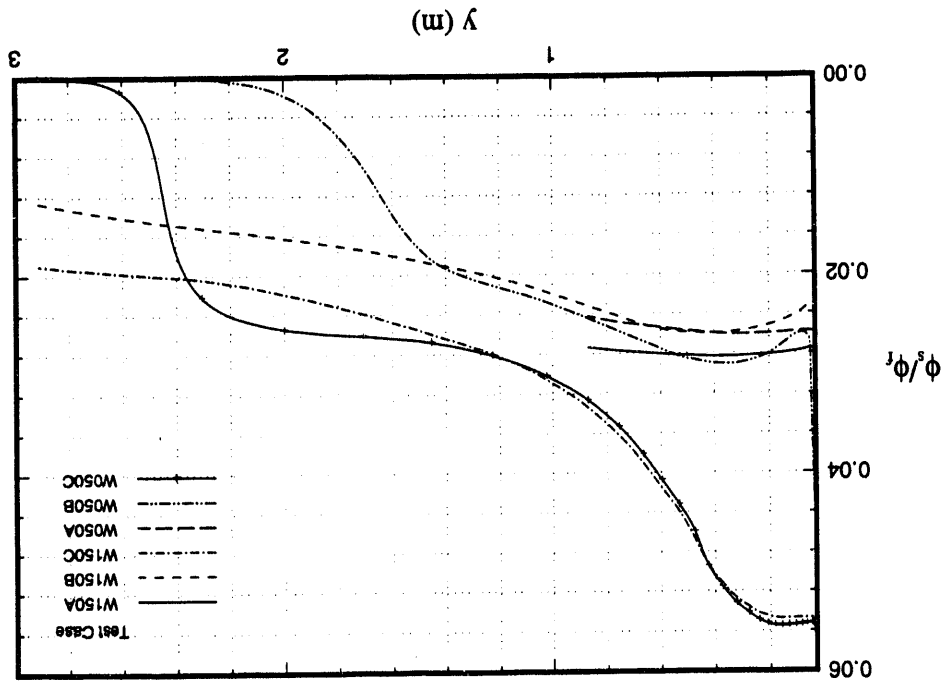


Figure 3.44 Normalized Particle Concentrations of Medium Particles Along Tank Wall for Various Test Cases



4.0 Mixing System Requirements

This Section presents mixing system requirements and recommendations for jet mixing pumps in INEL tanks. In the first section, several analytical models are developed which relate mobilization and suspension requirements with jet operating parameters. In the second section, the models are evaluated based on the assumed material properties and results from the numerical simulations. The final section presents some mixing system design recommendations.

4.1 Analytical Models

This section presents analytical models that are used to determine the mixing pump operating conditions and configurations required to mobilize settled solids and maintain solids in suspension. The models are developed based on conservative assumptions that capture essential features of a jet mixing system.

4.1.1 Necessary Conditions for Effective Mixing

The processes involved in mobilizing and suspending solids in tanks using jet mixing pumps are complex. However, several important requirements for successful mixing can be identified. The following conditions are fundamental to effective mixing:

1. The jet must produce sufficient shear stress on the floor to erode the solids.
2. The amount of mass eroded by a jet must be greater than the amount of mass which settles outside the jet's range of influence.
3. The effective cleaning radius (ECR) of a jet must be greater than or equal to the distance from the jet nozzle to the tank wall.
4. The jet must create a continuous upward vertical velocity at the tank wall or else solids will accumulate.
5. The magnitude of vertical velocities at the tank wall must be sufficient to lift solid particles to near the liquid surface.
6. The rate of work produced by the jet in suspending particles must be sufficient to overcome the rate of gravitational work on the suspended particles.
7. For rotating mixing jets, the rate of rotation must be large enough to prevent a net accumulation of solids on the floor.

The conditions for successful mobilization and solids suspension are not, in general, independent from each other. The first two conditions involve erosion and deposition requirements necessary for both mobilization and solids suspension. Conditions 6 and 7 relate primarily to solids suspension. Conditions 3 through 5 pertain not only to jet operating parameters but also to the number and placement of the mixing pumps.

4.1.2 Erosion and Deposition Models

The results of the numerical simulations demonstrated that the normalized floor shear stress near the tank wall was approximately constant for a given jet orientation. This can be expressed, in general, as

$$\tau_f / \rho_f (u_0 d_0)^2 = c_\tau \quad (4.1)$$

The constant, c_τ , is dependent on 1) the jet orientation relative to the cooling coils, 2) the location of the jet relative to the tank wall, and weakly dependent on 3) the height of the fluid. In order for erosion to occur, the erosion model given by Equation (2.8) states the condition

$$\tau_f / \tau_e > 1, \quad (4.2)$$

where τ_e is the critical shear stress for erosion. Combining the above two expressions gives the condition

$$u_0 d_0 > \sqrt{\tau_e / c_\tau \rho_f} \quad (4.3)$$

Equation (4.3) sets a lower limit on the nozzle discharge parameter ($u_0 d_0$) in order for erosion to occur and provides a means for satisfying condition 1. It also shows the dependence of the jet discharge parameter on the critical shear stress for erosion.

Condition 2 states that the net mass erosion rate in the region of the jet's influence must be greater than the net mass deposition rate outside this region of influence. In order to model this condition, consider a reference frame which rotates with the jet as shown in Figure 4.1. The region of the jet's influence can be approximated as the area of an angular segment of the effective cleaning radius given by

$$A_e = R_c^2 \theta_j / 2, \quad (4.4)$$

where θ_j is the spreading angle of the jet and R_c is the effective cleaning radius. The area outside the jet influence is given by

$$A_d = (\pi R_c^2)/2 - A_e = R_c^2(\pi - \theta_j)/2. \quad (4.5)$$

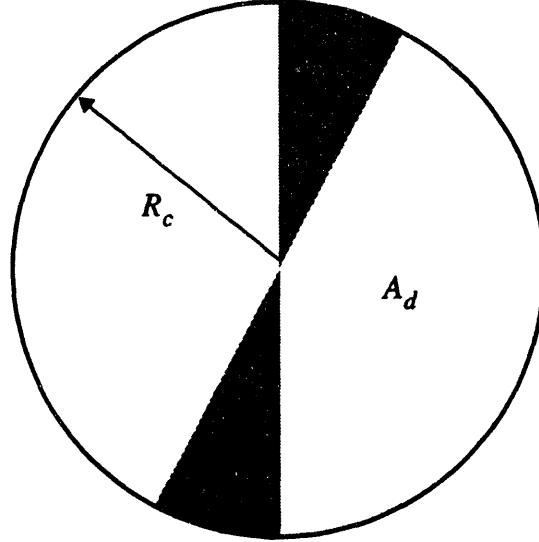


Figure 4.1 Erosion and Deposition Areas Within the Effective Cleaning Radius

The rate at which mass is eroded or deposited is given by Equations (2.8) and (2.9) which are rewritten here for convenience:

$$\dot{m}_e = E(\tau_f/\tau_e - 1) \quad \tau_f \geq \tau_e \quad (4.6)$$

$$\dot{m}_d = u_s \phi_s (1 - \tau_f/\tau_d) \quad \tau_f \leq \tau_d \quad (4.7)$$

Because these expressions give the mass flux (rate of mass flow per unit area), the total mass flow rates are obtained by integrating them over the areas of influence. The shear stresses in Equations (4.6) and (4.7) can be replaced with conservative mean values for erosion ($\bar{\tau}_e$) and deposition ($\bar{\tau}_d$). These average shear stresses can be related to the jet discharge parameter by

$$\bar{\tau}_e = \bar{c}_e \rho_f (u_0 d_0)^2 \quad (4.8)$$

$$\bar{\tau}_d = \bar{c}_d \rho_f (u_0 d_0)^2 \quad (4.9)$$

where the constants \bar{c}_e and \bar{c}_d can be determined from the simulation data.

With these simplifications, integration of Equations (4.6) and (4.7) over the affected areas results in

$$\begin{aligned}\dot{M}_e &= 2A_e \dot{m}_e = R_c^2 \theta_j E (\bar{c}_e \rho_f (u_0 d_0)^2 / \tau_e - 1) & (u_0 d_0)^2 > \tau_e / (\bar{c}_e \rho_f) \\ \dot{M}_e &= 0 & (u_0 d_0)^2 \leq \tau_e / (\bar{c}_e \rho_f)\end{aligned}\quad (4.10)$$

$$\begin{aligned}\dot{M}_d &= 2A_d \dot{m}_d = R_c^2 (\pi - \theta_j) u_s \phi_s (1 - \bar{c}_d \rho_f (u_0 d_0)^2 / \tau_d) & (u_0 d_0)^2 < \tau_d / (\bar{c}_d \rho_f) \\ \dot{M}_d &= 0 & (u_0 d_0)^2 \geq \tau_d / (\bar{c}_d \rho_f)\end{aligned}\quad (4.11)$$

These two equations give the total mass erosion and deposition rates, \dot{M}_e and \dot{M}_d , respectively. In order for the total mass erosion rate to be greater than the total mass deposition rate, the following condition must hold:

$$\dot{M}_e / \dot{M}_d = \frac{\theta_j E (\bar{c}_e \rho_f (u_0 d_0)^2 / \tau_e - 1)}{(\pi - \theta_j) u_s \phi_s (1 - \bar{c}_d \rho_f (u_0 d_0)^2 / \tau_d)} > 1 \quad \tau_e / (\bar{c}_e \rho_f) \leq (u_0 d_0)^2 < \tau_d / (\bar{c}_d \rho_f). \quad (4.12)$$

This inequality can be rewritten

$$(u_0 d_0)^2 > \frac{1}{\rho_f} \left[\frac{\theta_j E + (\pi - \theta_j) u_s \phi_s}{\bar{c}_e \theta_j E / \tau_e + \bar{c}_d (\pi - \theta_j) u_s \phi_s / \tau_d} \right] \quad (u_0 d_0)^2 < \tau_d / (\bar{c}_d \rho_f) \quad (4.13)$$

Equation (4.13) must be satisfied for each particulate species. The settling velocity for each species is given by Equation (2.10), written here for convenience as

$$u_s = \frac{1}{18} g d_s^2 (\rho_s - \rho_f) / \mu_f \quad (4.14)$$

The average mass concentration of each particulate species can be related to the sludge thickness and fluid height by

$$\phi_s = (mf V_{sl} \rho_{sl} h_{sl}) / h_f \quad (4.15)$$

Here mf is the species mass fraction in the sludge, ρ_{sl} is the sludge dry bulk density, V_{sl} is the sludge void fraction, and h_{sl} is the sludge thickness. The mass concentration ϕ_s represents the

particle concentration in the tank fluid if all the solids were suspended. During the early stages of mobilization, it is unlikely the actual particle concentration will be as large as ϕ_s , because not all the particles have been suspended. However, the assumption that all the particles are suspended represents the worst case scenario for the models being developed.

There are several limits of Equation (4.13) that are worth noting. First, if the erodibility constant E is very small, the right hand side of the inequality limits to $\tau_d / (\bar{c}_d \rho_f)$. Hence the minimum jet discharge parameter depends on the critical shear stress for deposition and the constant (\bar{c}_d). For small values of \bar{c}_d , implying very low floor shear away from the jet, the jet discharge parameter will be large. Another limit occurs when the concentration of suspended particles or the settling velocity is very small. For this situation, the right-hand side limits to $\tau_e / (\bar{c}_e \rho_f)$, which is dominated by erosion properties. A third limit occurs when $\theta_j E$ is small compared with $(\pi - \theta_j) u_s \phi_s$ and \bar{c}_d is very small. In this limit, deposition is dominated by unhindered settling and the right-hand side is dominated by the term $\tau_e u_s \phi_s / (E \bar{c}_e \rho_f)$. Therefore, the critical shear stress for erosion and the erodibility constant are of equal importance.

Finally, it should be noted that if the inequality in Equation (4.13) is replaced with an equality, then the equation gives the minimum discharge parameter in order to keep solids suspended, since there would be no net mass accumulation to the floor.

4.1.3 Jet Rotation Rate and Mixing Time Models

This section presents models that can be used to indicate necessary pump rotation rates and mixing time required to mobilize and suspend the sludge. If the jets are rotating and Equation (4.13) is satisfied, there will be no net accumulation of solids on the tank floor. However, after each sweep of the rotating jet, some solids will accumulate regardless of pump rotation rate. These solids will be eroded during the next jet sweep. Therefore, the primary factor affecting pump rotation rate is the amount of material that can be allowed to settle on the floor at any given time. Settling material implies nonuniform concentrations of solids in the suspension. The faster the pump is rotated, the less time is available between jet sweeps for particle settling, and a higher percentage of solids will be maintained in suspension.

A relationship between jet rotation rate ($\dot{\omega}_j$) and the degree of uniformity (Φ) (defined as mass of suspended particles divided by the total particle mass) can be obtained by considering the amount of solids that settle on the floor between jet passes. The maximum amount of time which the jet is not passing over any given point within the ECR is equal to $(\pi - \theta_j) / \dot{\omega}_j$. The amount of mass (for a single species) that settles per unit area during this time is $\dot{m}_d (\pi - \theta_j) / \dot{\omega}_j$. This must be equal to the amount of mass per unit area that accumulates on the floor given by $mfV_{sl} \rho_{sl} \Delta h_{sl}$

where Δh_{sl} is the height of the accumulated solid species. Equating the mass settled with the mass accumulated and using Equations (4.7) and (4.9) results in

$$\dot{\omega}_j = \frac{(\pi - \theta_j) u_s \phi_s (1 - \bar{c}_d \rho_f (u_0 d_0)^2 / \tau_d)}{mfV_{sl} \rho_{sl} \Delta h_{sl}} \quad (u_0 d_0)^2 < \tau_d / (\bar{c}_d \rho_f) \quad (4.16)$$

Given the definition of ϕ_s in Equation (4.15), Equation (4.16) can be rewritten in terms of the degree of uniformity as

$$\dot{\omega}_j = \frac{(\pi - \theta_j) u_s (1 - \bar{c}_d \rho_f (u_0 d_0)^2 / \tau_d)}{h_f (1 - \Phi)} \quad (u_0 d_0)^2 < \tau_d / (\bar{c}_d \rho_f), \quad (4.17)$$

where Φ is formally defined as

$$\Phi = 1 - \Delta h_{sl} / h_{sl}. \quad (4.18)$$

The mixing time required to suspend the sludge can be modeled in a similar way. The mixing time (T_m) is the amount of time required to erode away the sludge layer of thickness h_{sl} . Because erosion and deposition are occurring simultaneously, the net erosion rate per unit area is equal to $\dot{m}_e - \dot{m}_d$. The mass per unit area of each sludge component is $mfV_{sl} \rho_{sl} h_{sl}$. The time required to erode the sludge is therefore $T_m = mfV_{sl} \rho_{sl} h_{sl} / (\dot{m}_e - \dot{m}_d)$. With the aid of Equation (4.6) - (4.9), the mixing time is expressed as

$$T_m = \frac{mfV_{sl} \rho_{sl} h_{sl}}{E(\bar{c}_e \rho_f (u_0 d_0)^2 / \tau_e - 1) - u_s \phi_s (1 - \bar{c}_d \rho_f (u_0 d_0)^2 / \tau_d)} \quad \frac{\tau_e}{\bar{c}_e \rho_f} \leq (u_0 d_0)^2 < \frac{\tau_d}{\bar{c}_d \rho_f} \quad (4.19)$$

$$T_m = \frac{mfV_{sl} \rho_{sl} h_{sl}}{E(\bar{c}_e \rho_f (u_0 d_0)^2 / \tau_e - 1)} \quad (u_0 d_0)^2 \geq \tau_d / (\bar{c}_d \rho_f)$$

Equation (4.19) can be rearranged to give the jet discharge parameter in terms of the mixing time;

$$(u_0 d_0)^2 = \frac{mfV_{sl} \rho_{sl} h_{sl} / T_m + E + u_s \phi_s}{\rho_f (\bar{c}_e E / \tau_e + u_s \phi_s \bar{c}_d / \tau_d)} \quad \tau_e / (\bar{c}_e \rho_f) \leq (u_0 d_0)^2 < \tau_d / (\bar{c}_d \rho_f) \quad (4.20)$$

$$(u_0 d_0)^2 = \frac{\tau_e (mfV_{sl} \rho_{sl} h_{sl} / T_m + E)}{\rho_f \bar{c}_e E} \quad (u_0 d_0)^2 \geq \tau_d / (\bar{c}_d \rho_f)$$

4.1.4 Solids Suspension Models

Condition 5 stated that vertical velocities at the tank wall must be sufficient to transport settling particles upward to the fluid surface. This condition will be satisfied if the vertical velocity is greater than the settling velocity of the particles. Simulations showed that vertical velocities at the wall (v_f) scaled with the nozzle discharge parameter. This can be expressed as

$$v_f / (u_0 d_0) = c_v \quad (4.21)$$

where c_v is determined from simulation data. The condition will be satisfied when

$$v / u_s = c_v (u_0 d_0) / u_s > 1 \quad (4.22)$$

Condition 6 states that the rate of work produced by the jet in suspending particles must be sufficient to overcome the rate of gravitational work on the suspended particles. The rate of work produced by the jet is the total hydraulic power $\rho_j u_0^3 d_0^2$. The rate of work due to gravitational settling of one particle can be approximated by the drag on the particle ($6\pi\mu_f u_s d_s$) multiplied by the settling velocity. The total rate of work for each species of particles is the rate of work per particle multiplied by the total number of particles (n_s). The number of particles is related to the sludge thickness and species volume fraction (vf) according to $n_s = \pi R_c^2 h_{sl} vf / (\pi d_s^3 / 6)$. Not all of the flow work produced by the jet will go into resisting particle settling. Viscous shear will convert some of the jets power into heat. Furthermore, it is only the vertical component of fluid velocity that acts to counter the effects of gravity. On average, away from the jet, 1/6 of the fluid elements will be moving upward (due to three degrees of freedom of motion). Therefore, the condition will be satisfied to first order when

$$\rho_j u_0^3 d_0^2 > 216 \pi R_c^2 vf h_{sl} \mu_f u_s^2 / d_s^2 \quad (4.23)$$

Equation (4.23) must be applied for each of the species of particles present, with total power required being the sum of the power required for each species.

4.2 Model Results

In this section, the previously developed analytical models are evaluated for representative ranges of parameter values for the INEL mixing system. The correlation constants required by these models are obtained primarily from simulations of jets oriented perpendicular to the cooling coils. Because floor shear stresses were smallest for this orientation, the models will give conservative estimations. The results presented will be used to assess overall feasibility and guide in mixing system design recommendations.

4.2.1 Erosion and Deposition Results

Equation (4.3) gives the minimum acceptable nozzle discharge parameter required in order to erode the sludge material near the tank wall. Figure 4.2 shows $u_0 d_0$ plotted as a function of critical shear stress for erosion (τ_e) for a tank-centered jet ($\bar{c}_e = 0.00019 \text{ m}^{-2}$) and an off-center jet $\bar{c}_e = 0.0005 \text{ m}^{-2}$. Significant variation in $u_0 d_0$ is seen over the range of τ_e . The minimum $u_0 d_0$ required for a tank-centered jet is reduced by about 60% when the jet is in the off-center position. The values of $u_0 d_0$ required for larger τ_e are unfortunately large. A tank-centered jet with $\tau_e = 1.0 \text{ Pa}$ requires a minimum $u_0 d_0$ of approximately $1.9 \text{ m}^2/\text{s}$ ($20.5 \text{ ft}^2/\text{s}$). For a 15 cm (6 in.) diameter nozzle, this would correspond to a total hydraulic jet horse power of about 170 hp. However, this is just the minimum required to begin to erode the sludge. The actual power requirement would be larger in order to erode in a realistic time.

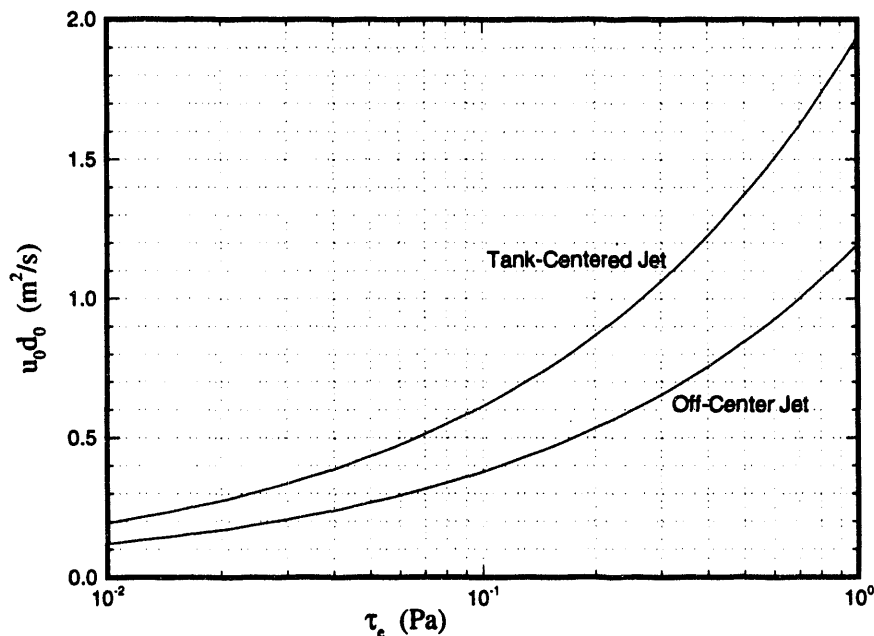


Figure 4.2 Jet Discharge Parameter Required to Erode Sludge Near Tank Wall

Equation (4.13) gives the minimum value of $u_0 d_0$ required in order for mobilization to occur for rotating mixing jets. In order to evaluate this expression, the mean correlation constants \bar{c}_e and \bar{c}_d must be determined from the simulation data. From Figure 3.16 it is seen that the average lateral shear stress is approximately one half the maximum center-line shear stress. This result implies $\bar{c}_e \approx c_e/2$. The constant \bar{c}_d was obtained by examining floor shear stress values far from the jet erosion area. A value $\bar{c}_d = 0.000064 \text{ m}^{-2}$ was found to represent several different test case results for tank-centered jets oriented perpendicular to the cooling coils and $\bar{c}_d = 0.00035 \text{ m}^{-2}$ for off-center jets. Equation (4.13) also requires the specification of the critical shear stress for deposition, τ_d . Due to lack of available data and in order to minimize the number of parameters, $\tau_d = \tau_e$ was assumed. This assumption is conservative because it results in a greater total deposition than if $\tau_d < \tau_e$.

Figure 4.3 shows values of $u_0 d_0$ obtained from Equation (4.13) for a tank-centered jet. Parameter conditions for this plot include $h_{sl}/h_f = 0.056$ (corresponding to a 5 cm sludge thickness and a 91 cm fluid height) and $E = .001 \text{ kg/m}^2\text{s}$. Results are shown for the three different particle species representing the sludge composition. Again, $u_0 d_0$ is seen to be strongly affected by the critical shear stress for erosion, with values being larger than those shown in Figure 4.2. The increase in $u_0 d_0$ is due to the fact that the jet must erode enough material to balance settling solids. Interestingly, $u_0 d_0$ is only weakly affected by particle characteristics. The reason for this will become clear momentarily.

Figure 4.4 shows the effect of the erodibility constant E on $u_0 d_0$. Again, only a small effect is seen. Figure 4.5 shows that jet location has a significant effect on $u_0 d_0$, with the minimum $u_0 d_0$ being reduced by about 40% for an off-center jet. Variations in fluid height and sludge thickness also were found to have little effect on the minimum $u_0 d_0$ required for mobilization. The reason for this can be understood by considering one of the limits of Equation (4.13) previously discussed. For the range of parameter conditions applicable to the INEL system, the terms in Equation (4.13) that contain the erodibility constant E are small compared with the other terms. This results in the limit $(u_0 d_0)^2 \approx \tau_e / (\bar{c}_d \rho_f)$. Hence, there should be a strong dependence on the constant \bar{c}_d which represents the mean floor shear in the deposition area outside the jet's direct influence. The effect of variations in \bar{c}_d are shown in Figure 4.6. As \bar{c}_d is increased (corresponding to higher background floor shear) $u_0 d_0$ decreases.

The value of \bar{c}_d derived from the simulations is believed to be conservatively low. Fluid motions away from the jet due to pump inlet entrainment, jet entrainment, large-scale circulations, and interaction from other jets (for multiple jet scenarios) will all act to increase \bar{c}_d .

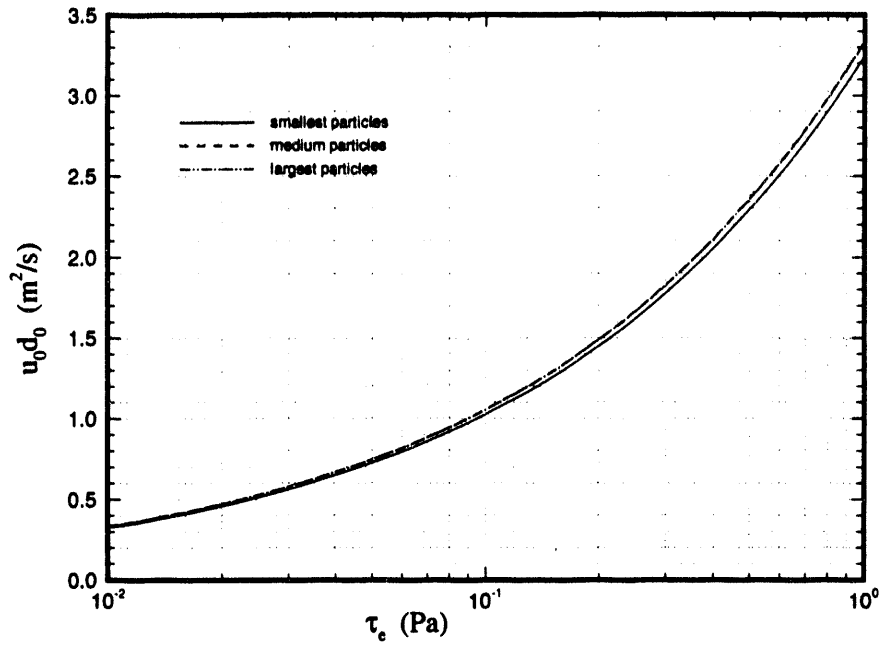


Figure 4.3 Effect of Particle Size on u_0d_0 for Tank-centered Jet

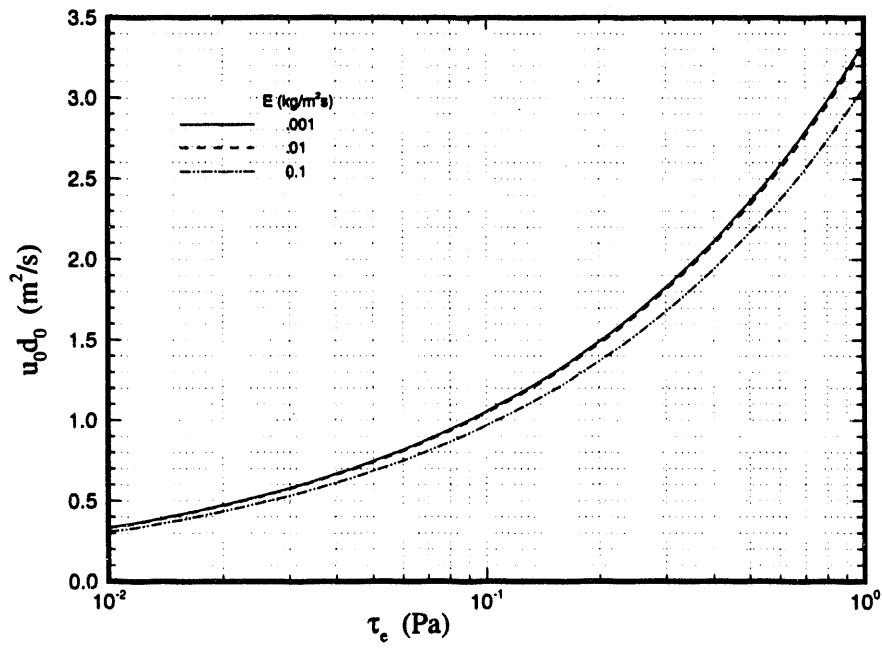


Figure 4.4 Effect of Erodibility Constant on u_0d_0 for Tank-centered Jet

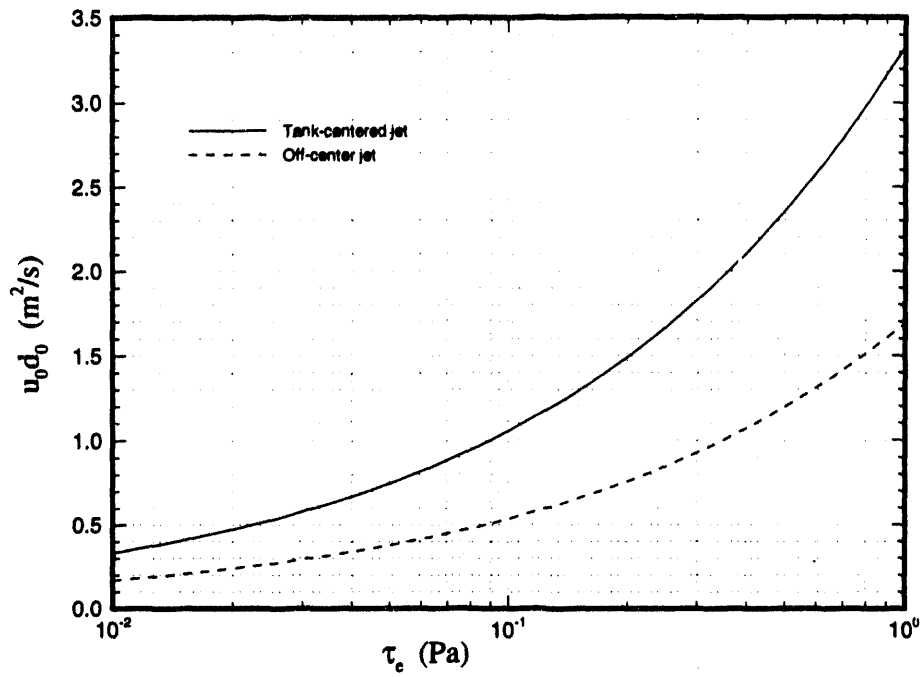


Figure 4.5 Effect of Jet Location on $u_0 d_0$

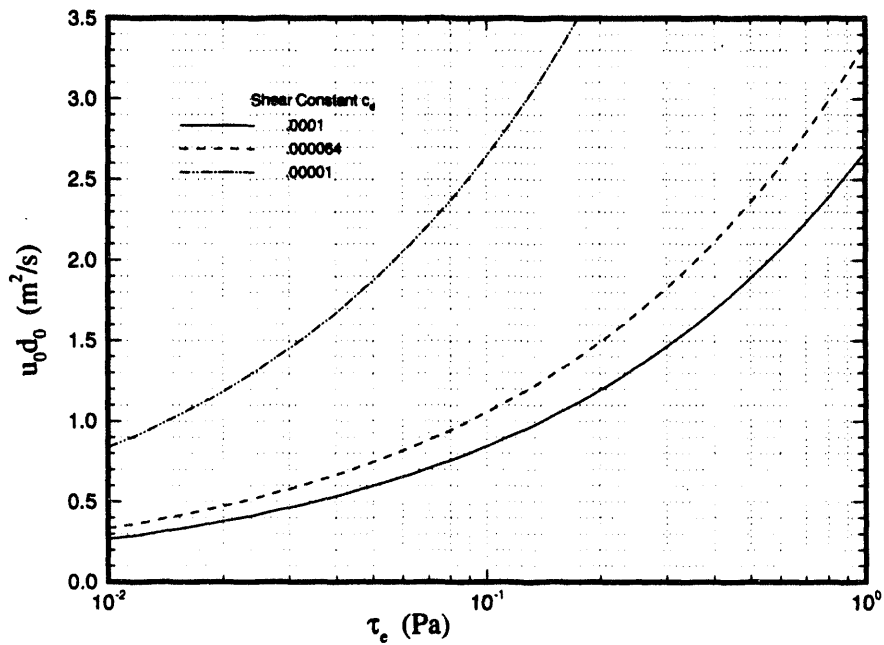


Figure 4.6 Effect of Background Shear Constant \bar{c}_d on $u_0 d_0$ for Tank-centered Jet

4.2.2 Mixing Time and Pump Rotation Results

Equations (4.17) and (4.20) relate jet discharge parameter ($u_0 d_0$) with jet rotation rate (ω_j) and mixing time (T_m). These expressions are functions of critical shear stress for erosion (τ_e) and deposition (τ_d), erodibility constant (E), particle settling velocity (u_s), suspended particle concentration (ϕ_s), fluid height (h_f), sludge thickness (h_{sl}), degree of uniformity (Φ), and the correlation constants (\bar{c}_e and \bar{c}_d). In order to graphically present the model predictions, base parameter values were chosen and then individual parameters were varied. The base values are $\tau_e = \tau_d = 0.1 \text{ Pa}$, $E = 0.01 \text{ kg/m}^2\text{s}$, $h_f = 91 \text{ cm}$, $h_{sl} = 5 \text{ cm}$, $\Phi = 0.95$, and $\bar{c}_d = 0.000064$. The correlation constant \bar{c}_e was 0.000095 for tank-centered jets and 0.00025 for off-centered jets. The suspended particle concentration ϕ_s was computed based on properties of the medium size (most populous) particles.

Figure 4.7 through Figure 4.12 show the relation between $u_0 d_0$ and mixing time for a range of parameter variations. Figure 4.7 shows results for the three different particle compositions of the sludge. The mixing time is strongly dependent on particle size and mass distribution. The discontinuity in the curves for the large and medium particles represents the transition to the hindered deposition regime. For short mixing times, a large value of $u_0 d_0$ is required. This increases the level of background shear enough to prevent any deposition from occurring away from the jet. Settling begins when $u_0 d_0$ is reduced to the value $\sqrt{\tau_d / (\bar{c}_d \rho_f)}$ and below. In this hindered deposition region, the effect of particle size is incidental. Figure 4.8 shows the effect of varying the erodibility constant. A similar behavior is observed, where mixing time increases with increasing E . Figure 4.9 shows the effect of liquid height on mixing time. For shorter mixing times, the behavior is independent of fluid height. This is true because the fluid height is only important when deposition is occurring. Figure 4.10 shows the effect of sludge thickness on mixing time. Again, a strong dependence is seen for shorter mixing times, where an increase in mixing time is seen with increasing sludge thickness. Figure 4.11 shows the effect of critical shear stress for erosion on mixing time. For small values of τ_e , the curves truncate at a certain mixing time. This occurs when the jet discharge parameter decreases to a value $(u_0 d_0)^2 = \tau_e / (\bar{c}_e \rho_f)$. Below this value, erosion cannot occur. For larger τ_e , $u_0 d_0$ is limited to the minimum value required for erosion given by Equation (4.13). Figure 4.12 shows the same plot for an off-center jet, where similar results are seen.

Figure 4.13 through Figure 4.16 show the dependence of jet rotation rate (revolutions per hour) on $u_0 d_0$ for the same parameter variations discussed above. The range of $u_0 d_0$ is limited to values greater than the minimum required for erosion and less than the value where deposition cannot occur. Above this latter value, there are no requirements on rotation rate. The trends are consistent with those for mixing time. However, an additional dependence on the degree of uniformity is seen.

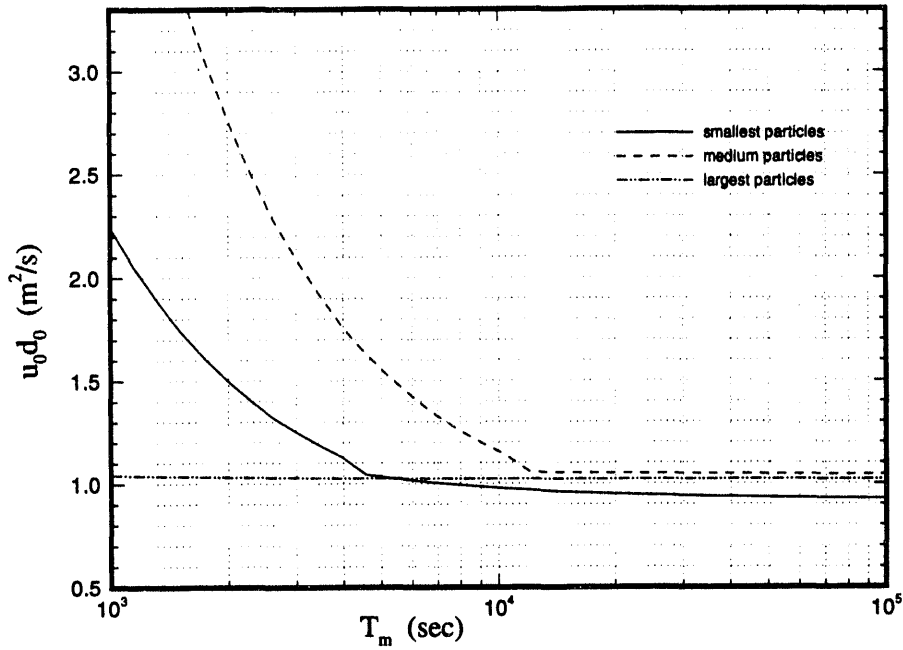


Figure 4.7 Effect of Particle Size on Mixing Time for Tank-centered Jet

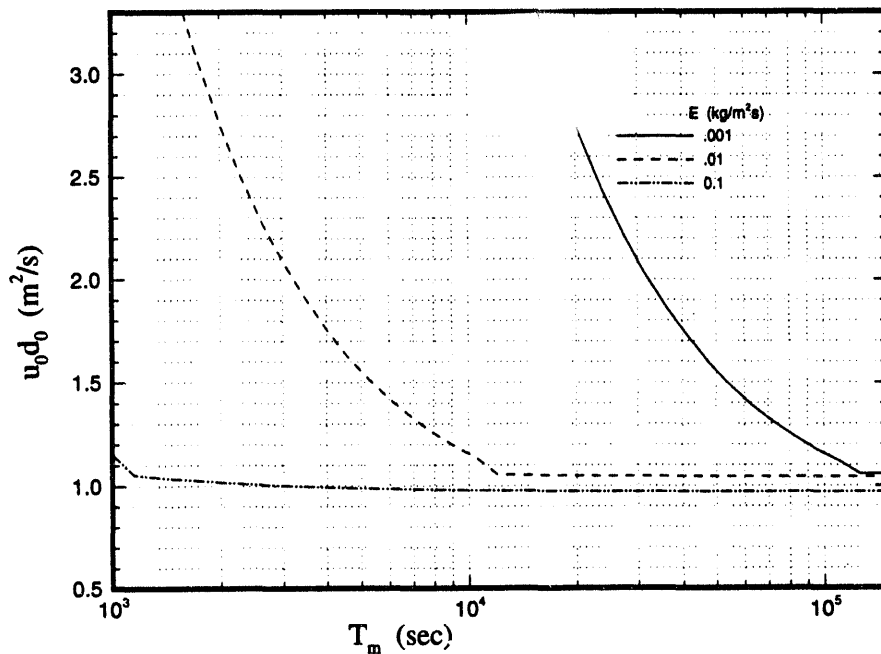


Figure 4.8 Effect of Erodibility Constant on Mixing Time for Tank-centered Jet

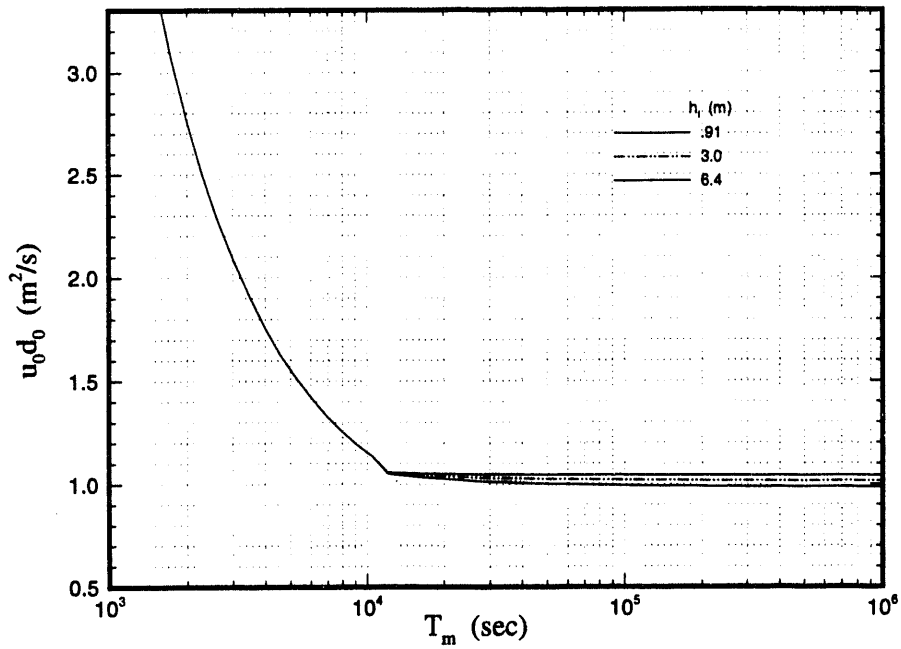


Figure 4.9 Effect of Fluid Height on Mixing Time for Tank-centered Jet

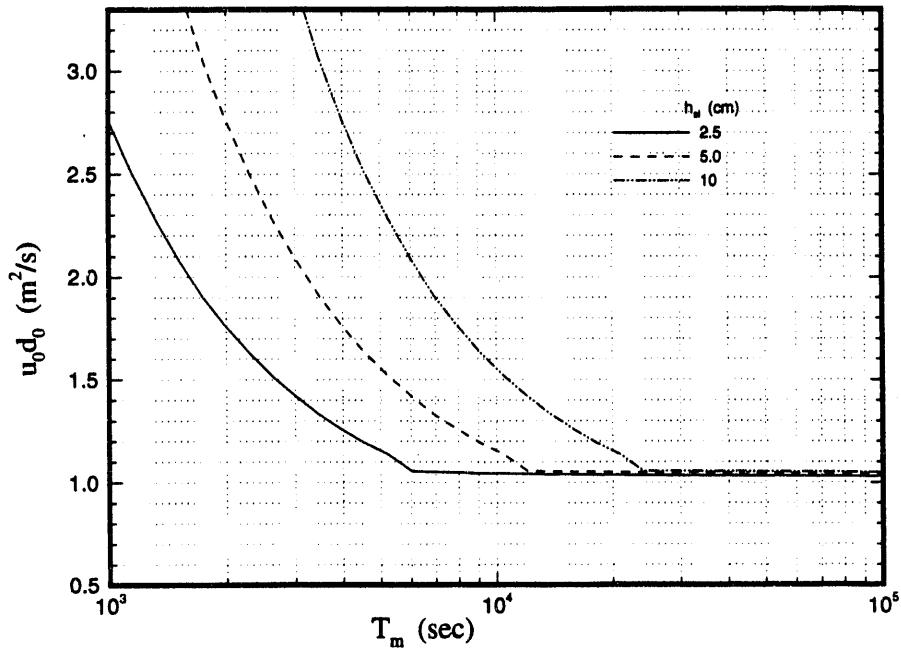


Figure 4.10 Effect of Sludge Thickness on Mixing Time for Tank-centered Jet

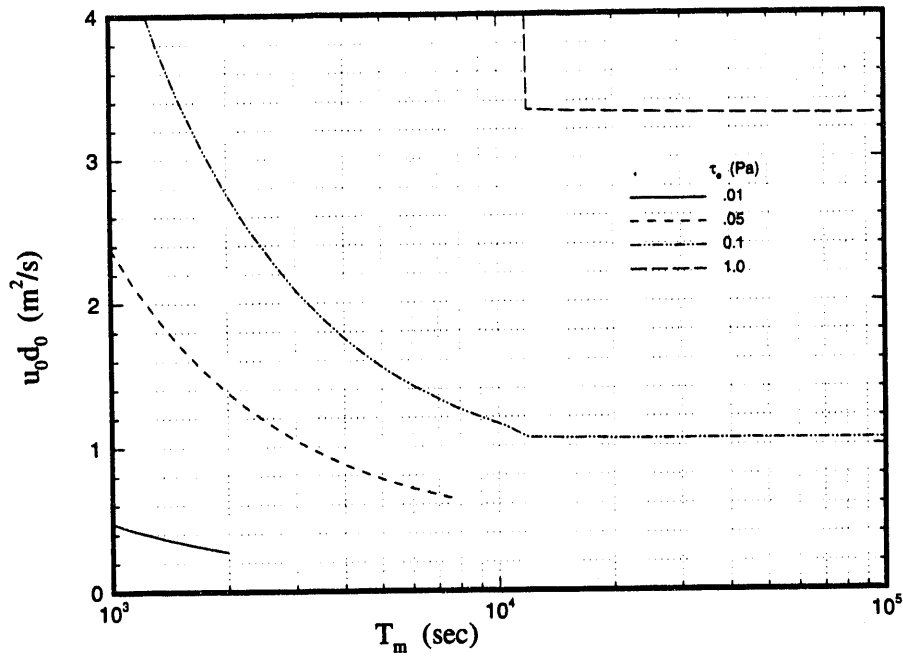


Figure 4.11 Effect of Critical Shear Stress for Erosion on Mixing Time for Tank-centered Jet

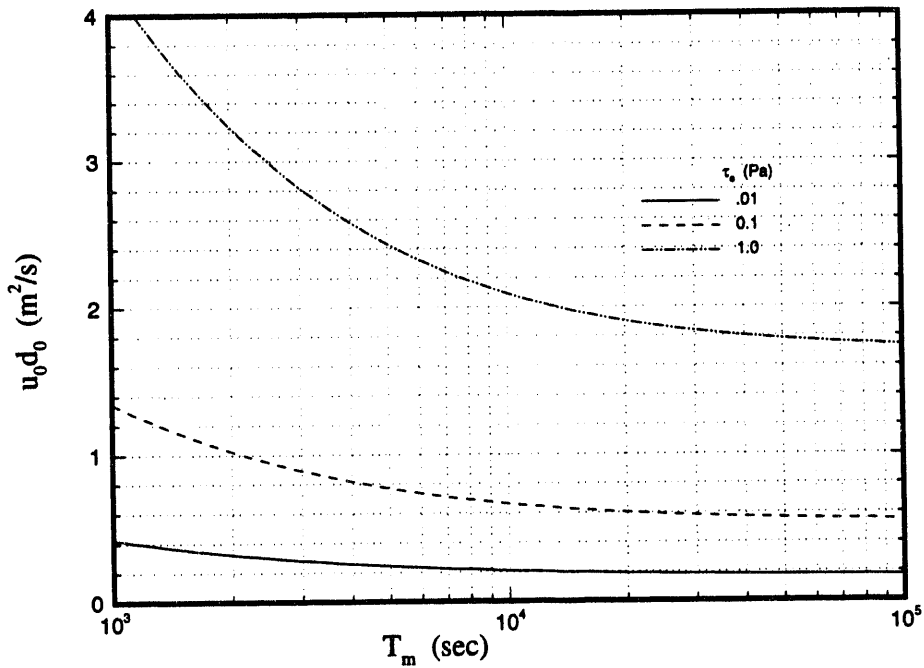


Figure 4.12 Effect of Critical Shear Stress for Erosion on Mixing Time for Off-center Jet

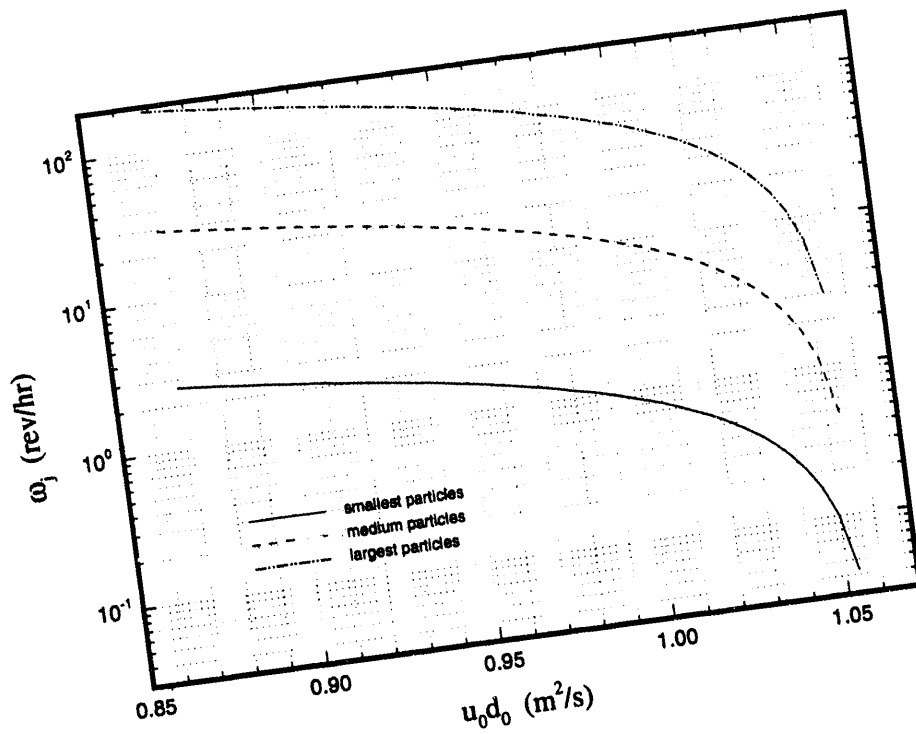


Figure 4.13 Effect of Particle Size on Jet Rotation Rate for Tank-centered Jet

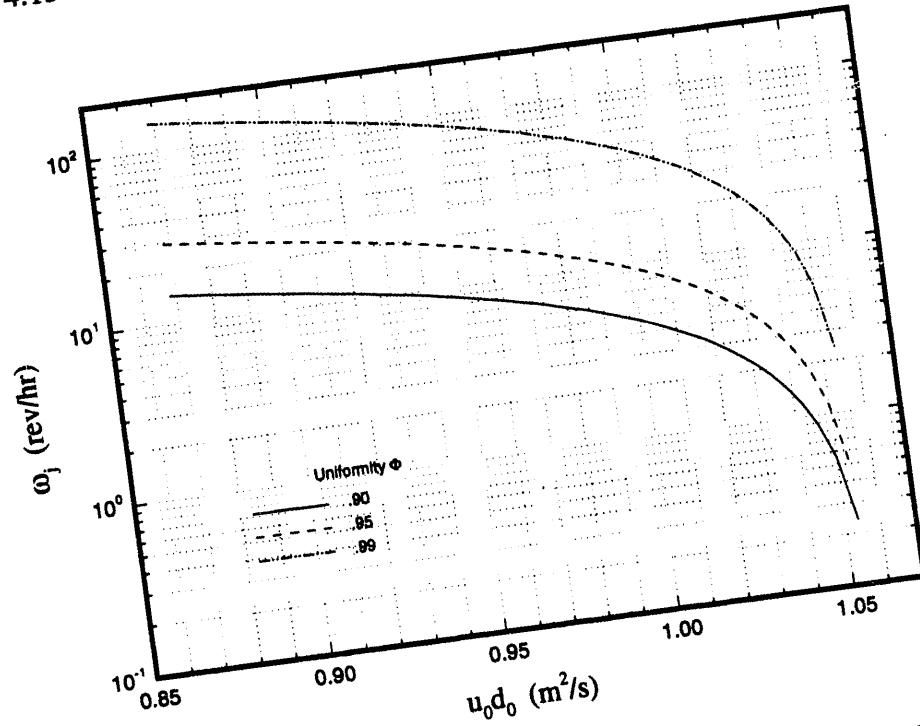


Figure 4.14 Effect of Degree of Uniformity on Pump Rotation Rate for Tank-centered Jet

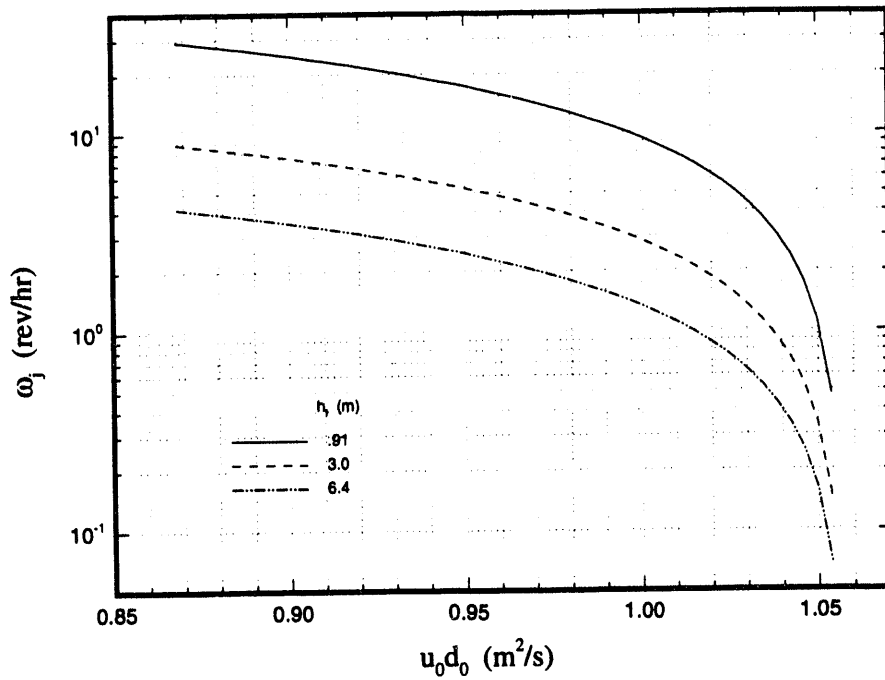


Figure 4.15 Effect of Fluid Height on Jet Rotation Rate for Tank-centered Jet

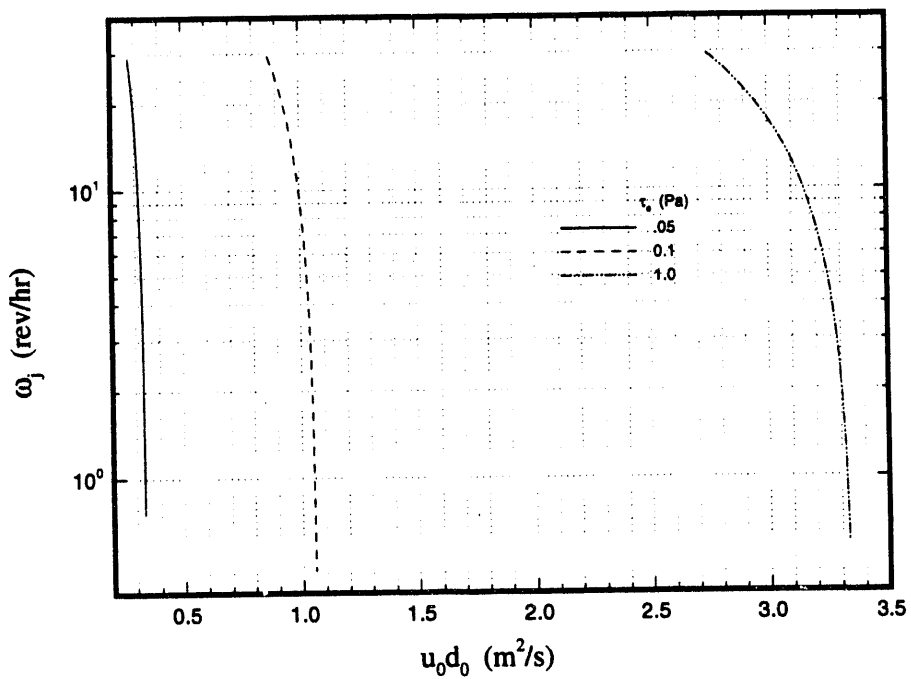


Figure 4.16 Effect of Critical Shear Stress for Erosion on Jet Rotation Rate for Tank-centered Jet

4.2.3 Solids Suspension Results

Equation (4.23) relates the jet hydraulic horsepower to the rate of gravitational work due to particle settling. The most conservative parameter values required to evaluate this expression are $R_c = R_T = 7.6$ m (25 ft) and $h_{sl} = 7.6$ cm (3 in.) which correspond to a single, tank centered pump with the maximum assumed sludge layer thickness. These produce values of the parameter $u_0^3 d_0^2$ equal to $0.53 \text{ m}^5/\text{s}^2$ which corresponds to a hydraulic jet horsepower of about 1 hp. This low value of jet horsepower is attributed to the relative thinness of the sludge layer. In light of this result, gravitational particle settling places no significant requirements on pump power.

Equation (4.22) related the jet discharge parameter to the velocity correlation constant (c_v) and the settling velocity (u_s). The value of c_v for tank-centered jets with $h_f = 91$ cm was determined from simulation data to be approximately 0.02. This value corresponds to the upward flowing region about 1 m from the wall. For the largest particles where $u_s = 0.022$ m/s, Equation (4.22) requires $u_0 d_0 > 0.9 \text{ m}^2/\text{s}$. Values of c_v for tank-centered jets with fluid heights greater than 91 cm and off-center jets were significantly larger, requiring a smaller jet discharge parameter.

4.3 Mixing System Design

This section addresses overall feasibility of using submerged liquid jets for heel removal and solids suspension in INEL waste tanks. Results of the numerical simulations and analytical models are analyzed to determine whether a suitable mixing system configuration exists.

4.3.1 Feasibility Assessment Approach

The results of the analytical models suggest that the minimum jet discharge parameter ($u_0 d_0$) required to erode and suspend the sludge material is dependent on many physical parameters. These include critical shear stress for erosion and deposition, the erodibility constant, the sludge thickness and particle attributes, fluid height, degree of uniformity, and jet location. The required mixing time (T_m) and jet rotation rate (ω_j) are also dependent on these parameters. Given the uncertainty in some of these parameter values, an assessment of feasibility is a challenging task. For example, $u_0 d_0$ has a strong dependence on the critical shear stress for erosion (Figure 4.5). The actual value of τ_c for the sludge may dictate whether or not a given pump configuration will be successful.

If one could show that the most conservative estimated parameter values (such as $\tau_e = 1\text{ Pa}$, $E = 0.001\text{ kg/m}^2\text{s}$, etc.) produce acceptable values of u_0d_0 , T_m , and ω_j , then it could reasonably be concluded that heel removal would be possible. However, if these conservative estimates produce unacceptable values of u_0d_0 , T_m , and ω_j , then the question of feasibility cannot be definitively answered without more accurate characterization of the sludge. Similarly, if the most favorable estimations of parameter values (such as $\tau_e = 0.01\text{ Pa}$, $E = 0.1\text{ kg/m}^2\text{s}$, etc.) produce unacceptable values of u_0d_0 , etc., then it could reasonably be concluded that heel removal would not be possible.

This principle is illustrated graphically in Figure 4.17 for the case of jet discharge parameter dependence on critical shear stress for erosion. The minimum value of critical shear stress for erosion has a corresponding jet discharge parameter $(u_0d_0)_{\min}$. If $(u_0d_0)_{\min}$ is too large (i.e. the corresponding horsepower is prohibitively high) then one could conclude that heel removal is not possible. Similarly, the maximum value of τ_e has a corresponding $(u_0d_0)_{\max}$. If the pump horsepower required to produce $(u_0d_0)_{\max}$ is acceptable, then heel removal is possible (assuming the mixing time and rotation rates are acceptable for the same scenario). If $(u_0d_0)_{\max}$ is not acceptable but $(u_0d_0)_{\min}$ is, then Feasibility is uncertain, and more precise specification of τ_e is required.

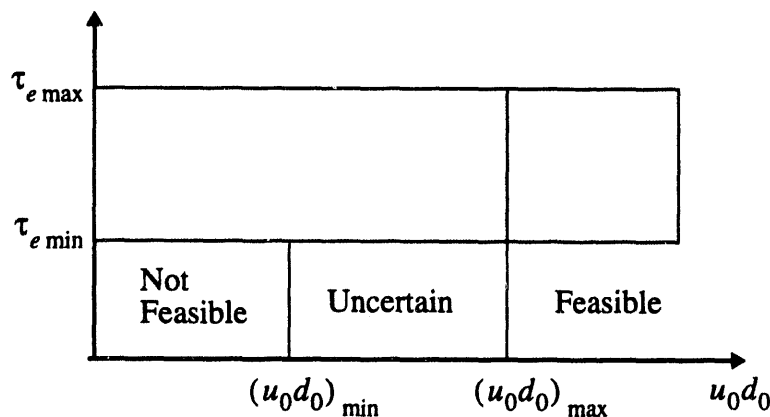


Figure 4.17 Graphical Illustration of Feasibility Assessment Approach

This process needs to be repeated for all parameters which have an estimated range of values. Mixing time and jet rotation rates also need to be considered since, for example, $(u_0d_0)_{\max}$ may be acceptable, but the corresponding value of T_m may be excessive, requiring a larger u_0d_0 in order to reduce T_m .

4.3.2 Feasibility Results

In this section, the results of the analytical models are evaluated in order to determine whether a positive feasibility assessment is possible, given the assumed ranges of parameter values for the INEL waste system.

The minimum value of $u_0 d_0$ required to mobilize the sludge was given by Equation (4.20). For tank-centered jets, $u_0 d_0$ was found to be most strongly dependent on τ_e . The value of τ_e was estimated to be 0.01 Pa to 1.0 Pa. For the lowest value of τ_e , the corresponding value of $u_0 d_0$ was determined to approximately 0.33 m²/s. For a 6 cm (2.5 in.) nozzle, this corresponds to a total hydraulic horsepower of 1.2 hp, with pump horsepower being somewhat larger. For a 5 cm sludge thickness, an erodibility constant $E = 0.001$ kg/m²s, and a 91 cm fluid height, the mixing time for the most populous particles is approximately 30 h, and the jet rotation rate is about 0.7 rev/h. Clearly, Feasibility is not ruled out because there would be no physical constraints on installing such a small pump.

The highest value of τ_e has a corresponding $u_0 d_0$ equal to 3.3 m²/s. For a 20 cm (8 in.) nozzle, this corresponds to a total hydraulic horsepower of approximately 340hp. Since pump horsepower would be even larger than this amount, this is clearly an excessive requirement. In light of this, the feasibility of using a single, tank-centered pump is uncertain, requiring more precise specification of critical shear stress.

It would be interesting to determine what maximum value τ_e can have in order for a tank-centered jet to be effective. A pump power of 150 hp and a pump efficiency of 50% results in a total hydraulic jet power of 75 hp. For an 15 cm (6 in.) square nozzle, this would require $u_0 d_0 = 1.8$ m²/s, with the corresponding τ_e of about 0.3 Pa. Mixing time for the most populous particles would be about 30 h with a jet rotation rate of about 1 rev/h for 95% uniformity and about 10 rev/h for 99% uniformity. For the largest particles, mixing time would be about 35 h. Mixing time for the smallest particles is about 11 h. If τ_e were somewhat less than 0.3 Pa mixing times would decrease. Increasing the fluid height would also cause mixing times to decrease.

Because the success of a tank-centered jet cannot be definitely determined, the question of using an off-center jet naturally arises. From Figure 4.5, the value of $u_0 d_0$ corresponding to $\tau_e = 1.0$ Pa is approximately 1.7 m²/s for an off-center jet. This corresponds to a total hydraulic jet power of approximately 45 hp for a 20 cm (8 in.) nozzle. This is within an acceptable range, even when considering total pump power which would be about 90 hp. For a 5 cm sludge thickness, an erodibility constant $E = 0.01$ kg/m²s, and a 91 cm fluid height, the mixing time for the most populous particles is approximately 5 days. If $u_0 d_0$ is increased to 1.9 m²/s (64 hp), then the

mixing time decreases to about 6 h. The mixing time will be different for different sludge thicknesses, fluid heights, and erodibility constants. If the upper limit of erodibility constant ($E = 0.01 \text{ kg/m}^2\text{s}$) is used, then a mixing time of approximately 2 days is required. There is no requirement on jet rotation rate for these situations because stresses are high enough to prevent settling.

4.3.3 Conclusions and Recommendations

Based on simulation data and analytical model results, feasibility of using a single jet mixing pump located near the tank center cannot be conclusively determined. The primary reason for this is uncertainty in the critical shear stress for erosion (τ_e) for the sludge in the INEL waste tanks. The results suggest, however, that if τ_e is less than about 0.35 Pa, a single pump with a jet discharge parameter of $u_0 d_0 = 1.8 \text{ m}^2/\text{s}$ ($19.4 \text{ ft}^2/\text{s}$) would be sufficient to mobilize and maintain solids in suspension, if it were located near the center of the tank. For a circular nozzle 20 cm (8 in.) in diameter, this would correspond to a total hydraulic jet power of about 62 hp and a pump power of about 124 hp assuming a 50% pump efficiency. If a 15 cm (6 in.) round nozzle were used, the required pump power would be about 164 hp. If a smaller nozzle was required due to manufacturing constraints, the required pump horsepower would increase further. Mixing times for these conditions range from about 5 to 30 hours depending on sludge particle characteristics and thickness. Minimum pump rotation rates range from 0.1 to 5 rev/h for a range of conditions.

If a single mixing pump were used, it should be located as close to the tank center as possible. For Tank WM-182, there is no existing riser near the tank center. Therefore, it would be necessary to install a new riser inside the man-way as shown in Figure 4.18. For Tank WM-188 (shown in Figure 4.19), the existing riser near the center of the tank would suffice. An alternative location would be inside the man-way as shown.

Using the estimated upper limit of critical shear stress for erosion of 1.0 Pa, model results suggest heel removal would be successful if two off-center pumps were used. These pumps should each have a jet discharge parameter of at least $u_0 d_0 = 1.7 \text{ m}^2/\text{s}$ ($18.3 \text{ ft}^2/\text{s}$). For a 20 cm (8 in.) diameter round jet nozzle, the models predict a total hydraulic jet power of at least 52 hp is required, corresponding to a pump power of approximately 105 hp per pump. If a 15 cm (6 in.) round nozzle were used, the required pump power would be about 138 hp per pump. The mixing time for this situation would be about 5 days. For a 20 cm diameter nozzle with a pump power of about 150 hp, mixing time would be reduced to about 5 h.

Ideally, each off-center pump should be located about one half the distance from the tank center to the outer wall along the tank center-line dividing east and west as shown in Figure 4.18 and Figure 4.19. This would maximize the propensity of the jet to erode the material on the northern and southern sides of the tanks. Unfortunately, there are no existing risers near these locations. Therefore, new risers would need to be installed in order to use a double pump configuration.

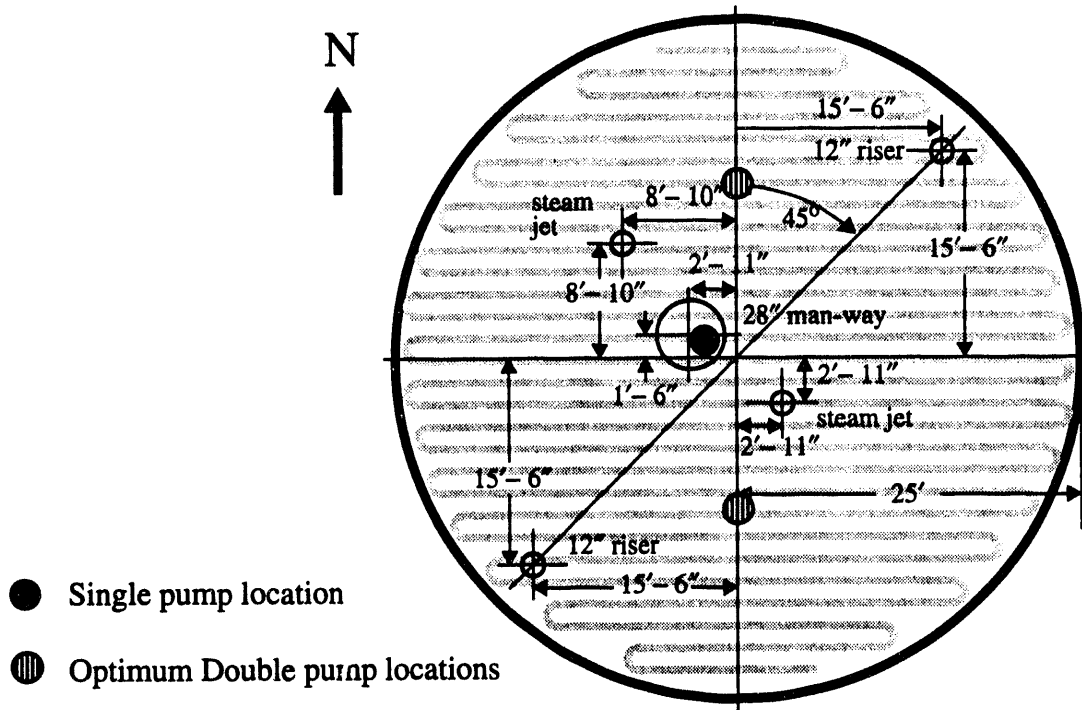


Figure 4.18 Recommended Mixing Pump Locations in INEL Waste Tank WM-182

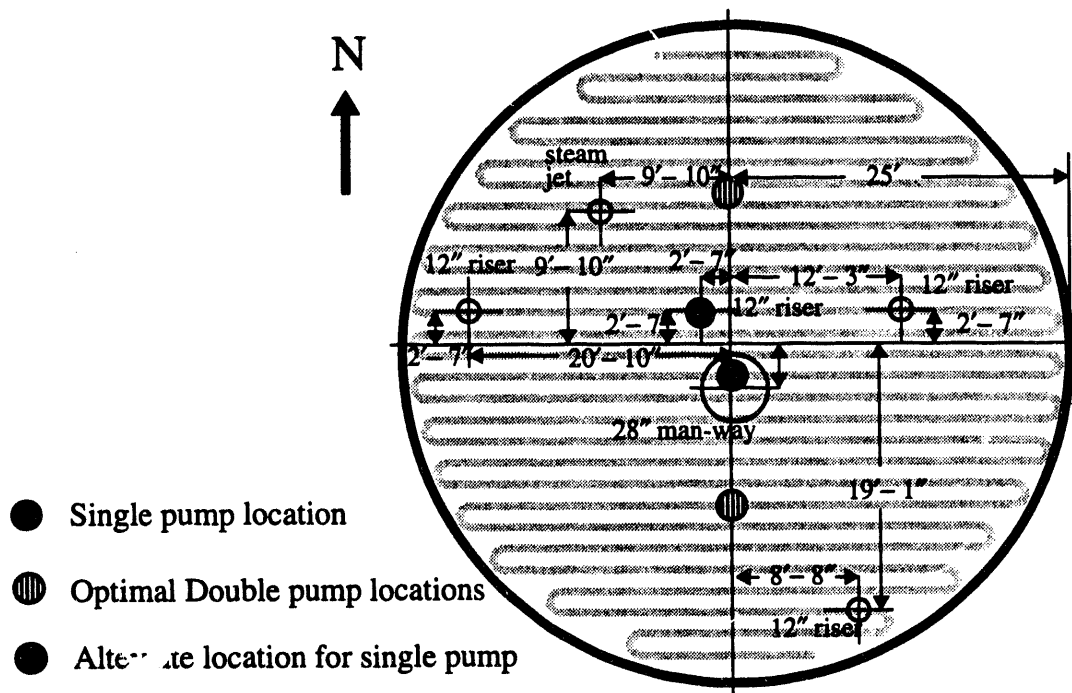


Figure 4.19 Recommended Mixing Pump Locations in INEL Waste Tank WM-188

While model results indicate that a double pump configuration would be adequate for even conservative values of critical shear stress for erosion (τ_e), difficulties associated with new riser additions may make this option unattractive. In light of this, it is imperative that INEL obtain more precise estimations of τ_e in order to determine whether a single pump located near the tank center would be effective. Model results indicate that if τ_e is determined to be less than about 0.35Pa, this option should be acceptable. The formulas for mixing time (Equation (4.19)) and rotation rate (Equation (4.17)) could be used as guides for pump sizing. In using these formulas, however, it would be helpful to have more precise estimates of particle properties such as size, density, and distribution by weight; sludge thickness; and erodibility constant (E).

The models developed in this study represent simplifications of extremely complex flow phenomenon. In light of this, it would be advisable for INEL to combine sludge characterization activities with carefully designed mobilization experiments. Experiments could identify important behaviors not captured by numerical simulations or analytical models. In particular, experimental observations of jets in shallow liquids and measurements of floor shear underneath the cooling coils would be helpful.

5.0 References

- Bamberger, J. A., L. M. Liljegren, and P. S. Lowery. 1993. *A Methodology to Predict Uniformity of Double-Shell Tank Waste Slurries Based on Mixing Pump Operation*. PNL-7665. Pacific Northwest Laboratory, Richland, WA.
- Dunn, I. S. 1959. "Tractive Resistance of Cohesive Channels." *Journal of the Soil Mechanics and Foundation Division*, No. SMC, Proc. Paper 2062, pp1-24.
- Flaxman, E. M. 1963. "Channel Stability in Undisturbed Cohesive Soils", *Journal of the Hydraulic Division ASCE*. Vol. 89, No. HY2, Proc. Paper 2462, pp. 87-96.
- Geisler, R. K., C. Buurman, and A. B. Mersmann. 1993. "Scale-up of the Necessary Power Input in Stirred Vessels with Suspensions." *The Chemical Engineering Journal*. Vol. 51, pp. 29-39.
- Krone, R. B. 1962. *Flume Studies in the Transport of Sediment in Estuarial Shoaling Processes*. Hydraulic Engineering Laboratory and Sanitary Engineering Research Laboratory, University of California at Berkeley, CA.
- Liljegren, L. M. 1993. *Similarity Analysis Applied to the Design of Scaled Tests of Hydraulic Mitigation Methods for Tank 241-SY-101*. PNL-8518. Pacific Northwest Laboratory, Richland, WA.
- Meyer, P. A. and J. A. Fort. 1994. *TEMPEST: A Computer Program for Three-Dimensional Time-Dependent Computational Fluid Dynamics, Volume 3, Validation and Verification, Version T*. PNL-8857, Pacific Northwest Laboratory, Richland, WA.
- O'Brien, J., S. Julien, and Y. Pierre. 1988. "Laboratory Analysis of Mudflow Properties." *Journal of Hydraulic Engineering*. Vol 114, No. 8.
- Onishi, Y. 1993. "Sediment Transport Models and Their Testing." NATO Advanced Study Institute: Lecture Series on *Computer Modeling of Free-Surface and Pressurized Flows*, June 28 - July 9, 1993, Pullman, WA.
- Partheniades, E. 1962. *A Study of Erosion and Deposition of Cohesive Soils in Salt Water*. Ph.D. thesis presented to the University of California at Berkeley, CA.
- Rajaratnam, N. 1976. *Developments in Water Science 5: Turbulent Jets*. Elsevier Scientific Publishing Company, Amsterdam, The Netherlands.
- Rouse, H. 1937. "Modern Conceptions of the Mechanics of Fluid Turbulence." *Transactions, ASCE*. Vol. 102, No. 1965, pp. 463-543.

Smerdon, E. T., and R. P. Beasley. 1961. "Critical Tractive Forces in Cohesive Soil." *Agricultural Engineering, St. Joseph, Michigan*, pp. 26-29.

Tatterson, G. B. 1991. *Fluid Mixing and Gas Dispersion in Agitated Tanks*, pp. 286-302, McGraw-Hill Book Company, Inc., New York.

Teeter, A. M. 1988. *New Bedford Harbor Project -- Acushnet River Estuarary Engineering Feasibility Study of Dredging and Dredged Material Disposal Alternatives - - Report 2. Sediment and Contaminant Hydraulic Transport Investigations*. US Army Corps of Engineers, Waterways Experiment Station, Vicksburg, Mississippi.

Trent, D. S. and L. L. Eyler. 1992. *TEMPEST: A Computer Program for Three-Dimensional Time-Dependent Computaional Fluid Dynamics, Volume 2, Input Instructions, Version T*. Battelle Memorial Institute, Pacific Northwest Laboratory, Richland, WA.

Trent, D. S., and T. E. Michener. 1993. *Numerical Simulation of Jet Mixing Concepts in Tank 241-SY-101*. PNL-8559. Pacific Northwest Laboratory, Richland, WA.

Vanoni, V. A., ed. 1975. "Sedimentation Engineering." *ASCE Manual and Reports on Engineering Practice*, ASCE, New York, New York.

DISTRIBUTION

**No. of
Copies**

2 DOE/Office of Scientific and
Technical Information

ONSITE

2 Westinghouse Idaho Company
M.R. Christensen

7 Pacific Northwest Laboratory
I.G. Choi, K7-15
L.L. Eyler, K7-15
P.A. Meyer, K7-15
E.W. Pearson, K7-15
Publishing Coordination
Technical Report Files (2)

Dist. 1

END DATE
5/26/94